

Mechanisms of Axonopathy in Krabbe Disease

BY

Ludovico Cantuti-Castelvetri
B.S., Università Vita-Salute San Raffaele, 2005
M.S., Università Vita-Salute San Raffaele, 2007

THESIS

Submitted as partial fulfillment of the requirements
for the degree of Doctor of Philosophy in Anatomy and Cell Biology
in the Graduate College of the
University of Illinois at Chicago, 2012

Defense Committee:

Scott T. Brady (Chair)
Ernesto R. Bongarzone (Advisor)
Jonathan Art
Raymond Roos, University of Chicago
Skip Binder, Northwestern University

TABLE OF CONTENTS

CHAPTER 1 INTRODUCTION	1
1.1 LYSOSOMAL STORAGE DISEASES	1
1.1.1 GENERALITIES	1
1.1.2 KRABBE DISEASE	2
1.1.3 PATHOPHYSIOLOGY OF KD	3
1.1.4 PSYCHOSINE	4
1.1.5 KD THERAPIES	6
1.1.6 PRIMARY VS SECONDARY NEURODEGENERATION IN KD	8
1.2 THE NEURON AND THE IMPORTANCE OF AXONAL STABILITY.	9
1.2.1 GENERALITIES	9
1.2.3 NEURONAL CYTOSKELETON	10
1.2.3 EXPRESSION OF NFs	11
1.2.4 PHOSPHORYLATION OF NFs	12
1.2.5 NFs INFLUENCE AXONAL CALIBER	12
1.2.6 AXONAL TRANSPORT	13
1.2.7 AXONAL TRANSPORT DEFECTS: THE DYSFEROPATHIES	15
1.3 THE IMPORTANCE OF THE SYNAPSE FOR THE NEURON AND ITS TARGETS: THE NEUROMUSCULAR JUNCTION	17
1.3.1 REGULATION OF THE MUSCLE GROWTH	19
1.4 THE TWITCHER MOUSE: THE MURINE MODEL OF KD	21
CHAPTER 2 RATIONALE & AIMS	24
CHAPTER 3 EXPERIMENTAL DESIGN	25
CHAPTER 4 MATERIALS AND METHODS	26
4.1 CELL CULTURES	28
4.2 MITOCHONDRIA LABELING AND TIME LAPSE MICROSCOPY	28
4.3 TISSUE COLLECTION, HISTOLOGY, AND IMMUNOHISTOCHEMISTRY	29
4.4 STEREOLOGY	30
4.5 WESTERN BLOTTING	30
4.6 GENE EXPRESSION ANALYSIS	32
4.7 ELECTROPHYSIOLOGY	33
4.8 SER/THR PHOSPHATASE ACTIVITY ASSAY.	34
4.9 ELECTRON MICROSCOPY	34
4.10 NISSL STAINING	35
4.11 SCIATIC NERVE LIGATION	35
4.12 VESICLE MOTILITY ASSAYS IN ISOLATED AXOPLASM	35
4.13 STATISTICAL ANALYSIS	36
CHAPTER 5 EXPERIMENTAL RESULTS	37
5.1 ACTIVATION OF THE PROTEIN DEGRADATION SYSTEM UNDERLIES THE MUSCULAR ATROPHY OF THE TWITCHER MOUSE.	37
5.2 THE TWITCHER NMJs HAVE NORMAL MORPHOLOGY.	38

5.3 TWITCHER NMJS APPEAR TO BE DYSFUNCTIONAL BY INCREASED LEVELS OF ACTIVE CASPASE 3 AND ABNORMAL EXPRESSION OF THE FETAL ACHR SUBUNIT.	43
5.4 AXONAL DYSTROPHY IN THE TWITCHER MOUSE.	44
5.5 AXONOPATHY STARTS BEFORE THE ONSET OF DEMYELINATION.	49
5.6 PERIPHERAL NERVES ARE AFFECTED OF AXONOPATHY.	49
5.7 NEURONAL LOSS IS A LATE EVENT IN THE TWITCHER MOUSE	50
5.8 DECREASE IN DIAMETER OF TWITCHER AXONS.	57
5.9 LOWER DENSITY OF NFs IN TWITCHER AXONS.	58
5.10 REDUCED PHOSPHORYLATION OF MUTANT NFs.	64
5.11 INCREASED ACTIVITY OF SERINE/THREONINE PROTEIN PHOSPHATASES IN TWITCHER SCIATIC NERVES.	65
5.12 PSYCHOSINE IS SUFFICIENT TO INCREASE PP1 AND PP2A ACTIVITY IN NEURONAL CELLS.	65
5.13 FAST AXONAL TRANSPORT IS REDUCED IN TWITCHER SCIATIC NERVES.	71
5.14 DEFECTS IN FAT INVOLVE GSK3B	75
5.15 PSYCHOSINE INDUCES KLC PHOSPHORYLATION THROUGH PP1 AND GSK3B	76
5.16 PSYCHOSINE IS PRESENT IN TWITCHER NEURONS.	82
5.17 PSYCHOSINE INHIBITS AXONAL TRANSPORT.	83
5.18 IN VIVO NEUROPROTECTION BY INHIBITION OF GSK3B.	87
CHAPTER 6 DISCUSSION	91
6.1 SUMMARY	91
6.2 AXONAL PATHOLOGY IN THE TWITCHER MOUSE.	92
6.3 MUSCULAR ATROPHY AS A CONSEQUENCE OF THE TWITCHER AXONOPATHY	94
6.4 ALTERATIONS IN NFs	96
6.5 FAST AXONAL TRANSPORT AS A PATHOLOGICAL MECHANISM IN KD.	98
6.6 IS PSYCHOSINE AS A NATURAL REGULATOR OF AXONAL PHOSPHOTRANSFERASES?	100
6.7 GALC DEFICIENCY MAY GENERATE A CELL AUTONOMOUS PATHOGENIC DEFECT IN NEURONS	103
6.8 NEURODEGENERATION AS A NEW TARGET FOR KD THERAPY.	104
6.9 RELEVANCE OF THIS STUDY IN OTHER LYSOSOMAL STORAGE DISEASES	106
CHAPTER 7 CONCLUSIONS AND FUTURE DIRECTIONS	108
REFERENCES CITED	110
CURRICULUM VITAE	131

Summary

In this work we describe the molecular mechanisms of axonal damage in Krabbe disease (KD). KD is a fatal genetic lysosomal storage disorder (LSD) caused by the loss of the lysosomal enzyme galactosyl-ceramidase (GALC). The deficiency causes the accumulation of galactosyl-sphingolipids. Psychosine, one of GALC substrates, is a lipid-raft associated neurotoxin believed to cause the death of myelinating cells in the CNS of affected patients. KD patients also suffer of neurodegeneration, due to axonal and neuronal deficiencies. Over the years, most studies have focused on the loss of myelin induced by psychosine, and have considered neurodegeneration as a consequence of demyelination. Recently, our laboratory showed that bone marrow transplantation (BMT) improved myelin preservation in Twitcher mice, the natural murine model for this disease, but it was insufficient to prevent neurodegeneration. There are various potential interpretations for this result. Neuronal loss and axonal degeneration in KD may start before oligodendroglia is affected, creating a progressive compounding factor contributing to the severity of the disease. Neurodegeneration may even be independent from demyelination.

We hypothesized that GALC deficiency causes a cell-autonomous defect in the mutant neurons, leading to neurodegeneration. By studying the Twitcher mouse, we show that the Twitcher axons are affected by a decrease in axonal caliber and by morphological abnormalities from the first postnatal days. Importantly, we show that these defects are at least partially caused by changes in two critical components of neuronal function: the neurofilament (NF) cytoskeleton and fast axonal transport (FAT). In particular, we provide evidence that psychosine alters the activities of critical phosphotransferases, interfering with the phosphorylation state of NFs and kinesin, one of the molecular motors responsible for FAT. Finally, we identify protein phosphatase 1 (PP1), protein phosphatase 2A (PP2A) and glycogen synthase kinase 3 β (GSK3 β) as the

phosphotransferases involved in psychosine toxicity. By injecting the newborn Twitcher mouse with an inhibitor of GSK3 β , we rescue the functionality of the mutant nerve to a significant level, further demonstrating the relevance of altered phosphorylation in the development of axonopathy in the Twitcher mouse.

In summary, these studies have shown that a sphingolipid can regulate NFs and FAT through specific phosphotransferases, and that this effect can cause axonal damage in KD. Pharmacological inhibition of these enzymes may provide new therapeutic alternatives to protect NFs and FAT in KD, therefore rescuing the mutant axons. Importantly, our studies also define a new mechanism by which psychosine, a substrate of a LSD, can cause axonopathy, raising the possibility that alterations in NFs and FAT might occur in other LSDs.

ACKNOWLEDGEMENTS

First, I would like to thank my Adviser, Dr. Ernesto R. Bongarzone, for his constant guidance and his patient supervision. We met eight years ago in Italy during my undergraduate degree. Since our collaboration started, he has spent every opportunity to patiently guide me through my mistakes and my successes. He showed how he deeply cared for my preparation. He has constantly worked to improve my scientific skills, from the work at the bench to the writing and communication skills required to present scientific results. His advice, support and friendship proved invaluable at both personal and scientific levels. It is really hard for me to describe how much I learned since I met him. He provided me with a friendly and cooperative scientific environment, where working was a challenging as well as pleasant experience for me.

I would like to thank all the people of the Bongarzone Lab for their scientific support and the pleasant times spent together. Thanks to Aurora, for all her terrific work with the difficult Twitcher colonies and the organization of the lab. Thanks to Ben Smith, Amy Hebert and Adam White, who constantly discussed my experiments and helped me to improve my writing skills (as well as to design innocent pranks on the new students). Thanks to Hongling Zhu and Agnieszka Kaminska for all their help with the injections on the Twitcher mice.

I also want to thank heartedly Dr. Maria Irene Givogri and her group, Kasia Pituch and Felecia Marattoli for the collaborations on RNA and DNA techniques and the qRTPCR protocols. Irene's motherly patience has taught me more than molecular biology, which by the way it proved fundamental for the PCR experiments of this work.

A special thank also goes to Marta Santos and Erik Maravilla, whose questions were a source of constructive discussions. I really want to thank Analis Moyano, Nicholas Cecchini and Kamila Krauze, who taught me the use of imaging software required for the figures of my thesis.

I would like to acknowledge Dr. Scott Brady, the head of the Anatomy and Cell Biology program, for providing me with the structure where to work towards my PhD. Many thanks to his collaborators, Gerardo Morfini and Gustavo Pigino, for teaching me how to isolate vesicles and how to prepare primary neuronal cultures. I also like to thank Dr. Brady and Bin Wang for providing me with several useful reagents (among which the extremely useful antibodies against kinesin). My thanks to the Department Office Team, Maria Carlstrom, Rory Sullivan, Mike Driscoll, Lea Smucker, Charles Snider and Sydelle Bautista for their constant help.

I want to express my deep appreciation to my Ph.D. committee: Dr. Scott Brady (chair), Dr. Jonathan Art, Dr. Raymond Roos, Dr. Skip Binder and Dr Ernesto R. Bongarzone. Their suggestions and feedback have been critical for the completion of my thesis.

Last, but not least, I want to thank my family, my mother Flaminia, my late father Nestore and my sister Maria Giulia. They supported me in every decision, even when this meant that to spend several years away from them. Without the support of my family, I would not have been able to come to Chicago and to UIC.

I thank the University of Illinois at Chicago, the Morton Cure Foundation, the Legacy of Angels Foundation and the National Institutes of Health for financially contributing to this work.

Sections of this dissertation are components of the following published manuscripts:

1: Castelvetri LC, Givogri MI, Zhu H, Smith B, Lopez-Rosas A, Qiu X, van Breemen R, Bongarzone ER. Axonopathy is a compounding factor in the pathogenesis of Krabbe disease. *Acta Neuropathol.* 2011 Jul;122(1):35-48.

2: Smith B, Galbiati F, Castelvetri LC, Givogri MI, Lopez-Rosas A, Bongarzone ER. Peripheral neuropathy in the Twitcher mouse involves the activation of axonal caspase 3. *ASN Neuro.* 2011;3(4).

3: Cantuti-Castelvetri L, Zhu H, Givogri MI, Chidavaenzi RL, Lopez-Rosas A, Bongarzone ER. Psychosine induces the dephosphorylation of neurofilaments by deregulation of PP1 and PP2A phosphatases. *Neurobiol Dis.* 2012 May;46(2):325-35.

Other sections of this dissertation are components of the following manuscripts in preparation:

4: Castelvetri LC, Lopez-Rosas A, Morfini G, Pigino G, Givogri MI, Brady ST, Bongarzone ER. Psychosine is a pathogenic sphingolipid that impairs fast axonal transport in Krabbe disease.

5: Castelvetri LC, Sural T, Lopez-Rosas A, Bongarzone ER. Axonopathy and muscle wasting in the Twitcher mouse: role of the AKT pathway in muscle degeneration.

LIST OF FIGURES

- Figure 1 Muscle wasting in the twitcher mouse.
- Figure 2 activation of the atrophy signaling pathways in the twitcher muscles.
- Figure 3 Activation of the ubiquitination system in the Twitcher muscles
- Figure 4 The Twitcher NMJs are not denervated.
- Figure 5 Counting of denervated NMJs
- Figure 6 Activation of caspase 3 in the axonal ending of the Twitcher mouse
- Figure 7 Counting of aCasp3+ NMJ in the twitcher muscles
- Figure 8 Alteration in the subunit composition of the AchR in the Twitcher muscle
- Figure 9 Axonopathy in the Twitcher spinal cord
- Figure 10 Progressive axonal degeneration in Twitcher axons
- Figure 11 Progressive demyelination in the Twitcher mouse
- Figure 12 Early signs of axonal dystrophy in the Twitcher mouse
- Figure 13 Axonal degeneration in the Twitcher sciatic nerve
- Figure 14 Glial apoptosis in the Twitcher spinal cord
- Figure 15 Neuronal apoptosis in the Twitcher spinal cord
- Figure 16 Chromatolysis in the Twitcher mouse
- Figure 17 Decrease in diameter of Twitcher axons
- Figure 18 Prevalence of small-diameter fibers in Twitcher sciatic nerves
- Figure 19 Lower density of NFs in the Twitcher mouse
- Figure 20 Lower levels of NFs in the Twitcher mouse
- Figure 21 Reduced phosphorylation of mutant NFs
- Figure 22 Increased activity of serine/threonine protein phosphatases in Twitcher sciatic nerves
- Figure 23 Psychosine is sufficient to increase PP1 and PP2A activity in neuronal cells NSC34
- Figure 24 Psychosine induces the dephosphorylation of NFs through PP1 and PP2A
- Figure 25 Evidence of defective axonal transport in the Twitcher mouse
- Figure 26 FAT is deficient in myelinated Twitcher axons
- Figure 27 GSK3 β regulates KLC phosphorylation
- Figure 28 Activation of GSK3 β in the Twitcher nervous system
- Figure 29 Increased KLC phosphorylation in the Twitcher nervous system
- Figure 30 Psychosine induces GSK3 β dephosphorylation
- Figure 31 Psychosine induces KLC phosphorylation
- Figure 32 Psychosine in Twitcher neurons
- Figure 33 Psychosine inhibits FAT
- Figure 34 Psychosine inhibits FAT through PP1 and GSK3 β
- Figure 35 Psychosine inhibits mitochondrial transport
- Figure 36 In vivo inhibition of GSK3 β prevents KLC phosphorylation
- Figure 37 In vivo inhibition of KLC phosphorylation restores the MCV in the twitcher animal.
- Figure 38 Model of psychosine-mediated axonopathy

ACRONYMS

Ach acetylcholine
AchR acetylcholine receptor
APP amyloid precursor protein
BMT bone marrow transplant
BTX α -Bungarotoxin
CMT combined therapy
CDK5 cyclin dependant kinase 5
CKII casein kinase II
CGT Ceramide Galactosyltransferase
CNS central nervous system
Erk1 extracellular signal regulated kinase 1
Erk2 extracellular signal regulated kinase 2
FAT fast axonal transport
GALC galactosylceramidase
GalCer galactosylceramide
GSK3 β Glycogen synthase kinase 3 β
HCT Hematopoietic Cell Transplantation
HSP60 heat shock protein 60
JNK c-Jun N-terminal kinases
KD Krabbe disease
KLC kinesin light chain
KHC kinesin heavy chain
M6P mannose-6-phosphate
MBO membrane bound organelle
MMD membrane microdomain
NCX1 Sodium calcium exchanger
NF neurofilament
NFL neurofilament light subunit
NFM neurofilament medium subunit
NFH neurofilament heavy subunit
NMJ neuromuscular junction
PNS peripheral nervous system
PKC protein kinase C
PP protein phosphatase
PP1 protein phosphatase 1
PP2A protein phosphatase 2A
SAPK1 stress activated protein kinase 1
SAT slow axonal transport
sPLA2 secretory phospholipase A2
TEM transmission electron microscopy
TUNEL Terminal deoxynucleotidyl transferase dUTP nick end labeling
Wt wild type
Twi twitcher
YFP yellow fluorescent protein

CHAPTER 1 INTRODUCTION

1.1 Lysosomal storage diseases

1.1.1 Generalities

The lysosome is the degradative organelle in the cell, discovered in 1955 by De Duve. The lysosome contains a wide array of hydrolases (at least 50), with tightly regulated catalytic activity and confined to the lysosomal milieu itself. Several types of macromolecules including antigen presentation proteins, neurotransmission and signal transduction components and numerous lipids are constantly delivered to the lysosome for degradation, their components being then recycled (Luzio et al., 2007).

Lysosomal storage diseases (LSD) are a large group of genetic disorders, resulting from the dysfunction of the one or more of the lysosomal proteins (Futerman and van Meer, 2004). Frequently, the mutations affect the activity of a specific lysosomal hydrolase, leading to the accumulation of its preferred substrate. However, mutations in lysosomal cofactors or sorting proteins can also affect the lysosomal catalytic activity. Most lysosomal enzymes are ubiquitous. However, the effect of the accumulation of a lysosomal substrate depends on the cell or tissue type in which the substrate is synthesized and with a high turnover. For example, all forms of Pompe disease, which is characterized by the accumulation of glycogen, involve severe myopathy, because of the critical role of glycogen in muscle metabolism. Several sphingolipidoses are characterized by severe neuropathology, because of the high levels of sphingolipids of the brain.

The correlation between the mutations and the symptoms is often unclear. Generally speaking, the severity of the symptoms can change, depending on the residual activity of the mutated lysosomal enzyme. The most aggressive forms of LSDs are caused by complete loss of function of the enzymes, while residual activity of the enzyme results in juvenile or adult forms, which develop symptoms more slowly. The nature of the symptoms is extremely specific for each LSD, possibly depending on the type of substrate accumulated. For this reason, a common pathogenic mechanism has not been identified.

Newly synthesized lysosomal enzymes are directed to the lysosomes by virtue of the mannose-6-phosphate (M6P), a residue attached to all lysosomal enzymes. Binding of the M6P to its receptor signals for its delivery to the lysosome. Importantly, the M6P receptor is present also on the cell membrane, which allows for the uptake of lysosomal enzymes from the extracellular milieu (Sando and Neufeld, 1977; von Figura and Hasilik, 1986). This principle, called cross-correction, is the basis of most of the LSD therapies (Fratantoni et al., 1968; Olsen et al., 1981). Wild type (Wt) cells can be administered to the patients, providing a source of the missing enzyme. Despite the ability of mutant cells to uptake the therapeutic enzymes and correct the deficiency, several lysosomal storage diseases are still incurable.

1.1.2 Krabbe disease

Krabbe disease (KD) is an autosomal recessive disease, first described by the Danish neurologist Knud Haraldsen Krabbe (Krabbe, 1916). The disease was named after him and later also known as globoid cell leukodystrophy, due to the presence of multinuclear (globoid) macrophages. KD is caused by the loss of function of the *GALC* gene. This gene encodes for the lysosomal protein β -galactosyl-ceramidase (GALC), which hydrolyzes the galactosyl ester bonds

of galactolipids, including galactosylceramide (GalCer), galactosylsphingosine (also called psychosine), and lactosylceramide (Igisu and Suzuki, 1984a; Aicardi, 1993; Suzuki, 1998; Wenger et al., 2000). More than 80 different mutations in the gene have been described, leading to different forms of the disease. The classic and most aggressive form of the disease is caused by a large 30kb deletion of the gene and by multiple widespread point mutations (Luzi et al., 1995; Rafi et al., 1995; Wenger et al., 2000). Several of these mutations clearly cause the infantile form of the disease if found in homozygosis. However, some mutations appear in heterozygosis or do not have a clear correlation with the phenotype. A possible explanation is the association of apparent disease-causing mutations to polymorphic changes. Several of these polymorphisms have been identified, which appear modify enzyme activity. For example, the C502T polymorphism, which is associated to the 30kb deletion, is widespread in Europe, while the G936A polymorphism is associated with a 12-base-deletion and 3-base-insertion in Japanese patients (Rafi et al., 1995; De Gasperi et al., 1996; Wenger et al., 1997; Xu et al., 2006). The infantile form of KD is characterized by the appearance of severe neurological symptoms around 6 months after birth. During the first months of age, KD patients are usually asymptomatic, and are often misdiagnosed. Eventually, neurological symptoms develop, including muscle rigidity and atrophy, hearing and vision defects and developmental regression. If left untreated, the disease leads to the death of the patient before 2-3 years of age.

1.1.3 Pathophysiology of KD

The GALC gene is localized in the chromosome band 14q31.3 (Cannizzaro et al., 1994). The gene is 57 kb long and is organized in 17 exons, of whom one is a GC-5' untranslated region (Luzi et al., 1995). The protein is synthesized as a 80 kDa precursor protein, with six potential

glycosylation sites. The precursor is further cleaved into the active 30 and 50 kDa subunits (Chen et al., 1993). GALC expression is ubiquitous, allowing KD diagnosis to be performed by determining GALC residual activity in fibroblasts, leukocytes and serum of potential patients. Despite the widespread expression of GALC, its deficiency has a tremendous impact on the nervous system, in particular on myelin. Likely, this is owed to the high proportion of lipids in myelin (70% among glycosphingolipids, phospholipids, cholesterol and glycolipids), with GalCer being the most abundant. GalCer metabolism follows myelination, which starts in the embryo and continues in the first two decades of life, before reaching a stable state with constant turnover. Myelin turnover occurs constantly, which illustrates the dramatic outcome that GALC deficiency brings to myelination. Interestingly, GalCer accumulates only during the first period of myelin turnover, triggering one of the hallmarks of the disease: the infiltration of hematogenous inflammatory cells in the nervous system and their transformation in multinucleated globoid cells (Kozutsumi et al., 2002). As the disease progresses, demyelination continues, with apparent increase of myelinating glia cell death. Curiously, GalCer does not accumulate any longer but decreases instead. This is paralleled by a constant and rapid increase in psychosine levels in the nerve tissue (Svennerholm et al., 1980). Because psychosine proved to be a potent neurotoxin, the role of psychosine in the pathogenesis of KD led to the formulation of the so called “psychosine hypothesis”. According to this model, psychosine accumulation in myelinating glia leads to the death of these cells and the consequent loss of myelin (Suzuki, 1998).

1.1.4 Psychosine

The psychosine hypothesis is the unchallenged model of KD. This model is supported by a great number of studies, which link psychosine accumulation to demyelination. Psychosine was

first isolated and quantified from the brain of KD patients in 1980. Its concentration was estimated to be 100 fold higher than in the age matched controls, which contain only trace amounts of this lipid (Svennerholm et al., 1980). Several studies followed with evidences of the severe sensitivity of myelinating cells to psychosine. For example, psychosine induced the apoptosis of oligodendrocytes in vitro through a mechanism involving the secretory phospholipase A2 (sPLA2) and the caspases 3, 8 and 9 (Zaka and Wenger, 2004; Giri et al., 2006). These results were later confirmed by the detection of some level of apoptotic oligodendrocytes in postmortem brains of KD patients (Jatana et al., 2002). Psychosine also affected Schwann cells by inducing morphological abnormalities, process retraction and, ultimately, cell death (Hannun and Bell, 1987; Yamada et al., 1996). Because of its unknown biological function and notorious toxicity, psychosine was defined as a “mistake of Nature” (Suzuki, 1998), even if different studies indicate that psychosine biological activity is not limited to the induction of apoptosis in glia. For example, when melanocytes, a highly proliferating cell type, are incubated with psychosine, cytokinesis is inhibited, resulting in the induction of multinuclear cells. This situation closely resembles the formation of the GLD characteristic globoid cells (Kanazawa et al., 2000). Inflammatory cells also respond to psychosine by activating inflammatory pathways, leading to cytokine production and induction of nitric oxide (Giri et al., 2002; Kagitani-Shimono et al., 2005; Formichi et al., 2007; Pasqui et al., 2007; Bashir and Haq, 2011).

While many pathways appear to be affected by psychosine, how psychosine activates any of these pathways remains unknown. White et al. showed that psychosine preferentially accumulates in membrane microdomains (MMR), signaling platforms rich in sphingolipids and cholesterol (White et al., 2009; White et al., 2011). Psychosine accumulation in MMRs alters their

composition, leading to the disruption of at least some of the MMR-dependent signaling enzymes, like protein kinase C (PKC) (White et al., 2009). Because of the pleiotropic nature of signaling cascades, disruption of MMRs and of their signaling cascades by psychosine can trigger completely different effects. Thus, while the molecular steps involved in psychosine's pathogenic mechanism are still unclear, our laboratory has postulated that disruption of lipid raft-signaling may be the common initiator of variegated downstream pathways which may vary in intensity depending on the cell type and the extent of psychosine accumulation.

1.1.5 KD therapies

The possibility for treatment of KD was first shown when peripheral nerves from the Twitcher mouse, the spontaneous model of the disease, were engrafted in a wild type host. This led to increased GALC activity in the graft, and led to increased number of myelinated axons, diminished edema, and lower number of globoid cells nine months after the engraftment (Scaravilli and Suzuki, 1983). This experiment proved that the reconstitution of GALC was indeed possible in the mutant tissue. Almost all the treatments of KD were thereafter based on the principle of restoring the missing enzymatic activity and clearing psychosine. Delivery of GALC to the mutant cells is indeed possible thanks to the cross-correction, the process by which lysosomal enzymes are secreted by a cell and taken up by neighboring cells. Delivery of GALC was achieved by several experimental approaches -transplantation of hematopoietic cells (HSC) or bone marrow (BMT), delivery of viral vectors encoding for the GALC gene- with the purpose of providing a source of the enzyme inside the tissue (Hoogerbrugge et al., 1988a; Hoogerbrugge et al., 1988b; Costantino-Ceccarini et al., 1999; Luddi et al., 2001; Escolar et al., 2005; McGraw et al., 2005). From the first works on cell transplant, it became clear that the enzyme replacement

is limited, slowing but not curing the disease (Yeager et al., 1984; Ichioka et al., 1987; Hoogerbrugge et al., 1988a; Hoogerbrugge et al., 1988b). Similar results were obtained in KD newborns transplanted with cord-blood cells (Escolar et al., 2005; McGraw et al., 2005).

The need for faster and improved GALC reconstitution led to the use of retroviral-, lentiviral- and adenovirus-associated based vectors to deliver the GALC transgene (Rafi et al., 1996; Costantino-Ceccarini et al., 1999; Luddi et al., 2001; Shen et al., 2001; Dolcetta et al., 2006; Lin et al., 2011a) Of relevance, injection of GALC+ retroviral vectors in the brain of newborn P0 Twitcher pups restored up to 15% of GALC activity and cleared 55% of psychosine, leading to the amelioration of the neurological phenotype. Earlier delivery of the vector in the uterus also showed neurological improvement, although long-term neurological symptoms occurred (Shen et al., 2001; Shen et al., 2005).

Ultimately, the various therapeutic strategies used so far have not been successful to halt the appearance of neurological symptoms in KD. The difficulties faced to treat KD, led the Bongarzone lab to start working on combining therapies for KD. In 2006, Dolcetta and Bongarzone produced and optimized the first lentiviral vector to express the murine GALC cDNA. This vector showed to permanently transduce all three neural cell types and to increase levels of GALC in the brain of the Twitcher mouse. However, intracranial treatment of Twitcher mice with this vector alone showed to be restricted to areas of injection and did not spread sufficiently in the rest of the nervous tissue, leading to minor improvement on the overall phenotype (Dolcetta et al., 2006). The GALC lentiviral vector was used in combination with BMT and showed to partially restore myelin and increase activity of GALC (up to 30%) in brain, spinal cord and sciatic nerves (Galbiati et al., 2009b). But even with this combined therapy, the

treated mutants survived to about 130 days, after which they developed neurological symptoms and died.

Altogether, the various strategies for therapy in KD have been disappointing. The accumulated experience from these studies points to: i) the delivery of the enzyme does not occur rapidly and vastly enough to correct for the enzyme deficiency before psychosine accumulates to toxic levels and ii) unidentified pathogenic mechanisms may be limiting the clinical value of the therapies. In these circumstances, the Bongarzone lab proposed a novel mechanism of axonal and neuronal dysfunction, which might contemporaneously compound demyelination in KD.

1.1.6 Primary vs Secondary Neurodegeneration in KD

Over the years, several research groups considered that the rapid deterioration of nerve conduction velocity and the onset of motor/cognitive phenotype affecting KD are primarily the consequence of myelin loss (i.e. secondary neurodegeneration). However, sporadic case reports detected signs of axonal and neuronal stress (Sourander and Olsson, 1968; Kurtz and Fletcher, 1970; Schlaepfer and Prensky, 1972; Duchen et al., 1980; Kobayashi et al., 1980; Jacobs et al., 1982; Nagara et al., 1982; Ohno et al., 1993; Matsushima et al., 1994; Taniike et al., 1999; Wu et al., 2000; Galbiati et al., 2007; Galbiati et al., 2009a). For example, large diameter axons are reduced in numbers in the Twitcher mouse but the cause for this was never explained (Jacobs et al., 1982). This deficiency in large axons was also noticed in some sural nerve biopsies from human patients (Schlaepfer and Prensky, 1972). Deficiency of large caliber axons may also contribute to slow nerve conduction. The Twitcher mouse also suffers of abnormal postural reflexes, grasp, limb strength, and some motor deficiencies at young age (Olmstead, 1987). Our own laboratory showed that a defective sympathetic innervation affects lymphoid organs such as

the thymus (Galbiati et al., 2007). In the latter study, it is relevant to note that most of the axons innervating lymphoid organs are unmyelinated, which hinted to the possibility that myelin-independent axonal defects may occur in this disease (i.e. primary neurodegeneration).

The importance of primary neurodegeneration in KD is also illustrated by recent works from our laboratory showing that a combination of BMT and lentiviral gene therapy for GALC was insufficient to prevent axonal damage in Twitcher mice (Galbiati et al., 2009b). Considering that neurons and axons develop before myelination of the nervous system, the timing for GALC correction could not be more critical: even when BMT is practiced on newborn KD animals, it takes about 30-40 days for donor derived cells (which can produce GALC) to infiltrate the nervous system (Wu et al., 2000; Galbiati et al., 2009b) and to start enzymatic cross-correction of host cells. We speculate then that by the moment donor cells arrive to the nervous system, extensive and likely irreparable damage occurred to neurons and axons. With this idea in mind, a new set of mechanistic questions was generated to understand the pathogenic mechanism mediating these defect.

1.2 The neuron and the importance of axonal stability.

1.2.1 Generalities

The neuron is one of the most polarized cell types of the body, with defined functional domains: the cell body (soma), the axon, the dendrites and the synapses. The axon alone represents 99% of the total cell volume, and can be very long (up to one meter long, in the case of some spinal cord motoneurons). Since most of the synthetic machinery is limited to the cell body, the neuron faces the unique challenge of constantly supplying the distant compartments with structural and functional components. Neurons therefore rely on a complex system of intracellular

transport, which constantly delivers vesicles and molecules to distant sites. The delivered molecules can reside along the axons for several weeks before reaching their final destination. Consequently, several neuronal proteins have an extremely long half-life to avoid degradation during transiting the axon. For example, neurofilaments (NFs), cytoskeletal proteins which provide mechanical resistance and diameter to the axon, are extremely resilient to proteases and can be detected in the cerebrospinal fluid after neuronal damage (Lycke et al., 1998; Malmstrom et al., 2003).

1.2.3 Neuronal cytoskeleton

The neuronal cytoskeleton has been the object of intense study for its critical role in neuronal development, maintenance and survival (Nixon and Shea, 1992; Perrot et al., 2008). The neuronal cytoskeleton is composed of microtubules, microfilaments and NFs. This work will focus on NFs, because of their critical role in axonal diameter and axonopathy.

NFs are neuron-specific intermediate filaments, and are among the most abundant of cytoskeletal components of the vertebrate myelinated axon. NFs are a combination of peripherin, α -internexin and the three forms of NF: the ~60 kDa subunit (NFL), the ~100 kDa subunit (NFM) and the ~120 kDa subunit (NFH) (Julien and Mushynski, 1998). NFs have a N-terminal head domain, a central α -helical core and a C-terminal tail. Individual subunits form parallel dimers, and two staggered dimers form anti-parallel tetramers by associating in their central core. Eight tetramers assemble to form 60 nm long filaments, which further assemble end to end (Angelides et al., 1989; Heins et al., 1993). During assembly, NFL functions as seeding subunit, on which NFM and NFH assemble. Contrarily to microtubules, NFs lack polarity. NFM and NFH tail

domains radiate outward from the NF bundle. The tails are enriched in Lys-Ser-Pro (KSP) repeats, which are phosphorylated during development to generate repulsive forces.

1.2.3 Expression of NFs

NF expression and phosphorylation are tightly regulated during development to ensure the proper development of the axon, as well the right targeting and positioning of the nerve endings (Nixon and Shea, 1992). Peripherin and vimentin, which also belong to the NF family, are expressed during neuritogenesis, remain high during axonal development and are progressively replaced by the expression of NFL. NFM expression then follows during axonal growth, while NFH expression is prompted by synaptogenesis (Willard and Simon, 1983; Carden et al., 1987). After synaptogenesis, the expression of the three main NF subunits peaks and remains constant during neuronal life. Despite few differences in the animal models, a body of work shows that NF expression pattern is tightly regulated at both the transcriptional and translational level and strongly depends on the successful development of the axons. When the nerve is damaged, a regenerative process starts, which recapitulates the developmental regulation of NFs (Hoffman et al., 1985; Hoffman, 1988; Muma et al., 1990). After nerve damage, the mRNAs of the three NF subunits decrease, while peripherin and vimentin expression increase, to allow for neurite regeneration. During neurite outgrowth, the expression of the three NF subunits increases (Goldstein et al., 1988; Oblinger et al., 1989b; Oblinger et al., 1989a). These changes seem to depend also on the ability of the neurite to reach for the appropriate nerve target. For example, NFM expression does not occur in frog regeneration optic axons and lamprey spinal tracts if the axons do not follow the appropriate paths or do not reach their synaptic target (Zhao et al., 1995).

1.2.4 Phosphorylation of NFs

NFs are regulated by several post-translational modifications, such as phosphorylation, glycosylation, nitration, oxidation and ubiquitination (Perrot et al., 2008). Phosphorylation of NFs has been studied the most, as it is critical in almost all the biological functions of NFs. NFs are phosphorylated on their N-terminal heads and C-terminal tails on specific phosphorylation sites (Julien and Mushynski, 1982, 1983). Several serine/threonine phosphorylation sites were identified on both termini of NFs, although the tails contains up to 51 KSP repeats, which makes NFs the most phosphorylated proteins of the axon (Julien and Mushynski, 1982). NF phosphorylation follows a regulated topographic pattern. The heads are phosphorylated immediately after synthesis in the cell body, while the tails are phosphorylated mostly after their entry in the axonal compartment (Sternberger and Sternberger, 1983; Glicksman et al., 1987; Oblinger et al., 1987).

The overall levels of NF phosphorylation are the result of the balanced activities of protein phosphatases, mainly protein phosphatase 2A and 1, and of kinases, mainly cyclin dependant kinase 5 (CDK5), glycogen synthase kinase 3 β (GSK3 β) and casein kinase 1 and 2 (CK1 and CK2, respectively) (Floyd et al., 1991; Saito et al., 1995; Veeranna et al., 1995; Strack et al., 1997a; Nakamura et al., 1999; Brownlees et al., 2000). Balancing the activity of these two groups allows the neuron to spatially and temporally regulate NF phosphorylation.

1.2.5 NFs influence axonal caliber

NFs are pivotal in the radial growth of the axon, which occurs during axonal development to increase the conduction velocity of the electrical impulse. The link between NFs and axonal radius was first hinted by studies correlating NF numbers and densities, localization of NFs along

the axon and increased axonal calibers (Friede and Samorajski, 1970; Hoffman et al., 1984). The current model states that phosphorylation of KSP repeats generates high density of negative charges around the NF bundles, which then produce strong radial repulsive forces. These forces would then help in the radial expansion (i.e. increasing caliber) of the axon. This model has been supported by several observations. Weak repulsive forces are detected by atom force microscopy around the core (Brown and Hoh, 1997). These forces are absent when the side arms are enzymatically removed or dephosphorylated (Kumar and Hoh, 2004). Furthermore, disruption of the NFM gene or expression of a NFM gene with the deletion of its C-terminal (NFM^{tailΔ}) results in higher NF density and decreased axonal diameter (Garcia et al., 2003; Rao and Mayor, 2005).

The nerve conduction velocity depends on axonal caliber, internodal length and myelin thickness. Since internodal length and myelin thickness are directly proportional to axonal caliber, the regulation of NF phosphorylation has a tremendous impact on the speed of the action potential. For this reason, myelination and axonal radial growth are tightly regulated. Signals between the myelinating processes and the axon regulate NF phosphorylation and the radial growth of the axon. Any interference in this process might lead to alterations in the axonal radial growth. For example, loss of NF phosphorylation correlates with higher NF density and decreased axonal diameter in the dysmyelinating mouse model Trembler (de Waegh and Brady, 1991; de Waegh et al., 1992).

1.2.6 Axonal transport

Axonal transport is an extremely complex mechanism for the sorting and delivery of molecular cargoes and compounds to different cellular domains in the neuron. Axonal transport is divided in a slow and a fast component. Slow axonal transport (SAT) delivers microtubules and

neurofilaments at a rate of 0.2-1 mm per day and microfilaments and cytosolic proteins at 0.8-6 mm per day. Fast axonal transport (FAT) delivers Golgi-derived vesicles, endosomes, pre-lysosomes and autophagosomes at a rate of 100-400 mm per day (for a detailed review, see (Brown, 2003). Several organelles can have specific modes of transport. For example, synaptic vesicles move continuously along the axons, while mitochondria frequently stop and re-start, following a saltatory mode of movement (Lorenz and Willard, 1978; Grafstein and Forman, 1980; Morris and Hollenbeck, 1993; Ligon and Steward, 2000).

Axonal transport is based on a great variety of molecular motors, which move directionally along the axons by following microtubule polarity. Kinesin moves towards the positive end of microtubules, while dynein towards the negative end (Goldstein and Yang, 2000; Karcher et al., 2002). This work will focus on the effect of GALC deficiency on kinesin regulation.

Kinesin was first identified in axoplasm preparations and was then isolated as a heterotetramer consisting of two heavy chains and two light chains (Vale et al., 1985). Kinesin heavy chains (KHC) have a globular N-terminal domain which mediates microtubule binding and ATP hydrolysis. The central core forms a α -helical coiled-coil domain, necessary for dimerization. Kinesin light chains (KLC) mediate the binding of the motor complex to the transported cargo, either directly or through scaffolding proteins (Verhey et al., 1998). Once kinesin binds to its cargo and to a microtubule, ATP hydrolysis causes the change in the conformation of the KHC globular domain, so that kinesin processively walks along the microtubule (Yildiz et al., 2004).

How the neuron regulates the specific delivery to the right subcellular domain is still under investigation. It has been proposed that post-translational modifications of the kinesin

chains regulate the activity of the motor (Brady, 1995). One of such modifications is phosphorylation. Phosphorylation on specific epitopes on KLC or KHC regulates the binding to a specific cargo and the binding to microtubules. Therefore, the cross-talk between the phosphotransferase activity of the neuron and the different kinesins influences where and when the motor halts and releases its cargo. The neuron employs this system to deliver specific cargoes to discrete axonal subdomains. For example, synaptic vesicles are delivered to synapses, while ion channels are delivered to nodes of Ranvier. By controlling the localization of specific phosphotransferases, like GSK3 β , PKC, CKII or JNK, neurons control the delivery of specific cargoes to their functional domains (Morfini et al., 2002b; Morfini et al., 2004; Morfini et al., 2006; Morfini et al., 2007a; Pigino et al., 2009). For example, PP1 activation induces the decrease in CDK5 activity. This, in turn, causes the decrease in the inhibitory phosphorylation of GSK3 β . Active GSK3 β then directly phosphorylates KLC, inducing the release of its cargo. Interestingly, GSK3 β is associated with transported vesicles, suggesting that some regulators travel with along with kinesin. By localizing PP1 and CDK5 in sites of active delivery (e.g., the growth cone), GSK3 β -mediated KLC phosphorylation and the cargo release can be quickly triggered. Curiously, the GSK3 β phosphorylation of KLC is dependent on CKII phosphorylation of an adjacent phosphoepitope, which indicates that the cell can regulate kinesin activity by orchestrating different kinases.

1.2.7 Axonal transport defects: the dysferopathies

The complexity of the neuronal architecture and size highlights the tremendous importance of axonal transport for neuronal survival. A significant body of evidence links defects in axonal transport to several, seemingly unrelated, neuropathies. Specifically, defects in either

the amounts or the proper regulation of the molecular motors are sufficient to impair the ability of the neuron to supply its distal compartment, ultimately causing synaptic loss and axonal damage. These diseases have been collectively called dysferopathies (from the Greek 'phero', to carry or transport), as they all have defects in axonal transport.

As an example of the functional relevance of axonal transport, mutations in Kinesin-1A and Kinesin-1B lead to forms of hereditary spastic paraplegia and Charcot-Marie-Tooth, respectively (Zhao et al., 2001; Reid et al., 2002). Importantly, several kinases, which regulate transport, are over-activated in neuropathies and appear to cause altered activities of kinesin. For example, some presenilin-1 mutations, which can lead to Alzheimer's disease, increase GSK3 β activity, leading to KLC phosphorylation and increased detachment of its cargoes (Kanaan et al., 2011). Similarly, in Huntington's disease and in spinal bulbar muscular atrophy, the stress-activated protein kinase JNK3 is overactivated, which also leads to KLC phosphorylation and cargo release (Morfini et al., 2006; Morfini et al., 2009a).

The importance of these alterations in the motor-associated signaling stems from the subtle but significant damages that can build up along the affected axons over time. If kinesin activity is deregulated, focal blockades of transport may occur, resulting in the local accumulation of unsorted material. Axonal swellings and varicosities may eventually appear which are followed by axonal damage and breakdown. The detection of such morphological changes was made possible by the employment of electron microscopy and a new generation of fluorescent reporter genes, which are expressed only in subsets of axons (Feng et al., 2000; Tsai et al., 2004; Coleman, 2005; Castelvetti et al., 2011). The fine imaging of the neurites in these models revealed that these morphological changes –altogether named “axonal dystrophy”- occur early in the disease, before the onset of the symptoms. Importantly, the cell death machinery that mediate apoptosis of

neurons, does not seem to play a role in this type of axonal damage. In fact, inhibition of apoptosis, either genetically or pharmacologically, does not prevent axonal dystrophy and axonal retraction (Sagot et al., 1995; Burne et al., 1996; Whitmore et al., 2003). In contrast, the lack of supply to the distant synapses causes their shutdown and, if the defect is not corrected, axonal retraction (Kornek et al., 2001; Tsai et al., 2004; Coleman et al., 2005). Indeed, several neuropathies show such a mode of axonal degeneration –called “dying-back”- in which synaptic loss and retraction of the axonal endings are the causes of the symptoms and in which cell death plays a secondary role.

1.3 The importance of the synapse for the neuron and its targets: the neuromuscular junction

The importance of the synaptic contact for neuronal survival can be exemplified by the studies on the neuromuscular junction (NMJ), the synaptic connection between the motoneuron and the skeletal muscle. The NMJ is formed by two components: the presynaptic nerve terminal which releases the neurotransmitter acetylcholine (Ach), and the postsynaptic endplate, the specialized muscle membrane enriched in Ach receptors (AchR). The development of NMJs is a multistep process which requires the precise coordination between the developing nerve fibers and the growing muscles.

The development of the mouse NMJ starts during the embryonic life (E12-E14) and progresses until the second postnatal week. Several neuronal and muscular factors regulate NMJ development. Of these, Ach seems fundamental for the development of both the innervating neuron and the muscle fiber, called myofibril (Oppenheim, 1984; Kablar et al., 1999; Kablar and Rudnicki, 1999; Heeroma et al., 2003). The first connections are established after the AchRs

cluster on the center of the developing myofibril (Mishina et al., 1986; Witzemann, 1989; Witzemann et al., 1989). While this process is largely under the molecular control of the muscle, it is also critical for the development of the nerve. Several nerve endings contact the patch of AchRs, which represent the rudimentary endplate (Ontell and Kozeka, 1984). However, these multiple contacts are progressively lost in favor of individually innervated myofibers (Brown et al., 1976; Betz et al., 1979). Importantly, Ach seems critical for this selection, as the increased activity of neurotransmission in one of the fibers results in the negative selection of the supernumerary ones. During this selection period, the neuronal fiber with the highest electrical activity induces the retraction of the excessive nerve endings from the endplate (O'Brien et al., 1978; O'Brien and Vrbova, 1978; Thompson et al., 1979; Thompson, 1983; Henneman, 1985). The release of a limited supply of survival factors from the muscle further stabilizes the connection (English and Schwartz, 1995; Kwon and Gurney, 1996; Snider and Silos-Santiago, 1996). At the end of the second postnatal week through adulthood, every endplate will be innervated by a single, functional nerve ending.

The molecular composition of the AchR plays a major role in the selection of the innervating neuron. The fetal Ach receptor is composed of five subunits (two α , one β , one δ and one γ subunit) (Sakmann, 1978; Mishina et al., 1986; Numberger et al., 1991). The γ subunit is particularly important because it allows the muscle to spontaneously contract, which is critical for the growth of the muscle (Numberger et al., 1991; Duclert and Changeux, 1995). After the nerve ending contacts the muscle membrane, the sustained release of Ach from the nerve terminal triggers a switch in gene expression from the γ isoform to the homologous, Ach-dependent ϵ isoform (Numberger et al., 1991; Duclert and Changeux, 1995). The ϵ receptor is considered the adult form of the AchR and is expressed by most skeletal muscles after P20 (Witzemann et al.,

1996). However, the γ subunit can be re-expressed if the activity of the NMJ is compromised. Re-expression of the γ subunit is observed in the adult muscle if the relative nerve is transected, a condition that causes the retraction of the innervating axons and, consequently, the functional decoupling of neuron and muscle (Witzemann et al., 1989; Li et al., 2008; Kong et al., 2009). The sharp decline in the Ach release and in the electrical activity of the NMJs induce the upregulation of the fetal AchR. The reappearance of the AchR possibly represents a mechanism to allow for the reestablishment of new NMJs. Consistently with this idea, the expression of the γ isoform following denervation disappears if the transected fibers regenerate and reestablish the NMJ (Witzemann et al., 1989; Li et al., 2008; Kong et al., 2009).

1.3.1 Regulation of the muscle growth

The change in NMJ activity significantly affects the development and the growth of the muscle. During the innervation of the skeletal muscle, the myofibrils undergo extensive growth. Because 70% of the fiber volume is represented by myofibrillar proteins, the overall growth of the fiber is the result of the balance between protein synthesis and degradation. Conditions leading to increased muscle activity, e.g. repeated contraction and stretching, significantly increase protein synthesis over protein degradation. The outcome is the strong increase in protein synthesis and, consequently, in muscle mass (hypertrophy). Inactivity has the opposite effect, shifting the balance from synthesis to degradation and causing a decrease in muscle mass (atrophy). Although the molecular mechanisms of this balance are not fully understood, the protein kinase AKT has been identified as an important molecular switch between muscle hypertrophy and atrophy (Cho et al., 2001; Gosmanov et al., 2004; McCurdy and Cartee, 2005; McCurdy et al., 2005). Repeated contraction of the muscle induces the phosphorylation and activation of AKT at serine 473

(Ser473) and threonine 308 (Thr308) (Funai et al., 2006; Haddad and Adams, 2006). This has two consequences. First, active AKT phosphorylates the transcription factors FOXOs. FOXOs transcription factors control the expression of several muscle-specific ubiquitin ligases, like muscle ring finger 1 (MURF1) and muscle atrophy F-box (MAFbx, also known as atrogin-1) (Sandri et al., 2004; Stitt et al., 2004). These enzymes add the polypeptide ubiquitin (Ub) to proteins. Ubiquitinated proteins are marked for degradation by the proteolytic complex known as proteasome. Phosphorylation of FOXO proteins by AKT sequesters them in the cytoplasm, preventing them from reaching the nucleus and increasing the expression of MURF1 and atrogin-1. By preventing the expression of Ub ligases, AKT decreases protein degradation. On the other hand, active AKT phosphorylates the mammalian target of rapamycin (mTOR), and GSK3 β . Both proteins phosphorylate components of the translation machinery, therefore regulating the efficiency of the translation of mRNAs in the muscle cells. mTOR and GSK3 β phosphorylation by AKT significantly increases the rates of protein synthesis. AKT regulation of muscle mass has received increasing attention in the recent years, because of its role in both healthy and diseased muscle. Several pathological conditions, like cancer, renal failure and motoneuron diseases lead to muscle atrophy. In particular, diseases affecting motoneuron survival and function, like ALS, spinal muscular atrophy (SMA) and sarcopenia, lead to decrease in NMJ activity and, consequently, to muscle inactivity and atrophy (Paturi et al.; Leger et al., 2006a; Millino et al., 2009). The AKT pathway, together with the its downstream effectors FOXOs, mTOR, and atrogin-1 seem to be the molecular mediators of the observed atrophy (Dobrowolny et al.; Bodine et al., 2001; Leger et al., 2006b; Leger et al., 2006a; Millino et al., 2009). An important aspect of these observations is that AKT activity might be downregulated even in the absence of clear neuronal pathology. In particular, dephosphorylation of AKT and nuclear translocation of FOXO

proteins are observed in skeletal muscles of mouse models of ALS (Leger et al., 2006a). The trigger of muscle atrophy is not the loss of motoneurons, because protection of the neuronal soma does not prevent the pathology in the axons and the NMJs. Indeed, subtle changes in muscle stability might occur before clear signs of denervation (Dobrowolny et al., 2011).

In conclusion, the NMJ represents a clear example of how the synaptic connection is fundamental for the physiology of the neuron and its synaptic target. Conditions that affect the NMJ can easily compromise the survival of both neurons and muscle cells, leading to the dysfunction of the neuromuscular units.

1.4 The Twitcher mouse: the murine model of KD

The Twitcher mouse is a spontaneous animal model of KD, first discovered in 1976 in the Jackson Laboratory. The mutation in the GALC gene (*twi*) is autosomal recessive and causes premature degradation of GALC mRNA, leading to the complete loss of function of the gene (Kobayashi et al., 1980). The mutant appears normal during the first two weeks of life. The first neurological symptoms appear around 20 postnatal days (P20), with inactivity and tremor, in particular of the head and the lower limbs. The size of the mutant is generally smaller and progressive weight loss is observed before the onset of the symptoms. Mutants do not survive past P45. Histological evaluation revealed that the Twitcher pathology resembles the human disease, with widespread demyelination, axonal degeneration and inflammation (Duchen et al., 1980; Nagara et al., 1982; Takahashi and Suzuki, 1982; Takahashi et al., 1983; Mikoshiba et al., 1985; Nagara et al., 1986). The characteristic multinucleated globoid cells are typically observed, especially around the brain capillaries (Duchen et al., 1980). Finally, the accumulation of psychosine was demonstrated for both CNS and PNS and was found to correlate with the severity

of the disease (Igisu and Suzuki, 1984a, b; Shinoda et al., 1987). The Twitcher mouse therefore represents a reliable model of KD, and it has provided an invaluable tool to study the effect of GALC deficiency on the nervous system.

Several works point out the occurrence of axonal defects in both CNS and PNS of the mutant (Krabbe, 1916; Sourander and Olsson, 1968; Dunn et al., 1969; Schlaepfer and Prensky, 1972; Baker et al., 1990). Despite of the acceptance of axonal abnormalities in this mutant, the study of this aspect has remained neglected. However, in the past years the Bongarzone laboratory observed that neurodegeneration might be a critical determinant of the Twitcher symptomatology. For example, Galbiati et al., showed that the loss of innervating fibers of the thymus are the likely cause of the thymic atrophy of the Twitcher, which has severe consequences on the production of lymphocytes (Galbiati et al., 2007). It is possible that other organs might be similarly affected. The skeletal muscle is particularly interesting, because myofibers require a constant electrical input from neurons to survive and grow. Actually, the Twitcher mouse is affected by muscle weakness, which further develops in paralysis of the lower limbs and difficulty in feeding. It is possible that a defect in the innervating fibers might influence the muscles of the mutant. In line with this idea, a reduction in MCV is observed in the sciatic nerve before the onset of demyelination (Dolcetta et al., 2005; Smith et al., 2011). Because the propagation of the electrical impulse also depends on the diameter of the axon, the propagation defect can also be caused by the decrease in diameter of the Twitcher fibers (Jacobs et al., 1982). No fiber loss is apparently observed in twitcher nerves (Jacobs et al., 1982). This suggests that the axonal defects compromise the ability of the axon to sustain its functions. In recent years, several neurodegenerative diseases have been described, with a similar axonal dysfunction in the absence of neuronal loss. In these diseases, defects in the supply mechanisms of the axon have been

observed. Defects in FAT or in the axonal cytoskeleton are of special interest, because they can affect axonal stability and synaptic transmission in the absence of apparent histological changes. In the specific case of the Twitcher mouse, we have no knowledge of the effect of GALC deficiency on the axonal supply machinery.

In summary, some of the neurological defects in Krabbe disease appear to rely on axonal and neuronal dysfunction. The pathogenic mechanisms mediating these defects have remained unclear. We think that psychosine may exert deleterious defects on multiple levels, which may include deregulation of axonal stability, leading to muscle wasting and atrophy as seen in the twitcher mutant. With these background, we propose to explore various aspects of axonal degeneration in Krabbe disease, using the twitcher mouse as our experimental model.

CHAPTER 2 RATIONALE & AIMS

Therapeutic targeting demyelination provides little benefit to animal models and patients with KD, showing the need for new insights into the pathological mechanisms of this disease. Experimental evidence indicates the existence of an early neurodegenerative component, which appears independent of demyelination (Galbiati et al., 2007; Galbiati et al., 2009b). The existence of an early neuronal insult, which apparently and irreversibly affects axonal function, represents a serious obstacle to the current therapies. Because the mechanisms mediating neurodegeneration in KD have remained unaddressed, my study will focus on the characterization of the temporal and anatomical progression of neurodegeneration and the identification of the pathogenic mechanisms using the Twitcher mouse as an animal model of KD.

The hypothesis of this study is that increasing concentrations of psychosine trigger a direct insult to mutant axons, by altering the signaling regulating two critical components of neurons: the neurofilament cytoskeleton and fast axonal transport.

The hypothesis was tested through the following aims:

1) To determine whether neurodegeneration in KD is a dying-back neuropathy, characterized by synaptic loss and axonal retraction.

2) To determine the condition of the neurofilament cytoskeleton and its role in axonal maturation of KD.

3) To determine if fast axonal transport is defective in KD.

CHAPTER 3 EXPERIMENTAL DESIGN

Goal 1. To determine the extent of synaptic loss in KD. This analysis determined the number of denervated or degenerating neuromuscular junctions (NMJs) of the soleus muscles by immunostaining for Alexa-555 conjugated α -bungarotoxin (to label the acetylcholine receptors) or for active caspase 3. The analysis was conducted on the TWI-YFPax, a Twitcher mouse model expressing yellow fluorescent protein (YFP) in subsets of spinal cord motoneurons, which allows YFP tracing of axons. RT-PCR analyses for the main isoforms of the acetylcholine receptor were performed to understand whether the expression of receptor subunits was affected by denervation. The activation of the atrophic pathway AKT/GSK3 β /ubiquitin was examined to elucidate the extent of muscular atrophy induced by the loss/dysfunction of NMJs.

Goal 2. To assess the role of neuronal loss in KD. Apoptosis of the neuronal soma is considered a late event in dying-back neuropathies. To measure for apoptotic neurons, stereological quantification of dying (TUNEL+) neurons (NeuN+) was performed on coronal sections of P7, P15 and P30 WT and Twitcher spinal cords. Cords were also stained using the Nissl technique to determine soma degeneration chromatolysis.

Goal 3 To determine the density of the NF cytoskeleton in KD. Transmission electron microscopy was performed on coronal sections of P12 and P35 WT and Twitcher sciatic nerves and the density of NFs was measured. The diameter of the fibers was also measured and compared to the NF density.

Goal 4 To determine the amount and phosphorylation levels of the major NF subunits.

Spinal cord and sciatic nerves of P7, P15 and P30 Wt and Twitcher animals were processed by immunoblotting to measure for total and phosphorylated NFM and NFH. Immunohistochemistry for these NFs was also performed on P30 Wt- and Twi-YFPax cords and sciatic nerves.

Goal 5 To assess the involvement of PP1 and PP2A in NFs dephosphorylation in KD.

Protein lysates and longitudinal sections from sciatic nerves of P7, P15 and P30 Wt and Twitcher mice were processed to determine the enzymatic activity (colorimetric assay) and distribution of PP1 and PP2A (immunohistochemistry).

Goal 6 To measure the efficiency of anterograde FAT in KD peripheral nerves.

For this, ligations of sciatic nerves in P7 and P30 Wt and Twitcher live mice were performed. After 2 hours, the proximal and distal stumps (relative to the spinal cord) and the non-ligated controlateral sciatic nerve were processed for immunoblots for antibodies against cargo markers. Band intensity was quantified with ImageJ and normalized against that of the loading control.

Goal 7 To determine whether FAT inhibition in KD is caused by deregulated

phosphorylation of kinesin. To check for changes in phosphorylation of motors, lysates of P7, P15 and P30 Wt and Twitcher spinal cords and sciatic nerves were immunoblotted with antibodies against total and a phospho-sensitive KLC epitope recognized by the monoclonal antibody 63-90. In addition and because the 63-90 epitope is phosphorylated by GSK3 β , we analyzed for the activation of this kinase by immunoblotting for total and phosphorylated (inactive) GSK3 β .

Goal 8 To determine whether psychosine is a pathogenic compound that deregulates NF phosphorylation. To examine this question, we focused on the effect of psychosine on protein phosphatases 1 and 2A (PP1 and PP2A). For this, phosphatase activities were measured in lysates from NSC34 cells after treatment with psychosine in the presence and absence of phosphatase inhibitors. This analysis was complemented with immunoblotting for total and phosphorylated NFs.

Goal 9 To determine whether psychosine is a pathogenic compound that deregulates FAT. To address this question two in vitro assays were performed. First, squid axoplasm preparations were incubated with psychosine and vehicle. The transport rates of cargoes were measured by optical microscopy. Second, the effect of psychosine on movement of mitochondria was measured in NSC34 cells after in vivo labeling with Mitotracker Green. Both experimental settings were used in the presence or absence of specific kinase and phosphatase inhibitors, to determine which phosphotransferase enzyme/s mediates the psychosine's effect on FAT.

CHAPTER 4 MATERIALS AND METHODS

4.1 Cell cultures

Cell cultures of cortical neurons were prepared as previously described (Kaech and Banker, 2006). Briefly, E16 pregnant females were sacrificed, the brains of the litter were collected and the cortex was isolated. The cortices were chopped as finely as possible, treated with 0,25% trypsin and then passed through a fire polished pipette. The cells were then plated in DMEM (Mediatech) supplemented with 10% (w/v) fetal bovine serum (FBS) and, after 2 hours, the medium was changed to Neurobasal medium supplemented with 1X B27. NSC34 cells were grown in DMEM supplemented with 5% (w/v) FBS, L-glutamine (Gibco) and penicillin/streptomycin (Gibco). For the experiment, the cells were serum deprived for 12 hours before the addition of the different treatments. Psychosine and D-sphingosine were purchased from Sigma and resuspended in ethanol to the desired concentration. For the treatment with okadaic acid, the inhibitor was added together with psychosine. For the treatment with TDZD8, the inhibitor was added 30 minutes prior to addition of psychosine. Both inhibitors were purchased from Calbiochem.

4.2 Mitochondria labeling and time lapse microscopy

The treatment of the cells with the different sphingolipids was performed as described above. After the treatment, the cells were incubated for 20 minutes at 37 °C with 75 nM Mitotracker G (MTG; Invitrogen) in growth media. At the end of the incubation, the medium was replaced with fresh media, and the recording was performed by taking a picture every 10 seconds for 5 minutes. The number of mitochondria sprinting along the neurites was counted.

4.3 Tissue collection, histology, and immunohistochemistry

Animals were anesthetized and perfused with saline. Tissues for psychosine determination, and immunoblot were frozen in liquid nitrogen. Tissues for immunohistochemistry and regular histology were postfixed in 4% paraformaldehyde/phosphate buffer saline (PBS) for 18 h, embedded in sucrose, and embedded in OCT. Appropriate blocks of tissue were separated and processed for electron microscope imaging. Cryosections (50 μm for muscle sections, 20 μm for sciatic nerve and spinal cord sections) were mounted onto superfrost slides. For immunofluorescence staining, sections were dried for 15 minutes at 37°C, and washed in PBS. The sections were blocked/permeabilized in 5% (w/v) bovine serum albumin, 0.5% (v/v) Triton X-100/PBS for 1 h at room temperature and incubated with primary antibodies (diluted in 2% BSA (w/v), 0.5% (v/v) Triton X-100/PBS buffer) for 12 hours at 4°C, with mild agitation. The following antibodies were used: NeuN (Abcam; 1:100), phosphorylated NF-M/NF-H (1:1000; SMI31R, Covance), dephosphorylated NF-MNF-H (1:250; SMI32, Covance) and active caspase 3 (1:250; Cell Signaling). For neuromuscular junction staining, muscle sections were blocked/permeabilized in 4% (w/v) BSA/0.1% (v/v) Triton/PBS for 2 hours at room temperature, incubated with a NF-H antibody (Cell Signaling; 1:250) and then with Alexa Fluo 488 αBTX (Invitrogen; 1:500) in blocking solution for 48 hours. Slides were rinsed in PBS and incubated with fluorescent secondary antibodies (Alexa 488) for 1 h at room temperature, washed in PBS and mounted with Vectashield (Vector, Burlingame, CA). Confocal microscopy was performed using a confocal laser Meta Zeiss scanning microscope. Terminal deoxynucleotidyl transferase dUTP nick end labeling (TUNEL) assay was performed according to the manufacturer instructions (Roche). Briefly, sections were dried at 37°C, washed in PBS and permeabilized in 0.1% Triton X-100, 0.1% Na Citrate in PBS on ice for 2 minutes. Slides were incubated with

terminal transferase and labeled for 60 min at 37°C mounted with permount. In some experiments, sections were colabeled with antibodies against NeuN.

For light microscopy immunostaining, cryo-sections were treated with 0.3% (v/v) H₂O₂ 10% (v/v) methanol/PBS and then blocked/permeabilized with 0.1% (w/v) casein, 0.1% (v/v) Triton X-100 in PBS for one hour. Sections were incubated with antibodies against PP1 (PP1E9; 1:100; Santa Cruz) and PP2A (1:100; Cell Signaling) and developed with biotinylated secondary antibodies (Vectastain).

4.4 Stereology

For unbiased stereological studies on the spinal cord motoneurons, 30- μ m-thick spinal cord cross sections were selected (one every 10 sections) and stained accordingly. Quantification of positive cell markers was performed with design-based stereology system (StereoInvestigator version 8, MBF Bioscience, Williston, VT, USA). Briefly, the spinal cord ventral horns were traced under a 5X objective and TUNEL+ motoneurons were counted under 63X objective (Zeiss AX10 microscope, Carl Zeiss Ltd., Hertfordshire, England). The sampling parameters were set up according to the software guide to achieve the coefficient of error ranged between 0.09 and 0.12 using the Gundersen test, normally a counting frame size 100 x 100 μ m, optical dissector height 20 μ m, and an average of 10 sampling sites per section were chosen.

4.5 Western blotting

Tissues were homogenized in lysis buffer (1 mM PMSF, 2 mM sodium orthovanadate, 1 mM NaF, 20 mM Tris HCl pH 7.4, 1% (v/v) Triton X-100, 150 mM NaCl, 5 mM MgCl₂, 300 nM okadaic acid). Samples were briefly sonicated on ice and spun down for 5 minutes at 5000 rpm.

Protein concentration in the supernatant was quantified with the Bradford assay (Biorad) and equal amount of proteins were loaded on 4–12% Bis–Tris gels (Invitrogen). Proteins were transferred onto a polyvinylidene fluoride (Biorad). Blots were blocked in 5% milk, 1% BSA, 0.05% Tween 20 in TBS (blocking solution) and incubated with primary antibodies at 4°C overnight. Secondary peroxidase-conjugated antibodies were incubated at room temperature for 1 hour. The following primary antibodies were used: actin (1:3000; Sigma), phosphorylated NF-M/NF-H (1:10000; SMI31R, Covance), NF-L (1:7500; Cell Signaling), dephosphorylated NF-M and NF-H (1:2000; SMI32, Covance), total NFM (1:10000; clone RMO189), PP2A (1:2000; Cell Signaling) and PP1 (1:2000, Santa Cruz), anti HSP60 (1:200; Santa Cruz), anti SNAP25 (1:1000: Abcam), anti phosphorylated GSK3 β (pGSK3 β ; serine 9; 1:5000 Cell Signaling), anti total GSK3 β (1:5000; Cell Signaling), anti phosphorylated Akt (1:5000; Cell Signaling), anti total Akt (1:5000; Cell Signaling), anti ubiquitin (1:100; Santa Cruz), anti-KHC H2 (1:5000, kind gift of prof. Brady) and anti-phospho-KLC (63-90; 1:500; kind gift of prof. Brady). Membranes were developed using the Enhanced Luminescence kit (Thermo Scientific). For phosphorylated proteins, blots were probed for the phospho-sensitive antibody first, then stripped. For the stripping protocol, the membranes were incubated in stripping buffer (60 mM Tris-HCl, 2% (w/v) SDS, 0.7% (v/v) β -Mercaptoethanol) at 25 °C for 10 minutes and then at 55°C for 10 minutes. Blots were re-probed with the corresponding total antibody. Bands were semiquantified (Image J, NIH) and relative abundance of a particular protein was normalized to that of house-keeping proteins.

4.6 Gene expression analysis

RNA from tissue or cells was purified with the Trizol reagent (Invitrogen), according to the manufacturer's instructions. The quality of the RNA was determined by measuring the absorbance at 260 and 280 nm. Retrotranscription was performed using the Superscript III kit (Invitrogen) according to the manufacturer's instructions. Quantitative real-time PCR (qPCR) analyses were performed with primers specific for the following genes:

atrogin-1

forward: ATGAAGATGCCACACAAT

reverse: CATGAAACACAGACATTGCC

acetylcholine receptor β subunit

forward: ACCACGACGCACTGAAGG

reverse: GGTCCCGACGCTTGTGA

acetylcholine receptor γ subunit

forward: AGAACAATGTGGACGGTGTC

reverse: GCAGCCAGTAGATACACCG

NFM

forward: AATGAACTTCGGGGACC

reverse: CCCCTCTAGGAGTTTCCTGT

NFH

forward:GAAAAGCACCAAGGAGTCAC

reverse: TGGTGTTTCTCAGCTCACTG

60S acidic ribosomal protein P0 (RPLP0)

forward: TCGCTTTCTGGAGGGTGTC

reverse: CACAGACAATGCCAGGACG

Primers were tested on a standard curve and the efficiency and the correlation coefficient were higher than 90% and 0.990, respectively. PCR analysis was calculated with the Delta-delta Ct method (Livak and Schmittgen, 2001)

4.7 Electrophysiology

Motor conduction velocities (MCV) in sciatic nerves were measured according to previously described techniques(Dolcetta et al., 2005). Briefly, compound motor action potential (CMAP) was obtained, stimulating the nerve at the ankle and ischiatic notch with a pair of needle electrodes and recording in the distal hind limb muscles. The active electrode was placed in the middle of plantar muscles, whereas the reference was inserted subcutaneously in the second digit. MCV was measured by dividing the distance between the two points of stimulation by the difference between proximal and distal CMAP latencies. F-waves were recorded from proximal nerve segments and motor roots with the same montage as described for MCV (Toyoshima et al., 1986).

4.8 Ser/thr phosphatase activity assay.

PP1 and PP2A activities were measured using the Rediplate assay (Molecular probes) following the manufacturer's instructions. Enzyme activity was expressed as pmoles of substrate per mg of protein per minute.

4.9 Electron Microscopy

Sciatic nerves were quickly removed and fixed with 2.5% (w/v) glutaraldehyde and 2% formaldehyde (w/v) in cacodylate buffer. Samples were embedded in Araldite, and ultrathin sections (60 nm) were collected on Formvar-coated one-hole grids and stained with osmium tetroxide and lead acetate. For the quantitative analyses, thirty myelinated axons were randomly selected from each sample. A total of 3 nerves per condition were analyzed. Axonal diameters were measured and images were processed for counting of NF density as described (Cole et al., 1994). Briefly, the NFs were counted using a template of hexagons, each of which enclosed an area of 2.6 cm^2 (9 mm per side). All NFs were counted in every hexagon included within the axonal boundaries, as described earlier (de Waegh et al., 1992). We did not include any hexagons in the quantitative studies in which vesicular organelles occupied more than approximately 10% of the area of the hexagon or in which the NFs were not all in true cross sections of axoplasm. At this magnification, each hexagon represent a $5.8 \times 10 \text{ m}^2 \text{ m}^2$ region of axoplasm. Nerves from four mice from each line of transgenic mice and their age-matched controls were analyzed. The cross-sectional area of all individual axons was determined from 8 x 10 inch photographs at a magnification of 2000 x from the same section of sciatic nerve. The length and width of each axon (not including the axon sheath) was measured and then the area was determined.

4.10 Nissl staining

Sections (30 μm thick) were treated with 100% ethanol and xylene and then re-hydrated. Slides were immersed in 0.1% cresyl violet (prepared in distilled water and 3% acetic acid) for 5 min, before rinses in 1% acetic acid–70% ethanol and 1% acetic acid–100% ethanol and mounting with permount. Deeply stained motoneurons in the ventral horn were counted by stereology as viable Nissl+ cells.

4.11 Sciatic nerve ligation

For the in vivo study of FAT, animals were anesthetized and the right sciatic nerve was exposed and ligated using a surgical thread. The wound was sutured. The proximal and distal stumps (1mm from each side) were collected from the ligated nerve 6 h after surgery. The controlateral, unligated nerve was used as control of unaltered transport. The tissue was processed for immunoblot analysis for antibodies against SNAP25, HSP60, H2 and actin. Bands were semiquantified (Image J, NIH) and relative abundance of a particular protein was normalized to that of actin. The accumulation of the specific marker at the stump is proportional to the efficiency of the transport. TEM was performed on the ligated nerves as described above.

4.12 Vesicle motility assays in isolated axoplasm

Axoplasms were extruded from giant axons of squid (*Loligo pealii*) (Wood Hole Marine Biological Laboratory) as described previously (Szebenyi et al. 2003). Sphingolipids were diluted into X/2 buffer (175 mM potassium aspartate, 65 mM taurine, 35 mM betaine, 25 mM glycine, 10 mM HEPES, 6.5 mM MgCl_2 , 5 mM EGTA, 1.5 mM CaCl_2 and 0.5 mM glucose, pH 7.2) supplemented with 2–5 mM ATP to a final volume of 20 μl . The mix was then added to perfusion

chambers. Preparations were analyzed on a Zeiss Axiomat microscope with a 100x, 1.3 n.a. objective, and DIC optics. Hamamatsu Argus 20 Model 2400 CCD cameras were used for image processing and analysis. Organelle velocities were measured with a Photonics Microscopy C2117 video manipulator (Hamamatsu) by matching calibrated cursor movements to the speed of vesicles moving in the axoplasm. Limits to resolution in the light microscope preclude following individual organelles in axoplasm, but this method has proved highly reproducible. The rate of transport was plotted against the time. Each data point represents an average rate for particles moving in the specified direction in a field.

4.13 Statistical analysis

Where appropriate, results are the average from at least three independent experiments and are expressed as the mean \pm SE. Data were analyzed by the Student's t test and p values < 0.05 were considered statistically significant (*). Where experimental variable was investigated across different time points in Wt and Twitcher mice, the ANOVA test was used to calculate significance.

CHAPTER 5 EXPERIMENTAL RESULTS

5.1 Activation of the protein degradation system underlies the muscular atrophy of the Twitcher mouse.

The Twitcher mouse, an authentic mutant that models KD, is known to develop severe muscle atrophy of the lower limbs. This muscle waste is evident as early as P15 and worsens as the mutant enters more severe stages of the disease. Figure 1 shows images comparing the leg of twitcher and wild type littermates at 7, 15 and 35 days of age. Noticeable loss of muscle mass is observed at P15, which worsens at P35.

Muscle mass is regulated by the PI3K/AKT pathway, which modulates the balance between protein synthesis and protein degradation. This pathway is differentially regulated both in the developing muscle and in several pathological states, like denervation, ALS and spinal muscular atrophy (Bodine et al., 2001; Millino et al., 2009; Dobrowolny et al., 2011). To determine whether this pathway is involved in this disease, we quantified the fraction of phosphorylated AKT (serine 473) (pAKT), which directly correlates to its kinase activity. While a significant increase in pAKT was observed in the Wt tissue, concomitantly with the growth of the animal, a strong decrease in pAKT was observed in Twitcher soleus muscle protein extracts (Fig. 2A, and relative quantification in 2C). Inactivation of AKT has two important consequences on the muscle biology. First, it leads to the activation of GSK3 β , which then inhibits protein synthesis (Leger et al., 2006). In line with this observation, we detected a significant increase in the activation of GSK3 β in the Twitcher muscles (Fig. 2B, and relative quantification in 2D). Secondly, AKT phosphorylates the FOXO transcription factors, which keeps them in the cytosol. AKT inactivation releases the FOXO proteins from this inhibition, allowing them to translocate to

the nucleus and to increase the expression of the ubiquitin ligase atrogin-1 (Leger et al., 2006). Expression analysis detected a 1.5-fold increase in the mRNA levels of atrogin-1 in Twitcher soleus muscle at P15 (Fig. 3B), which rose to 14 fold in P30 mutant muscles (Fig. 3C). Analysis of the activation of the proteasome system was performed by western blot analysis for ubiquitinated proteins in extracts from muscles (Fig. 3D). Higher levels of ubiquitinated proteins were observed as early as P15 and more noticeably at P30 in mutant muscle extracts (Fig. 3D). These results indicate an undergoing pathological mechanism affecting some mutant muscles.

5.2 The Twitcher NMJs have normal morphology.

The changes detected in the Twitcher soleus muscle may be triggered by abnormalities in the NMJ structure, regulation and/or axonal innervation. To investigate this in more detail, we analyzed how the disease affects the nerve endings in NMJs of the soleus muscle in our new Twi-YFPax mouse line. The Twi-YFPax mouse is a cross between the original Twitcher strain and the reporter transgenic mouse Thy1.1-YFP, which expresses the YFP in subsets of neurons, allowing for fine morphological analysis of axons (Feng et al., 2000; Castelvetti et al., 2011). Longitudinal sections of P30 Wt- and Twi-YFPax soleus muscle were labeled with AlexaFluo-555 α -Bungarotoxin (BTX), which binds the α -subunit of the muscle acetylcholine receptor (AChR). In both Wt and Twi-YFPax mice, YFP+ axons were visualized ending in typical ramified structures, which colocalized with BTX labeling (Fig. 4). Surprisingly, NMJs with little or no BTX staining (a sign of denervated muscle) were scarce in mutant muscles, even at 30 days of age (Fig. 4S, 4T).

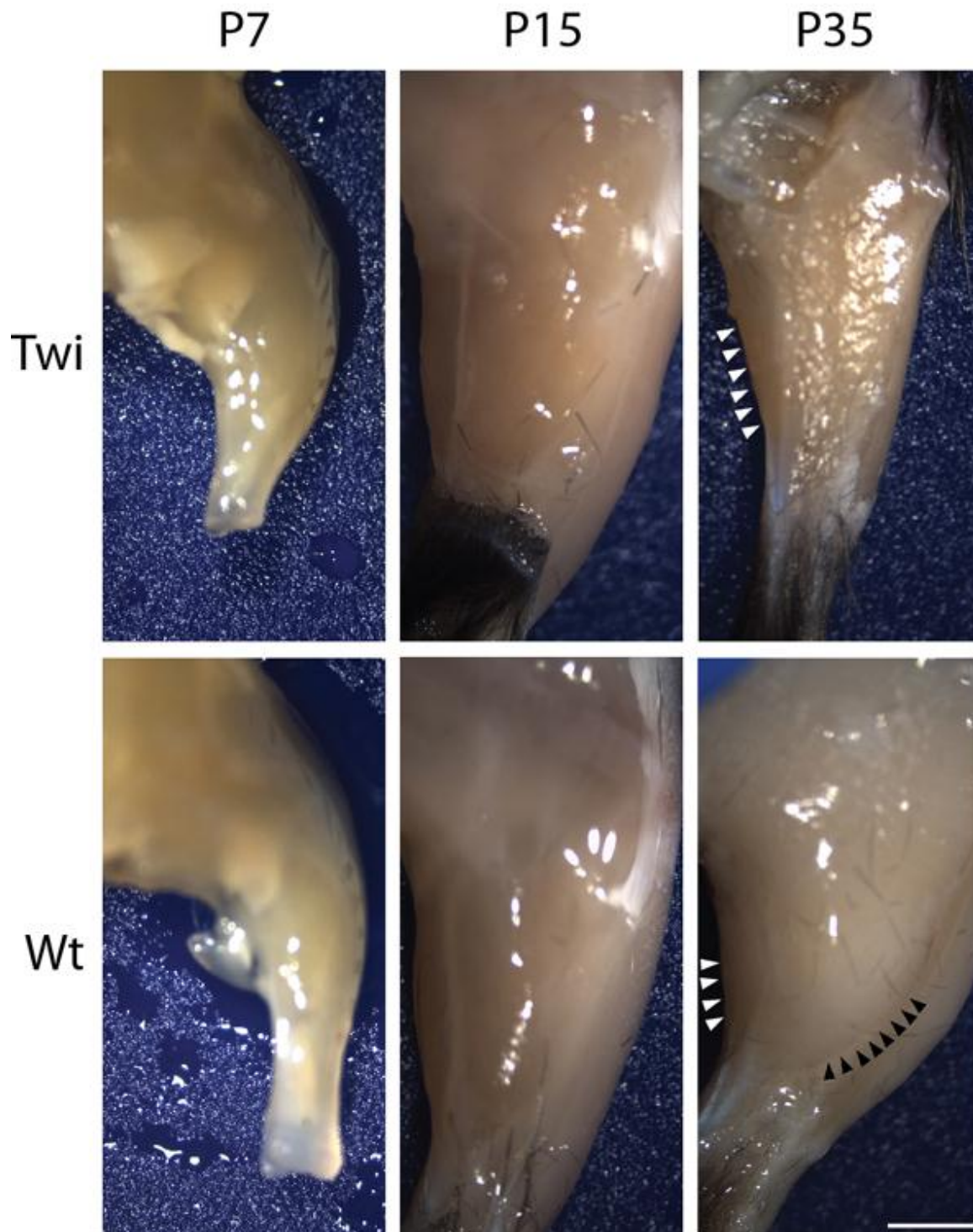


Figure 1 Muscle wasting in the Twitcher mouse

Representative pictures of the right leg of Twitcher (upper panels) and wild type (Wt, lower panels) mice after removal of the skin. The Wt muscle progressively increases in size, as expected during the postnatal growth. In the Twitcher animal, a strong reduction in muscle mass is observed at P35 (white arrows), which indicates severe muscle wasting.

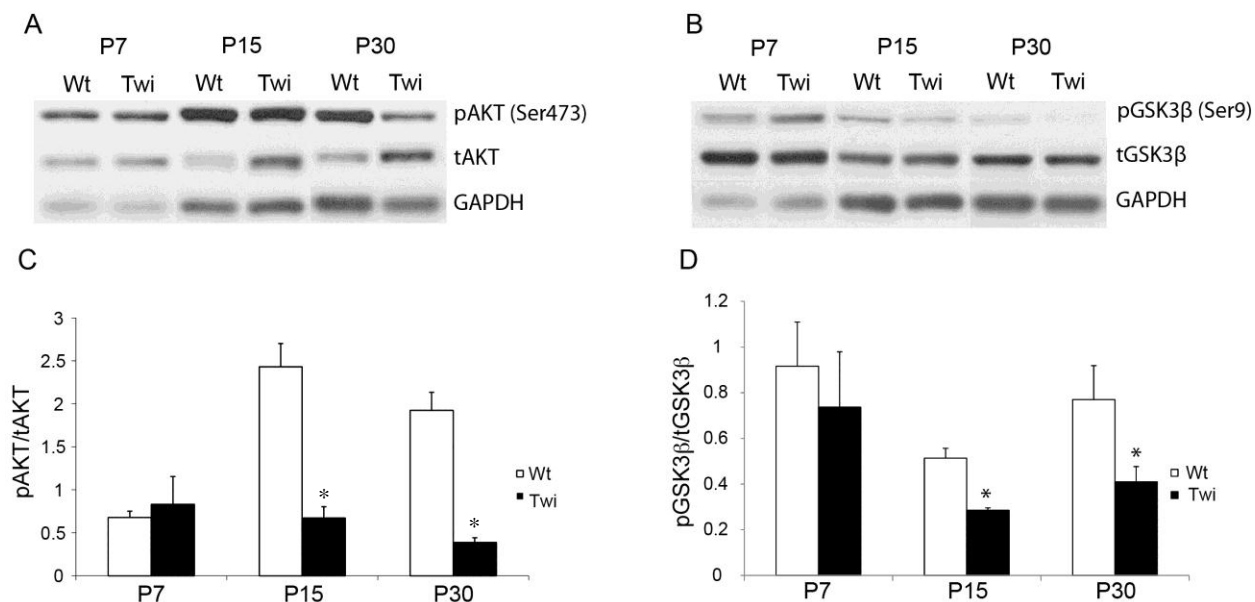


Figure 2 Activation of the atrophy signaling pathways in the Twitcher muscles

Western blot analysis of total and phosphorylated AKT (serine 473; active form) in P7, P15 and P30 soleus muscle protein extracts (A). Quantification is shown in C (n=3). Western blot analysis of total and phosphorylated GSK3β (serine 9; inactive form) in P7, P15 and P30 soleus muscle protein extracts (B). Quantification is shown in D (n=3). $p < 0.05$. Activation of both kinases can be observed at P15 and P30. Protein loading was determined with the antibody against GAPDH.

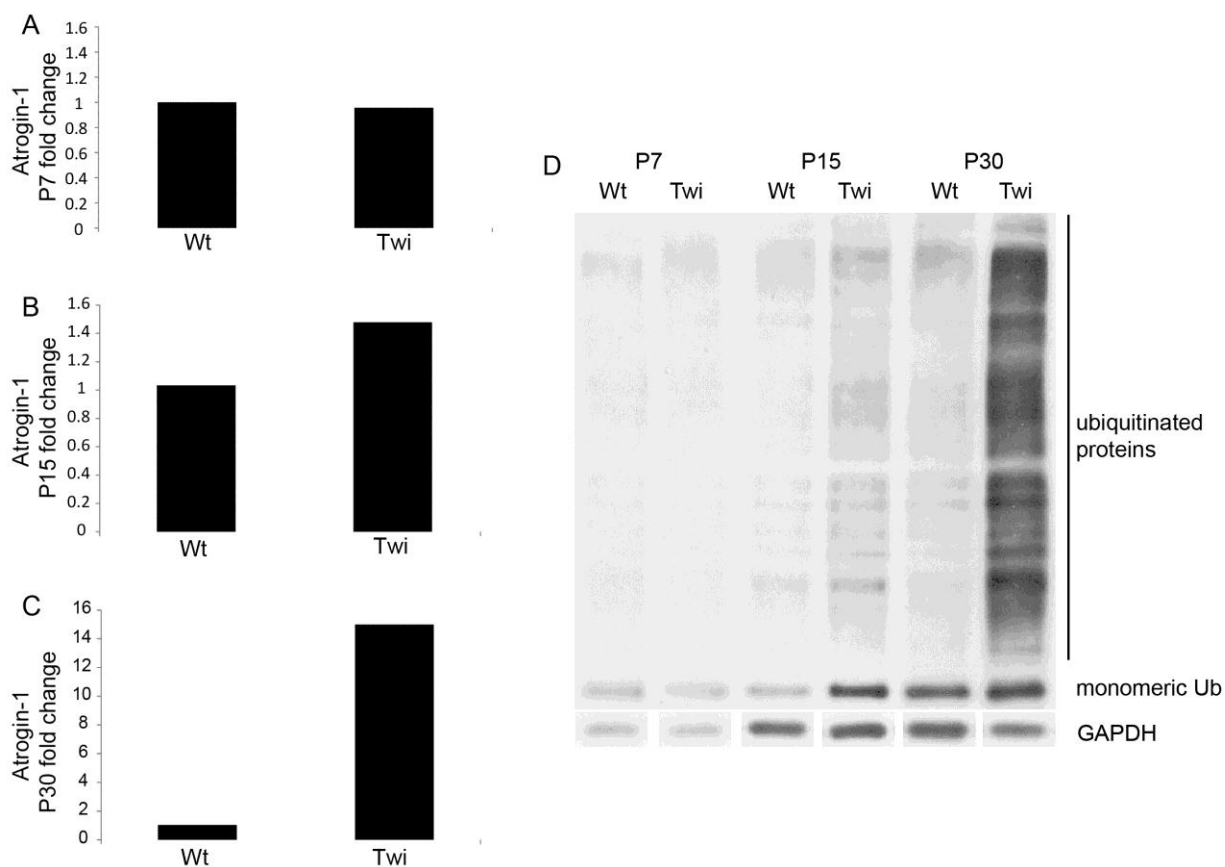


Figure 3 Activation of the ubiquitination system in the Twitcher muscles

qRT-PCR analysis for the ubiquitin ligase atrogin-1 on P7 (A), P15 (B), and P30 (C) soleus muscle extracts from Wt and twitcher mice. The analysis shows 1.5 and 14 fold increases in the atrogin-1 mRNA at P15 and P30 in the mutant, respectively. Data is expressed as -fold changes in the twitcher tissue with respect to the content in the wild type after normalization by the expression of RPLP0, as a housekeeping gene. n= 3 animals per genotype per time point. Differences at P30 were significant with $p < 0.05$. D) Western blot analysis for the ubiquitin antibody, showing the total tissue content of ubiquitinated proteins and the monomeric ubiquitin in P7, P15 and P30 soleus muscle protein extracts.

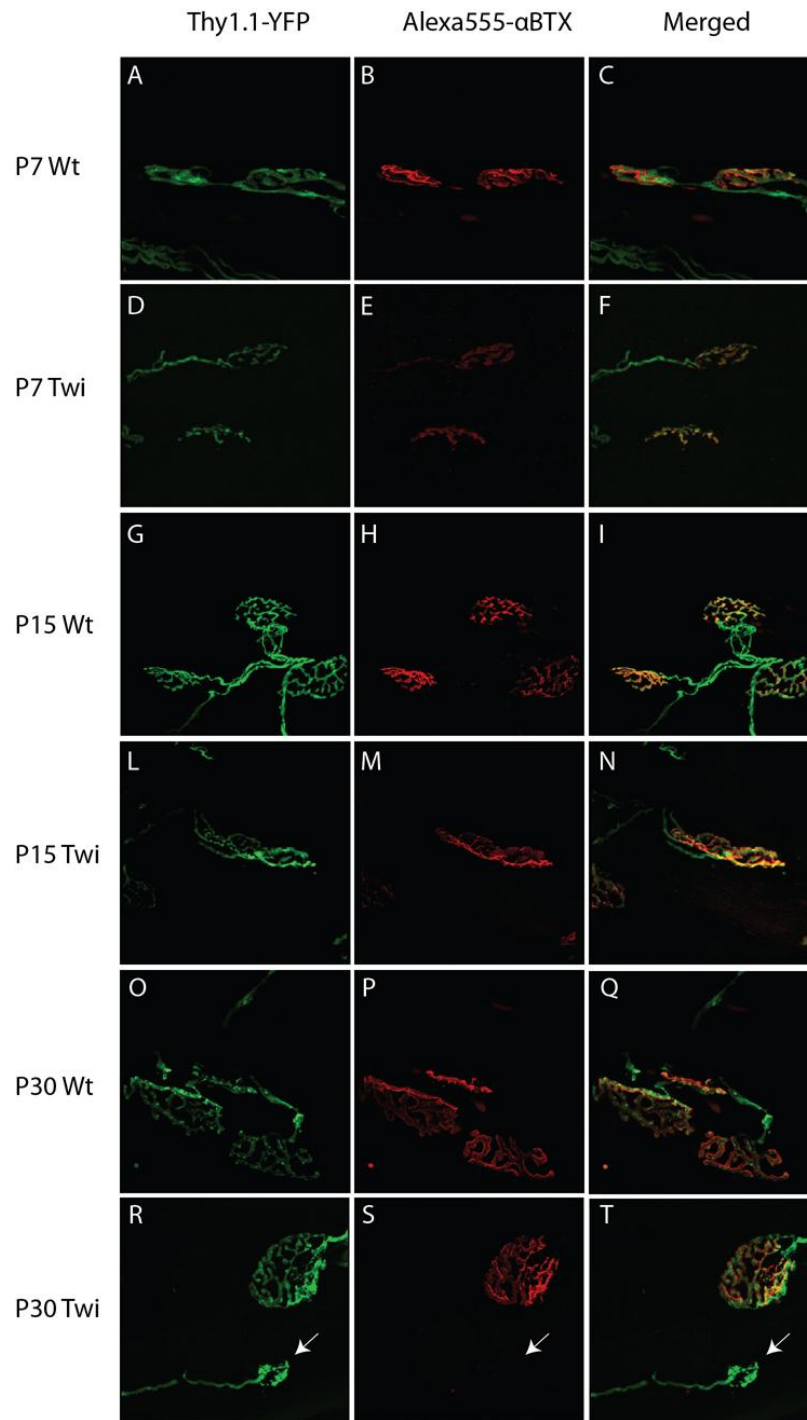


Figure 4 The Twitcher NMJs are not denervated.

Staining of longitudinal sections of the soleus muscle of Wt- and Twitcher-YFPax at P7, P15 and P30 with alexa555-conjugated BTX (red) to label AchRs. The axons are labeled by the transgenic YFP. The NMJs appear as pretzel-shaped structures, surrounded by the clustered AchRs. All the examined NMJs appeared normal at P7 (A-C for Wt and D-F for twitcher) and P15 (G-I for Wt and L-N for twitcher). Occasionally, retracting axons were observed in the P30 Twitcher tissue, which were also negative for the BTX (arrow in R-T).

Quantitative analysis showed the absence of significant differences in the number of double positive YFP+/BTX+ NMJs in mutants (Fig. 5), suggesting that denervation is per se unlikely to account for the loss of their muscle mass.

5.3 Twitcher NMJs appear to be dysfunctional by increased levels of active caspase 3 and abnormal expression of the fetal AchR subunit.

Muscle atrophy in the absence of clear denervation has been observed in some specific neurological diseases such as myasthenia gravis, Lambert-Eaton myasthenic syndrome and botulism (Pinter et al., 1995; Balice-Gordon et al., 2000; Kong et al., 2009) and may be consequent to dysfunctional NMJs. We examined two possible contributors to NMJ abnormalities. First, to examine the possibility that activation of caspases may be destabilizing Twitcher NMJs, we stained the Wt and Twitcher muscles for the active fragment of caspase 3. Effector caspases can be detected in developing NMJs or in NMJs of myopathological conditions such as the slow-channel syndrome (Vohra et al., 2004; Vohra et al., 2006; Keller et al., 2011). At P30, we detected numerous NMJs strongly stained for active caspase 3 in Twitcher muscle (Fig. 6R-6T). Interestingly, some mutant NMJs were lightly stained for the protease, suggesting that NMJs could be differentially affected in the mutant (arrowhead in Fig. 6L-6N). These results are in line with previous experiments from our laboratory showing the activation of caspase 3 in Twitcher axons (Smith et al., 2011). Counting revealed a significant increase of caspase 3+ NMJs in Twitcher muscles at P15 and P30 (Fig. 7B, 7C). Interestingly, mutant muscle cells were not stained by the caspase 3 antibody, suggesting that apoptosis is not a major component of muscle atrophy in this mutant.

Second, to determine changes in neurotransmitter receptor composition in NMJs, we analyzed the expression of the AchR subunits. The AchR is composed of five subunits (α , β , γ , ϵ and δ), which are developmentally regulated (Punga and Ruegg, 2012). The γ subunit is expressed during the embryonic life, and its expression is shut down after the NMJ is properly developed. Improper muscle innervation causes the reappearance of the γ subunit adult muscles, making this molecule a reliable marker of NMJ disease (Numberger et al., 1991; Buonanno et al., 1992). Unfortunately, commercially available antibodies against the γ subunit proved to be completely inefficient for either immunohistology or immunoblotting. Consequently, we opted for analyzing for changes in mRNA levels. qRT-PCR for the β and γ subunits were performed on Wt and Twitcher muscle RNA (P7, P15 and P30). While at P7 no changes were observed in the two isoforms, both mRNAs were significantly increased in P15 Twitcher muscles (Fig. 8). At P30, the expression of the γ subunit was about three fold increased (Fig. 8). Expression of the AchR γ subunit indicates either a delayed development of muscle fibers or a reexpression due to NMJs inability to transfer the nerve impulse to the muscle. This may represent a compensatory mechanism for the dysfunction of the presynaptic terminal.

5.4 Axonal dystrophy in the Twitcher mouse.

To analyze for axonal dystrophy, we used the Twi-YFPax, which permits an easy, fast and detailed fluorescent characterization of axonal morphology in various neuronal populations. These include neurons in the cortex (motor neurons in layers 2-6), cerebellum (some Purkinje neurons), hippocampus, dorsal root ganglia and spinal cord (particularly lower spinal cord motor neurons). This dissertation focused on axons within the spinal cord and sciatic nerve fibers.

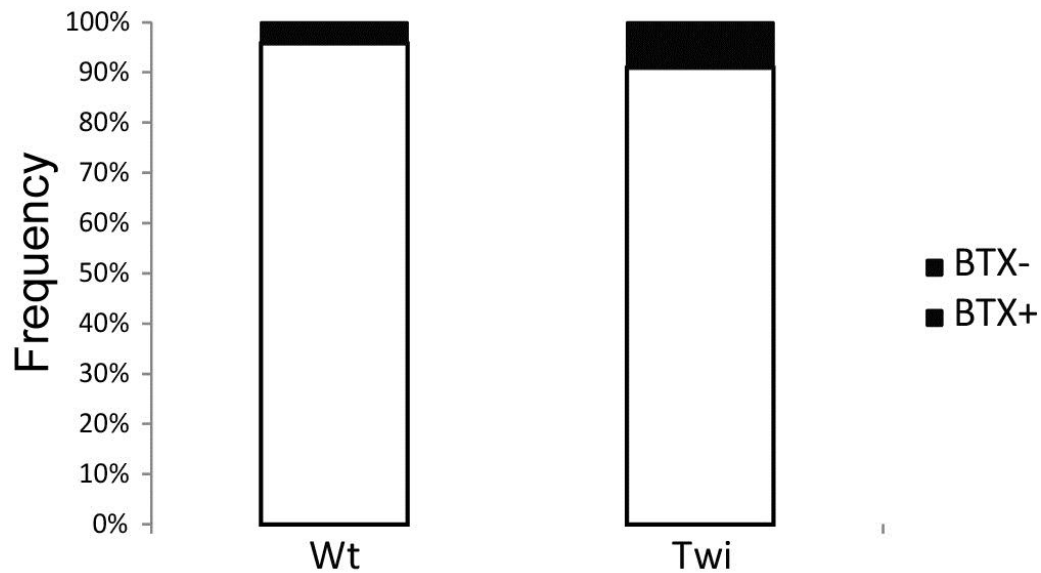


Figure 5 Frequency of denervated NMJs

Denervated NMJs (negative for the BTX) were counted at P30, the only time point when denervated NMJs were observed in the twitcher muscle. Data are expressed as percentage of the total counted NMJs (n= 3 animals per genotype). The percentage of BTX(+) NMJs is represented in white, while the percentage of BTX(-) NMJs is in black. The increase in denervated NMJs in the twitcher was not significant.

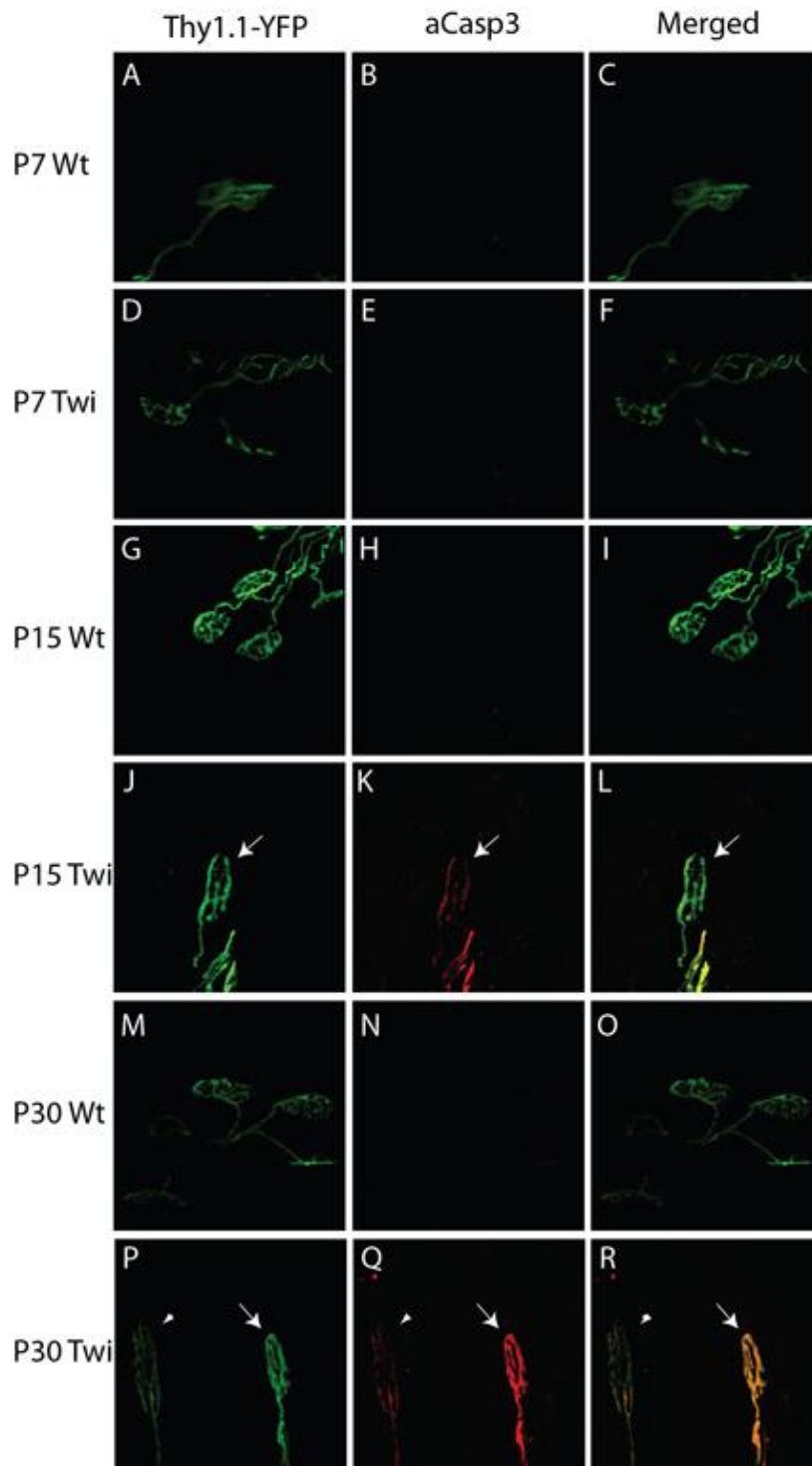


Figure 6 Activation of caspase 3 in the axonal ending of the Twitcher mouse

Immunostaining for the active fragment of caspase 3 (aCasp3, in red) in longitudinal sections of soleus muscle of Wt-YFPax and Twitcher-YFPax at P7 (A-F), P15 (G-L) and P30 (M-R). Several aCasp3+ NMJs were observed in the Twitcher muscle at P15 and P30 (arrows in J-L and P-R). Few NMJs were weakly labeled in the Twitcher muscles (arrowheads in P-R), suggesting different levels of caspase 3 activation.

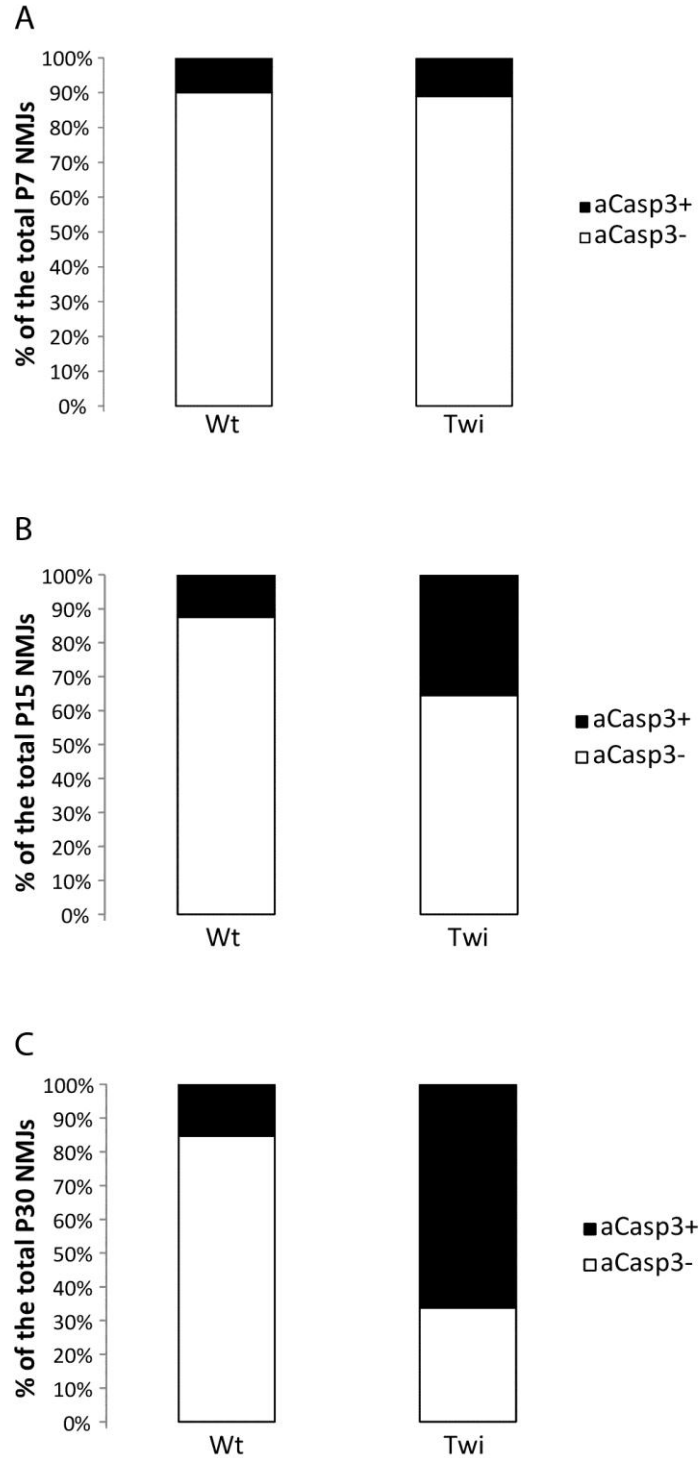


Figure 7 Frequency of aCasp3(+) NMJ in twitcher muscles

aCasp3(+) NMJs were counted in longitudinal sections of soleus muscles of Wt-YFPax and Twitcher-YFPax at P7 (A), P15 (B), and P30 (C). Data are expressed as percentage of the total counted NMJs (n= 3 animals per genotype and time point). The percentage of cCasp3(-) NMJs is represented in white, while the percentage of aCasp3(+) NMJs is in black. Differences at P15 and P30 were significant with $p < 0.05$.

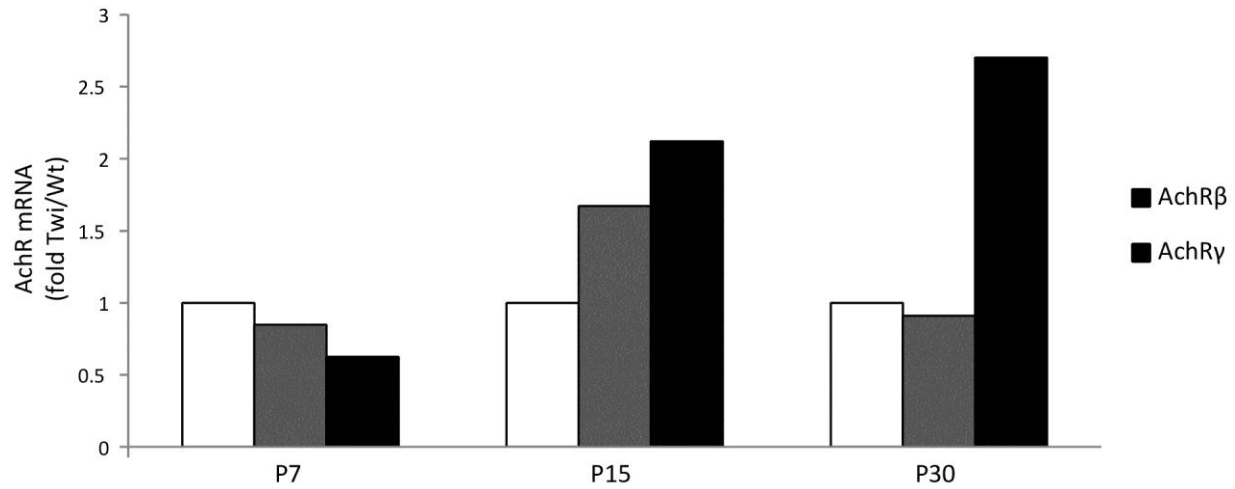


Figure 8 Alteration in the subunit composition of the AchR in the Twitcher muscle

qRT-PCR analysis for the β (adult) and γ (fetal) in soleus muscle RNAs isolated from Wt and twitcher mice at P7, P15 and P30, showing increased expression of the fetal subunit at P15 and P30. The β subunit also increased at P15. n= 3 animals per condition per genotype.

Confocal analysis showed a decrease in the density of YFP+ axons in the lumbar spinal cord of P30 Twi-YFPax mice. This was particularly evident in ventral white matter (Fig. 9A, 9B). In coronal sections, some mutant axons appeared with swellings (insets in Fig. 9A), suggesting local accumulations of YFP. This observation was confirmed by confocal analysis of longitudinal sections of the spinal cord (white arrows in Fig. 9E). Some axons showed breaks or transections (blue arrows in Fig. 9E) suggesting severe structural disruption. Orthogonal confocal analysis demonstrated that these pathologic profiles were abnormal structures contained within mutant axons (Fig. 10A to 10C). Wild type samples were completely devoid of these profiles (Fig. 10D).

5.5 Axonopathy starts before the onset of demyelination.

Myelination of the central nervous system appears normal in the early postnatal life of the Twitcher mouse. Published studies (Nagara et al.; Suzuki and Suzuki) and our own examination (Fig. 11) show that the onset of demyelination starts around the third week of postnatal life of Twitcher mice. Examination of Twi-YFPax mutants showed axonal swellings and varicosities already within the ventral white matter as early as P7 (arrows in Fig. 12A-12B), but not in the age-matched controls (not-shown). Axonal profiles increased in frequency in the spinal cord of older mutants (Fig. 12C-12E) but not in control tissue (Fig. 12F). The appearance of axonal profiles (swellings or varicosities) at such early postnatal ages and in the absence of demyelination suggests unexpected premature neuronal vulnerability in this disease.

5.6 Peripheral nerves are affected of axonopathy.

The observation of a progressive axonal dystrophy in the spinal cord prompted us to investigate axonal damage in the sciatic nerve, as this nerve carries some of the longest axons. Similarly to what we found in the spinal cord, swellings and varicosities were detected in sciatic nerves. While these were evident at P15 (arrows in Fig. 13B), we could not detect gross

morphological changes in axons from P7 mutant nerves (Fig. 13A). Axonal abnormalities became more evident with the onset of demyelination. At P30, axons in the mutant sciatic nerve appeared with multiple swellings and were frequently transected (arrows in Fig. 13C).

5.7 Neuronal loss is a late event in the Twitcher mouse

Axonopathy generally precedes apoptotic death. To address whether Twitcher neurons undergo cell death, coronal sections of the lumbar spinal cord from the Twitcher parental line and from wild type littermates were subjected to the TUNEL assay. The TUNEL assay identifies cleavages in DNA, and has served as a traditional method for detecting apoptosis (Gavrieli et al., 1992; Wijisman et al., 1993). As expected, TUNEL+ glial nuclei were detected in the white matter of symptomatic mutant mice. The frequency of these apoptotic glia in presymptomatic (P7-P15) Twitcher mice was minimal and not significantly different from wild type littermates (Fig. 14A). However, TUNEL+ glia sharply increased as Twitcher mice developed the disease, reaching stereological significance when mutants passed the onset of the disease (P30) (Fig. 14A). Figure 14D-14F shows TUNEL+ glial nuclei within the ventral white matter in lumbar spinal cord samples from P30 Twitcher. These results are in line with previous studies showing apoptotic death of oligodendrocytes in the Twitcher animals, (Taniike et al., 1999; Jatana et al., 2002).

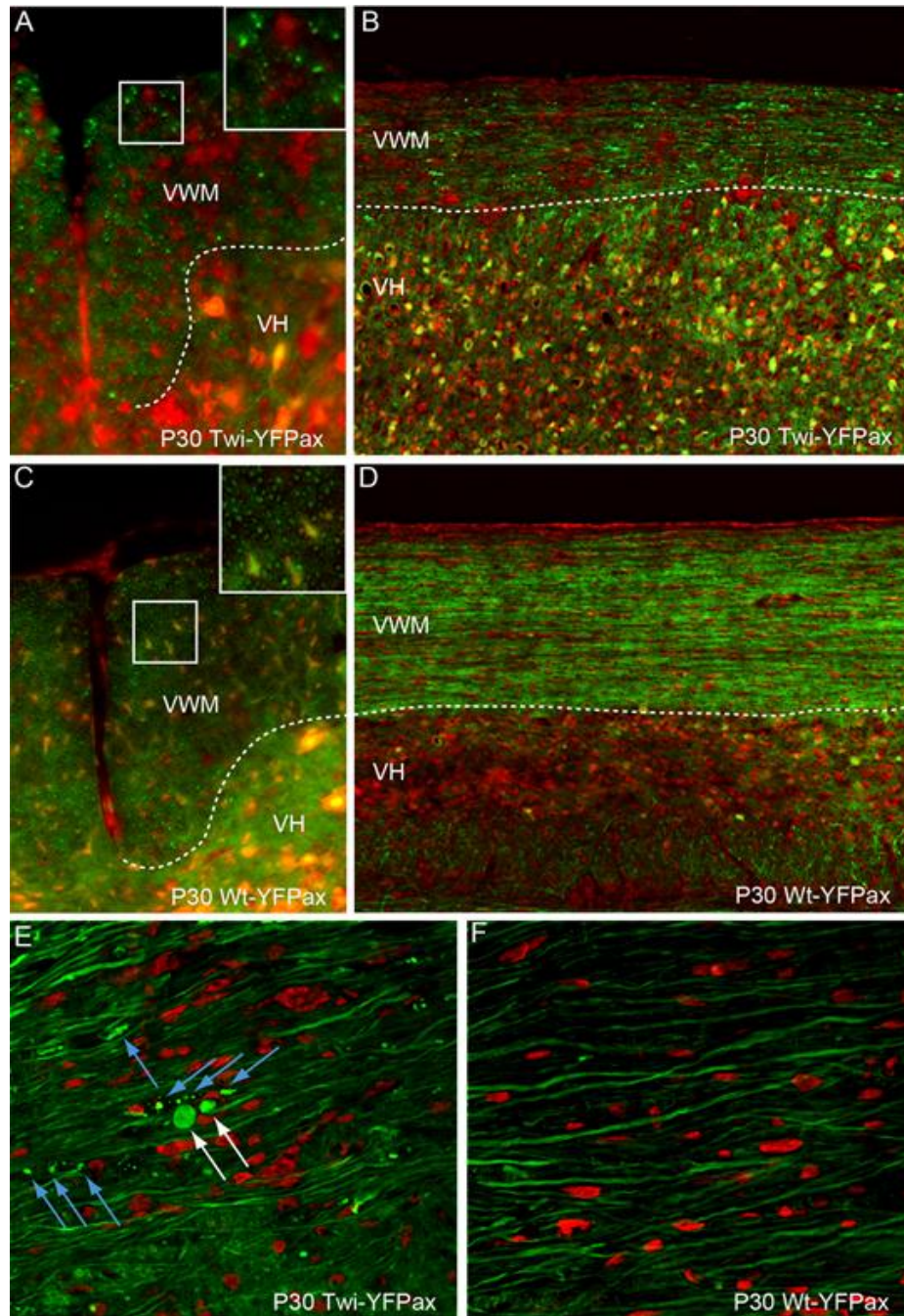


Figure 9 Axonopathy in the Twitcher spinal cord

Coronal (A, C) and longitudinal (B, D) sections from postnatal day 30 (P30) Wt-YFPax and Twi-YFPax were observed with a confocal microscope to detect axonal dystrophy. VWM ventral white matter, VH ventral horn. Inset boxes are higher magnifications from boxed areas in the ventral white matter. Magnification X200. Red fluorescence is propidium iodide. E-F) Longitudinal sections from P30 Twi-YFPax and Wt-YFPax were confocally imaged to identify axonal abnormalities. White arrows point to swellings and blue arrows to breaks or transected areas in mutant axons. Red fluorescence is propidium.

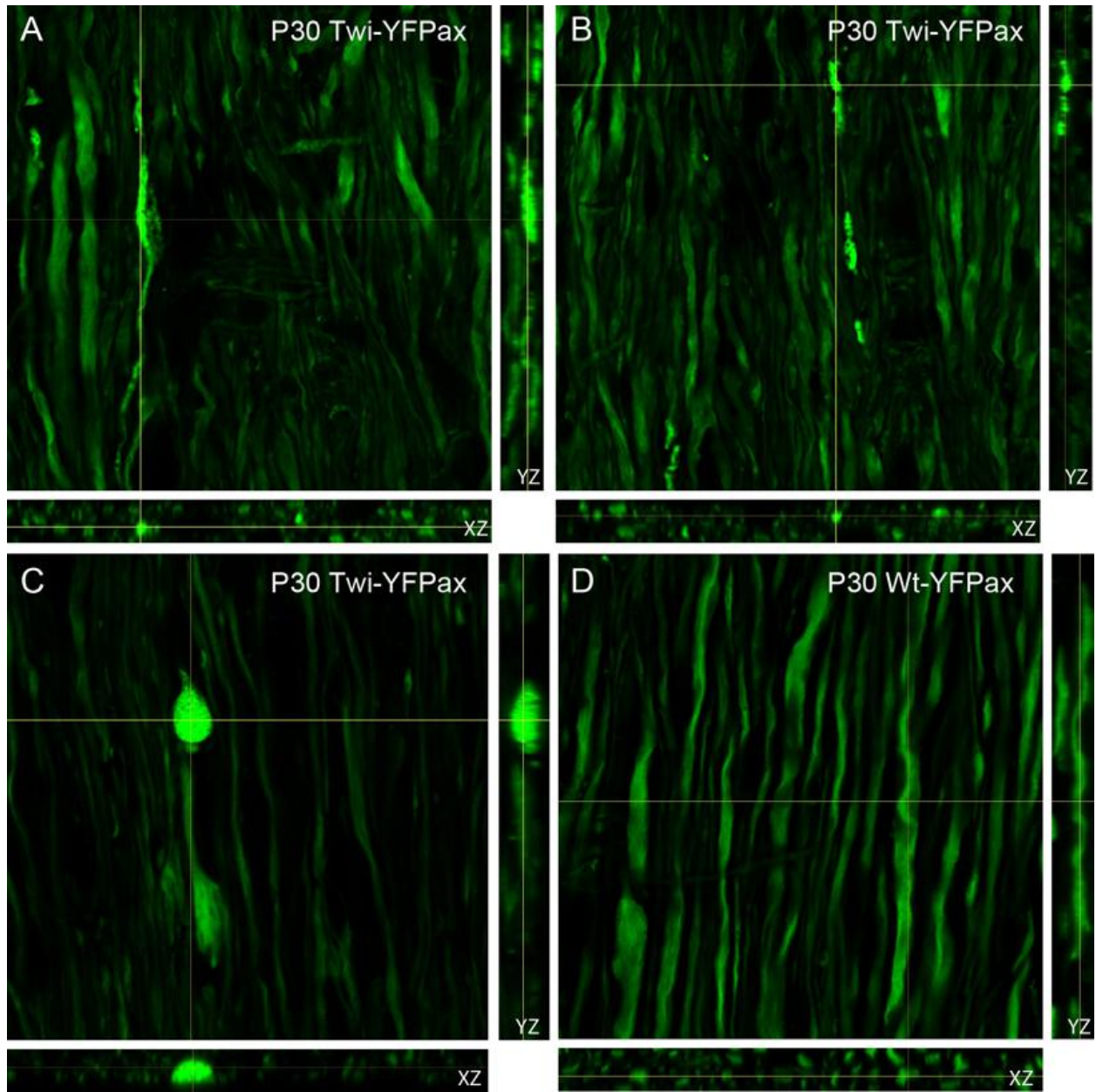


Figure 10 Progressive axonal degeneration in Twitcher axons

Confocal imaging revealed different stages of axonal degeneration in Twitcher axons. Z-stacking confocal imaging was performed on longitudinal sections of P30 spinal cord. White arrows point to three different stages of axonal degeneration in the Twitcher mouse (A–B). Orthogonal reconstructions show the YZ and XZ axes. White lines point to selected axonal alterations. These pathological profiles were not detected in any wild-type tissue analyzed (X1,000)

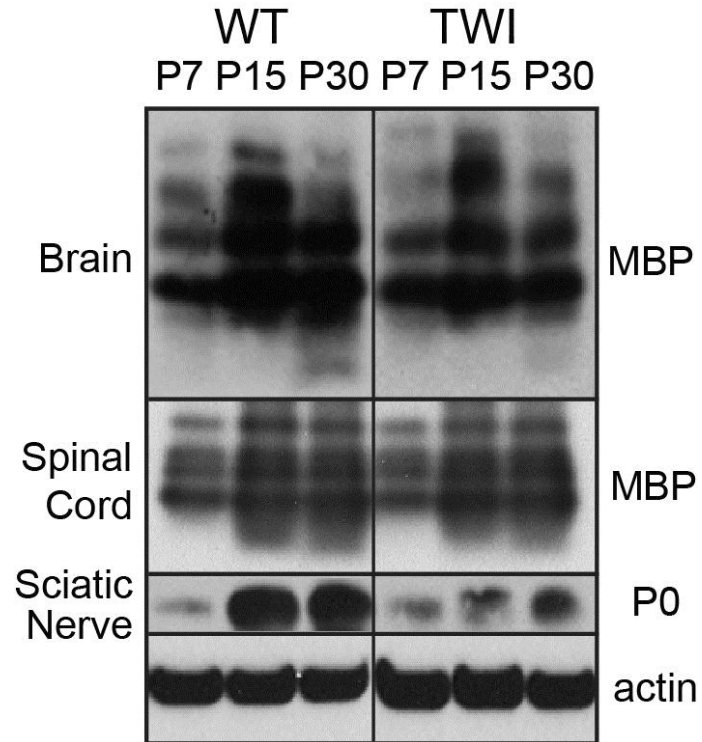


Figure 11 Progressive demyelination in the Twitcher mouse

Western blot analysis for the expression of MBP in brain and spinal cord and P0 in sciatic nerve lysates from P7, P15 and P30 Wt and twitcher mice. MBP and P0 are reduced in the twitcher tissues during aging. Actin was used as loading control.

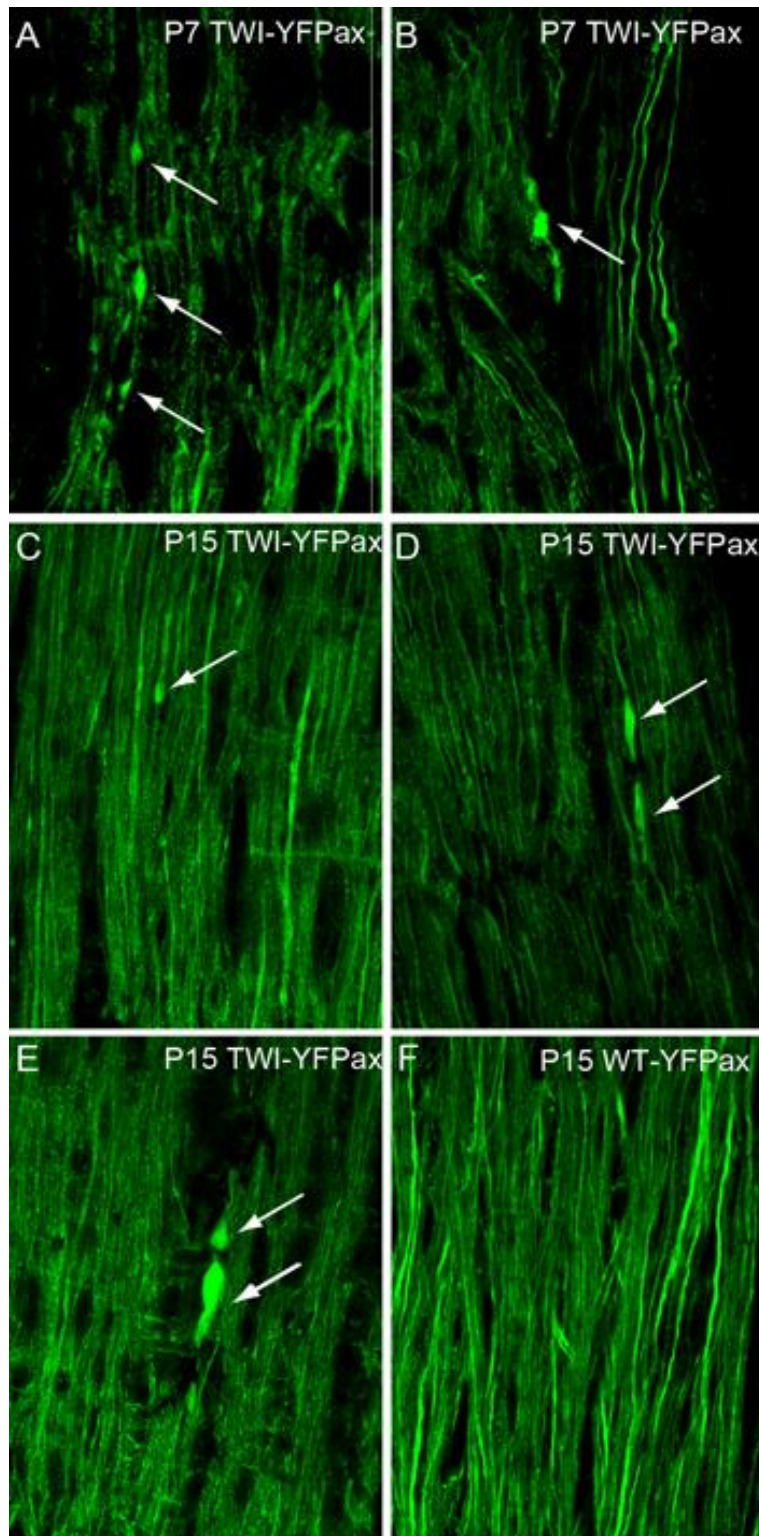


Figure 12 Early signs of axonal dystrophy in the Twitcher mouse

Confocal imaging of longitudinal sections from P7 (A, B) and P15 (C–F) lumbar spinal cords revealed axonal swellings (arrows) at 7 days of age in the Twitcher spinal cord. These pathological profiles were not detected in any wild-type tissue analyzed. Magnification x650

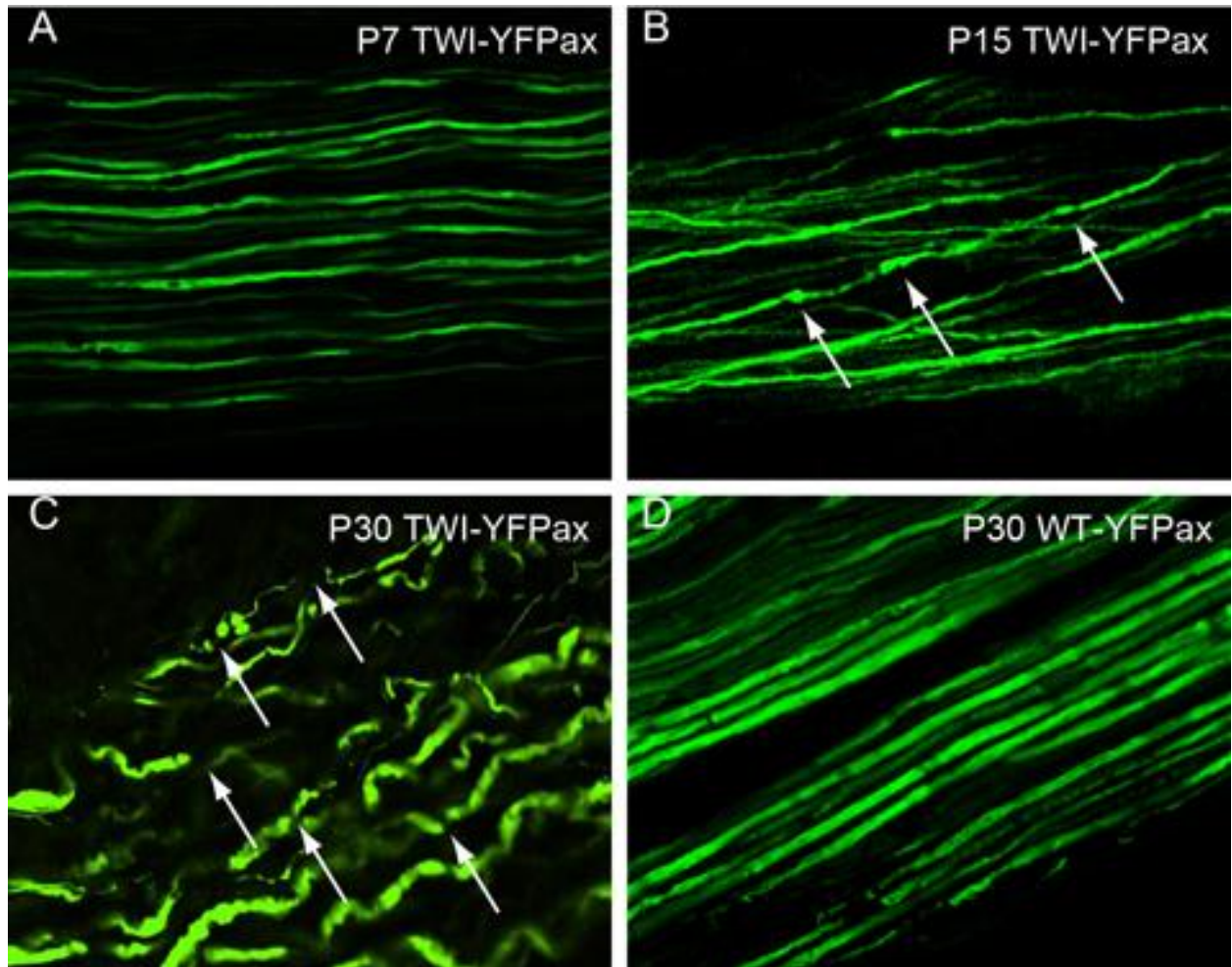


Figure 13 Axonal degeneration in the Twitcher sciatic nerve

Confocal imaging of longitudinal sections from P7 (A), P15 (B) and P30 (C) sciatic nerves revealed axonal dystrophy in P15 and P30 (arrows) but not in P7 nerves of the mutant mouse. These pathological profiles were not detected in any wild-type tissue analyzed. Magnification x650

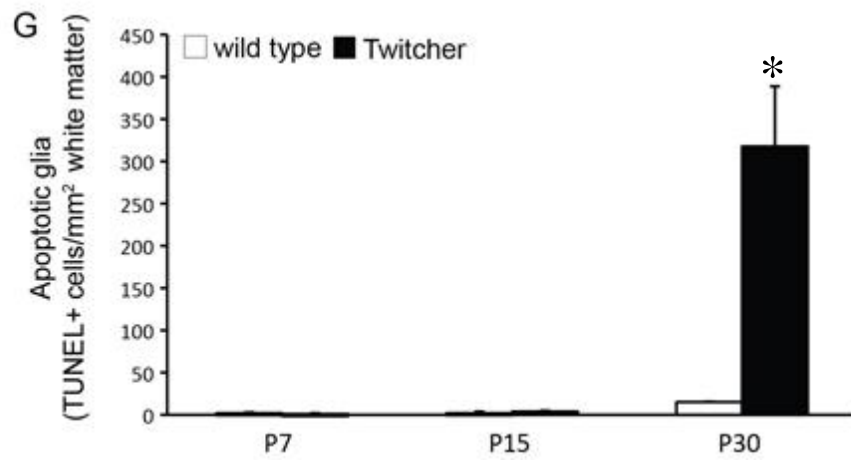
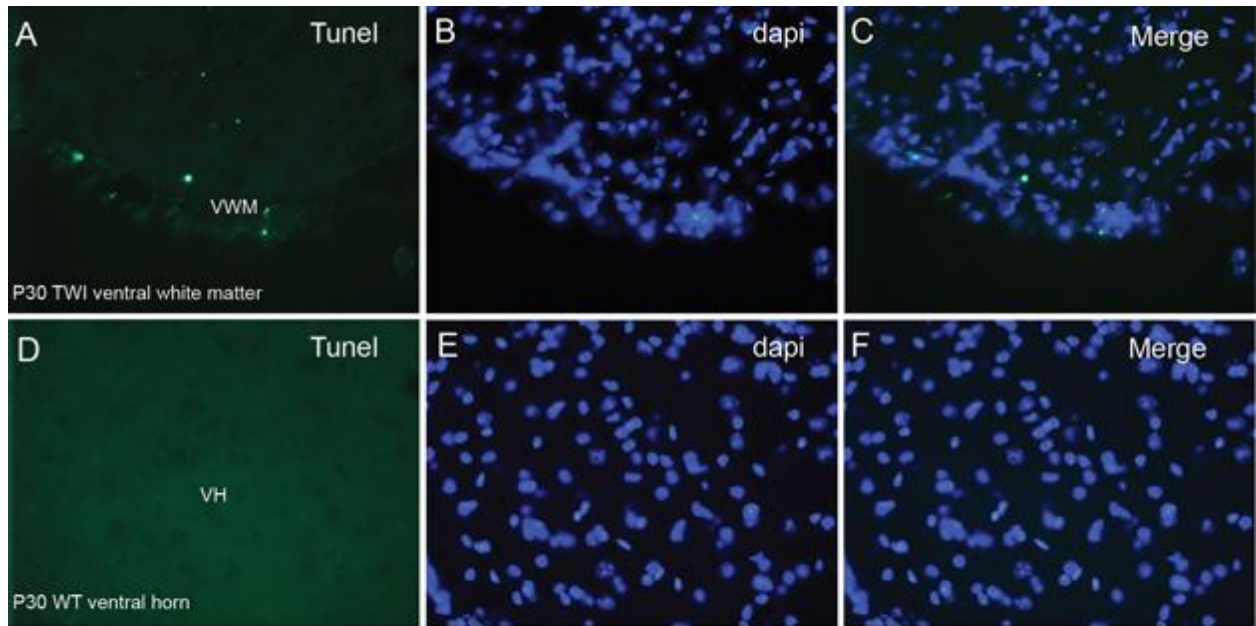


Figure 14 Glial apoptosis in the Twitcher spinal cord

TUNEL staining (green) of twitcher (A-C) and Wt (D-F) P30 spinal cords revealed the presence of cell death in the mutant white matter at late stages of the disease. Magnification x400. TUNEL+ glia counts confirmed the appearance of apoptotic glia at P30, but not at P7 and P15 (G). Counting was expressed as TUNEL+ cells per square mm. n=3 mice. p<0.05

Notably, some large TUNEL+ motorneurons were also detected in the gray matter of Twitcher mice but only when mutants were symptomatic (P30) (Fig. 15B). However, we did not detect any TUNEL+ motorneuron (or any other spinal neuron) at earlier time points (P7 and P15) (Fig. 15A) nor in tissues from wild type littermates at any of these time points. Co-staining for the neuronal nuclear marker (NeuN) confirmed the neuronal nature of these dying cells (Fig. 15C-15E). Stereological counting of TUNEL+ motorneurons confirmed these results (Fig. 15M). Stereological counting of total Neu+ neurons showed absence of significant differences between mutant and control littermates at any age (Fig. 15L), suggesting limited if any real loss of neurons. Interestingly, apoptotic neurons were mostly localized in the ventral horn of mutant cords and showed cytoplasmic rather than nuclear localization of the TUNEL staining (Fig. 15C). Although the reason for cytoplasmic localization of the TUNEL staining has not been explained, this pattern has been reported for neurons undergoing chromatolysis (Karnes et al., 2009). To examine this possibility, spinal cords from P7 and P15 Twitcher and wild type littermates were stained with the Nissl stain (Fig. 16A). The Nissl stain labels large stacks of rough endoplasmic reticulum and ribonuclear complexes (also called Nissl bodies), and its disappearance is a known endpoint for neuronal demise, (Cragg, 1970). Stereological counting of Nissl+ motorneurons showed a significant loss (~20%) of healthy (Nissl+) motorneurons as early as P7 (Fig. 16B) in the mutant cord. This loss increased to about 45% in P15 mutant mice (Fig. 16B).

5.8 Decrease in diameter of Twitcher axons.

To better understand the condition of the Twitcher axonopathy, we performed transmission electron microscopy (TEM) on coronal sections of sciatic nerves collected from WT and Twitcher mice at P12 and P30. Axonal diameter, which is usually affected during an ongoing

axonopathy, was measured and the frequency of axons calculated for mice at each age. Twitcher nerves showed fewer large-caliber axons as compared to controls already at P12 (Fig. 17A, 17B). As disease progressed, mutant nerves showed severe loss of myelin, edema (Fig. 17D, asterisk) and a visible reduction in the number of large-caliber axons (Fig. 17D, 17E). Even those mutant axons with no obvious demyelination showed smaller diameters (Fig. 17D, arrows). Frequency analysis confirmed these observations; at P12, mutant nerves contained higher numbers of axons with 2- to 3-micron calibers (Fig. 18A), and at P30, there was a significant ($p < 0.05$) shift to axons of smaller diameters, with the majority of mutant axonal caliber ranging between 1-5 microns (Fig. 18B). In contrast, the majority of WT axons grew in diameter as expected (Fig. 18A, 18B).

5.9 Lower density of NFs in Twitcher axons.

To determine whether the observed reduction in diameter of mutant axons involved alterations in the NF cytoskeleton, we examined NF density by TEM. Because NF density is affected by the level of myelination of the axon (Reles and Friede, 1991; de Waegh et al., 1992; Mata et al., 1992; Hsieh et al., 1994), we analyzed only mutant fibers that remained myelinated during the time-frame of our experiments (i.e., P12 and P30). Cross sectional and longitudinal imaging analysis showed that the spacing between NFs increased between P12 and P30 in WT nerve fibers (Fig. 19B, 19D, 19F), as expected for normal developing fibers, whereas Twitcher NFs appeared compacted at both time points (Fig. 19A, 19C, 19E), suggesting a failure in the mechanism regulating the spacing of these proteins. Quantitation of these observations by counting the NFs per random region of axoplasm revealed the expected decreased density of NFs (number of hexagons containing a given number of NFs/ $3.5 \times 10^{-2} \mu\text{m}^2$ area of axoplasm),

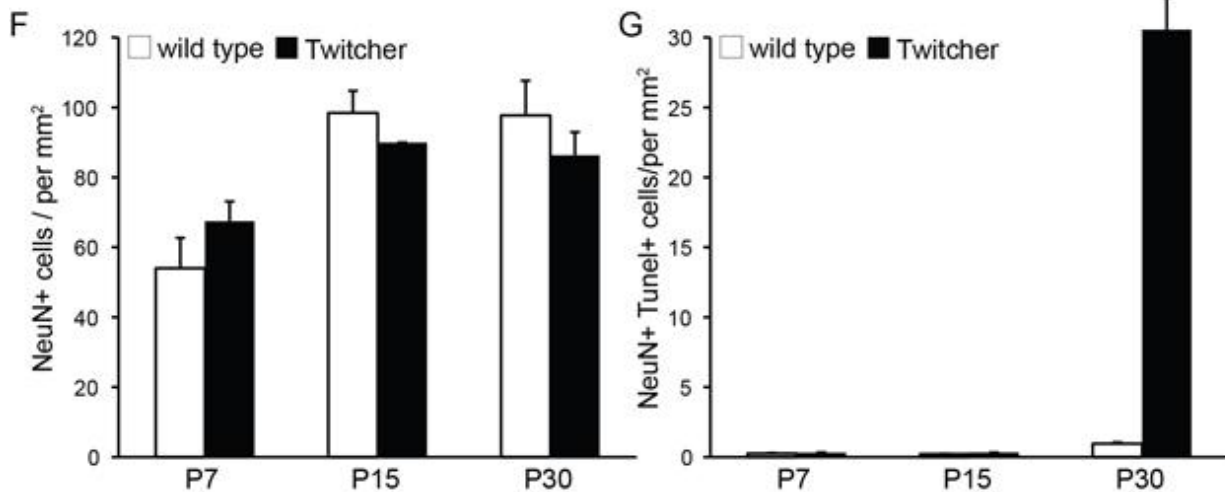
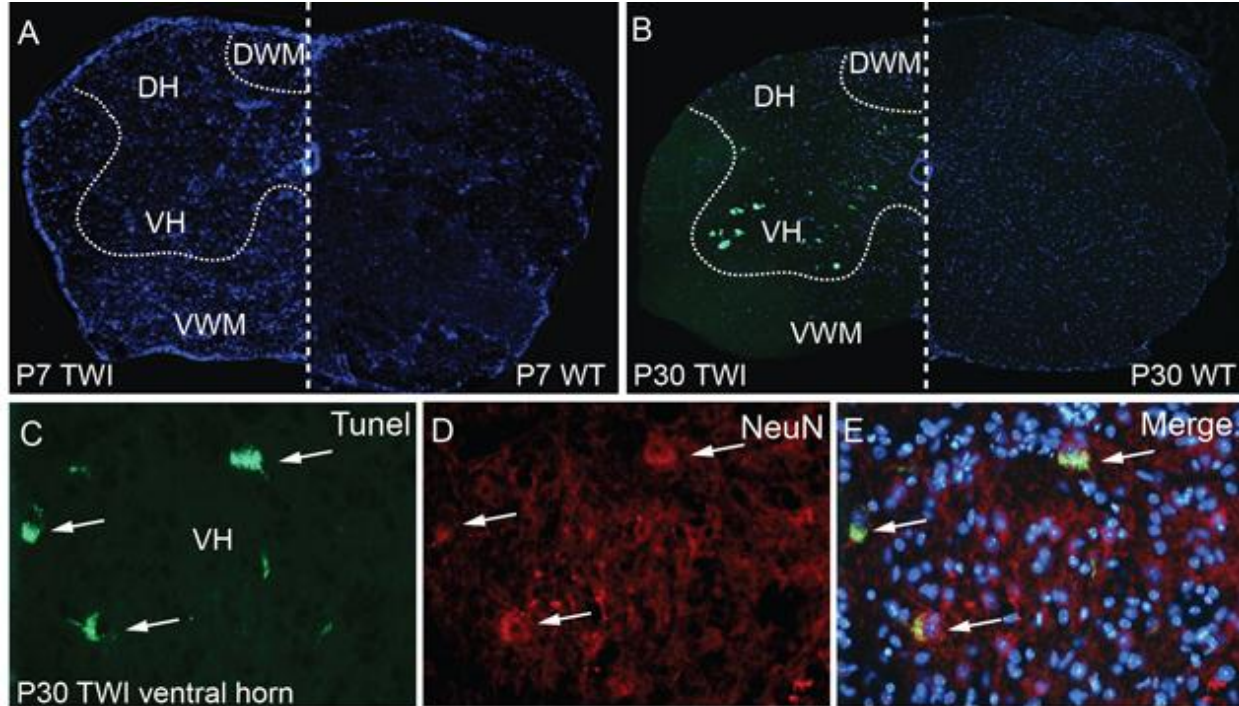


Figure 15 Neuronal apoptosis in the Twitcher spinal cord

TUNEL staining (green) of P7 (A) and P30 (B) Wt (right panel) and twitcher (left panel) spinal cords. TUNEL+ cells were detected in the ventral horn (VH), but not in the dorsal horn (DH) or in the ventral and dorsal white matter (VWM and DWM, respectively). Staining for TUNEL (green) and NeuN (red) showed that the TUNEL+ cells were neurons (C-E). Counting of the NeuN+ cells showed no significant change in the number of NeuN+ neurons in the VH (F). NeuN+ /TUNEL+ cells were observed only at P30 in the twitcher spinal cord (G). Counting was expressed as NeuN+ /TUNEL+ cells per mm². n=3 mice

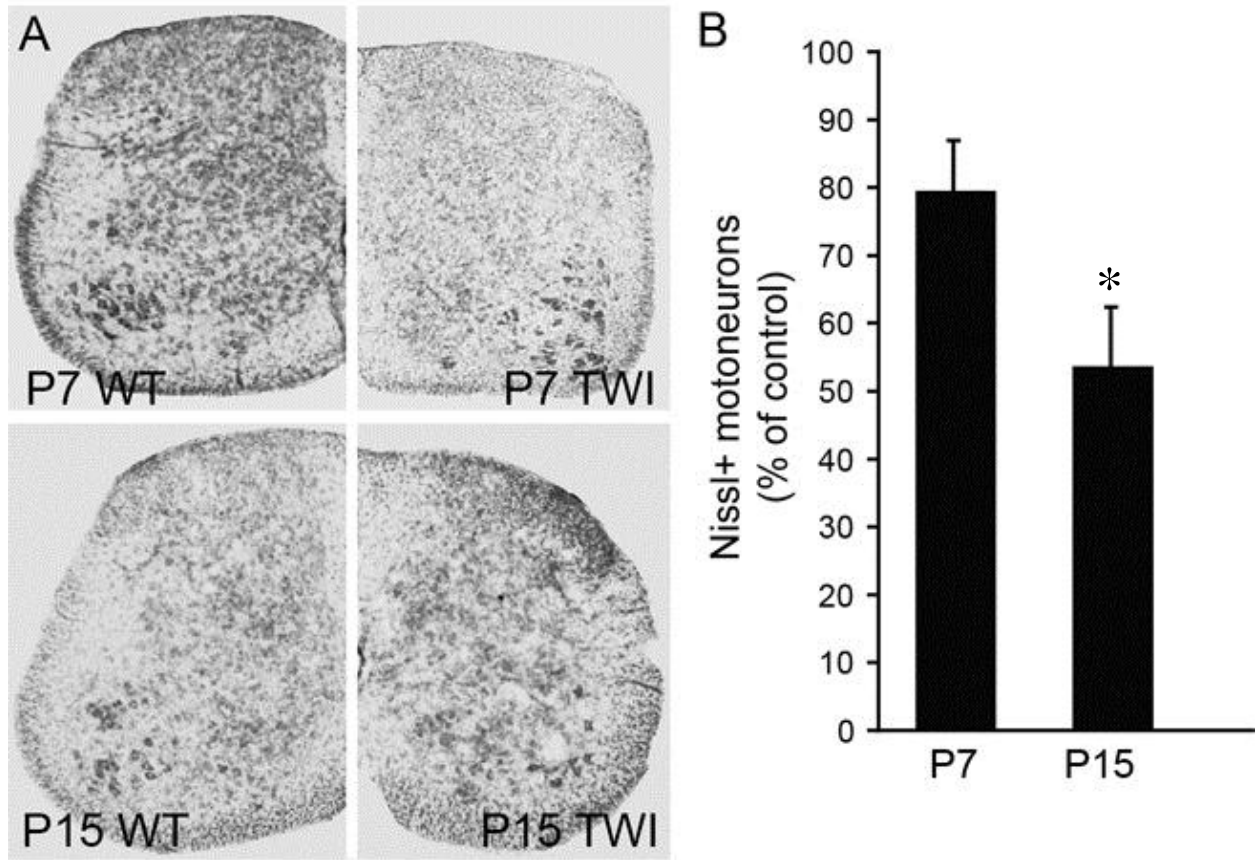


Figure 16 Chromatolysis in the Twitcher mouse

Coronal sections of Wt (left) and twitcher (right) lumbar spinal cords at P7 and P15 processed for Nissl staining show chromatolysis in the mutant tissue (A). Stereological counting of Nissl(+) motoneurons in the ventral horns of the Wt and twitcher spinal cord at P7 and P15. Counting was expressed as Nissl(+) motoneurons per mm^2 . $n=3$ mice. $p<0.05$.

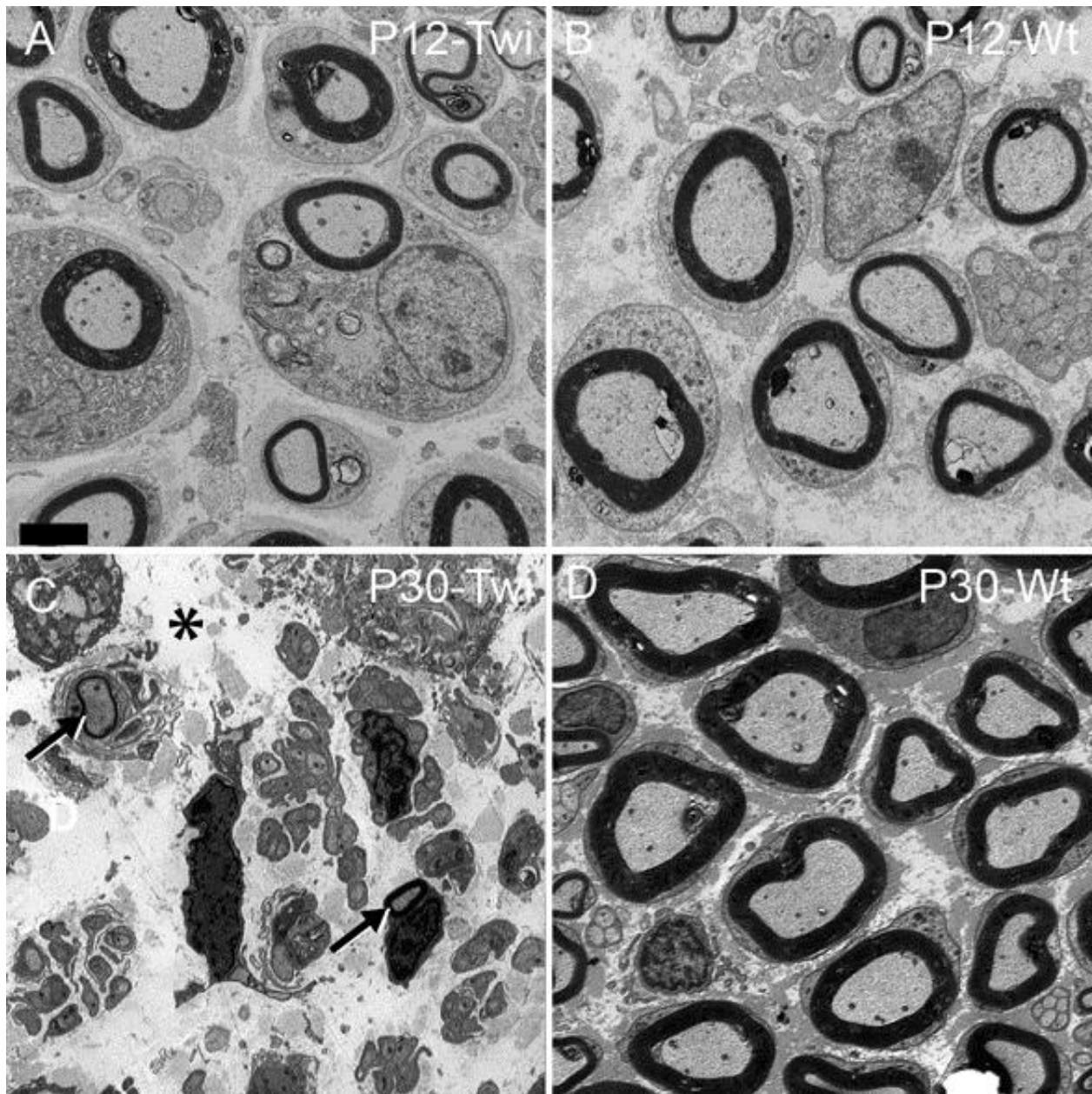


Figure 17 Decrease in diameter of Twitcher axons

Electron micrographs of coronal sections of Wt and twitcher sciatic nerves at P12 and P30 show a decrease in axonal diameter in the Twitcher fibers (A) as compared to age-matched Wt fibers (B). Severely demyelinated and abundant small diameter axons were clearly observed in older (P30) Twitcher nerves (C). All images are at the same magnification (bar in A=2 μ m). Arrows and asterisk in C point to myelinated axons and edema, respectively.

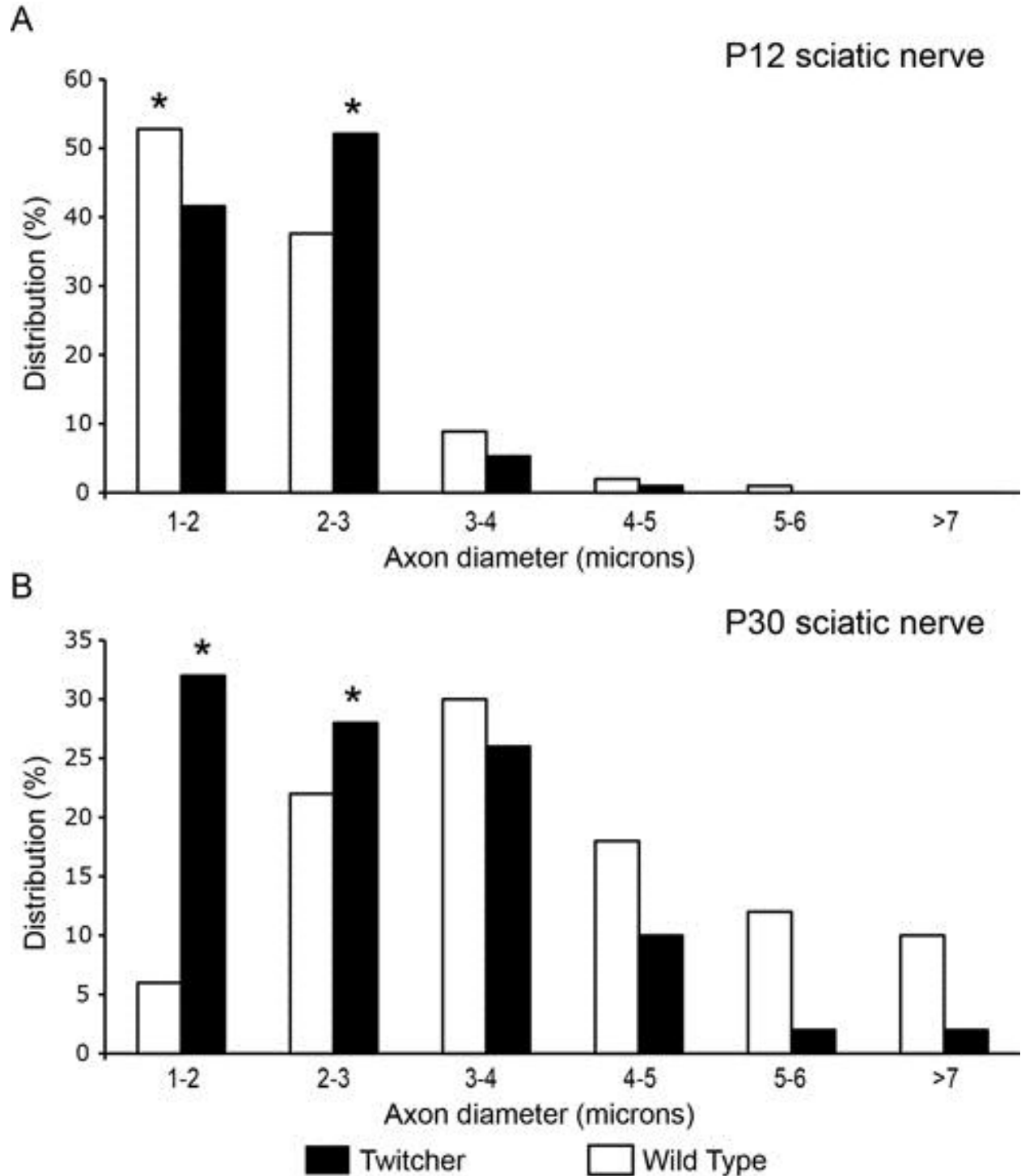


Figure 18 Prevalence of small-diameter fibers in Twitcher sciatic nerves

Distribution profiles based on axonal diameter in P12 (A) and P30 (B) sciatic nerves showed a growing increase in small-caliber axons. A minimum of 50 axons was counted per each nerve (n=3 nerves/time point/genotype). Data were analyzed by ANOVA/post hoc paired test. $p < 0.05$.

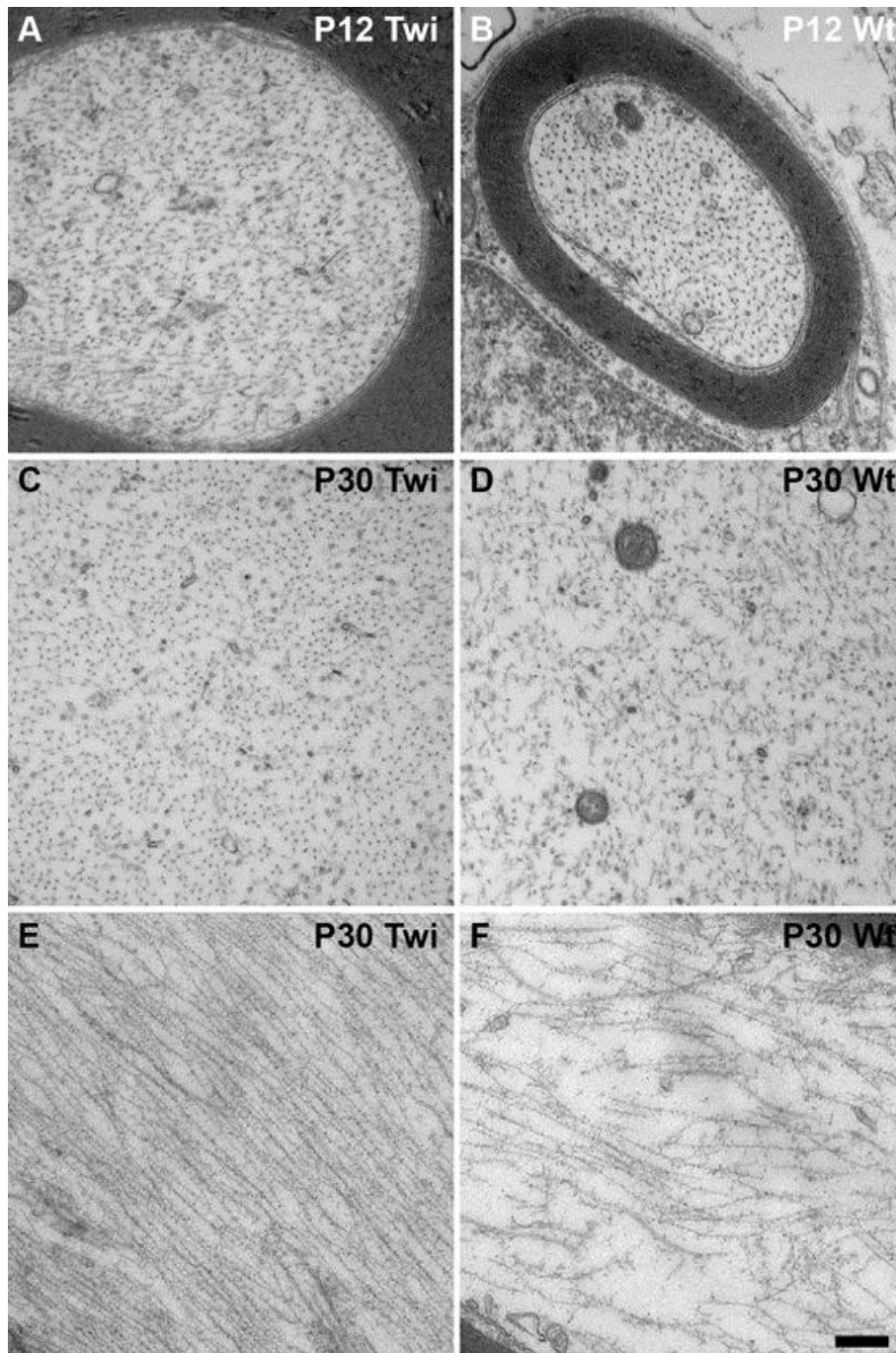


Figure 19 Lower density of NFs in the Twitcher mouse

Increased packing of NFs in Twitcher axons. A–D) High-magnification TEM of coronal sections of P12 and P30 sciatic nerves revealed slightly increased NF density at P12 (A) but significantly higher density at P30 in Twitcher axons (C) as compared to Wt axons (B and D, respectively). E,F) High-magnification TEM of longitudinal sections of P30 Wt (E) and twitcher (F) sciatic nerves showed several gaps among NF bundles in the Wt nerve. Twitcher NFs were tightly packed together, further confirming the increase in NF density in the mutant axons. (Bar=0.5 μm for A,B and =0.250 μm for C–F).

between P12 and P30 in WT nerves (Fig. 20A) but a consistently high NF density in Twitcher axons at both developmental times (Fig. 20B). Immunoblotting analyses of the total amount of NF proteins in sciatic nerves showed decreased levels of each NF protein in the nerves of Twitcher mice (Fig. 20C). Real-time PCR analysis of each NF mRNA revealed no statistically significant difference in the spinal cord of Twitcher and age-matched WT mice (Fig. 21P, 21Q), suggesting absence of gene transcription deficits.

5.10 Reduced phosphorylation of mutant NFs.

The higher densities of NFs in the mutant nerve suggested abnormal phosphorylation of NFs. To test this possibility, we first examined coronal sections of WT and Twitcher spinal cords stained for phosphorylated epitopes on NF-M and NF-H using monoclonal antibody SMI31; the number of SMI31+ fibers was noticeably reduced in Twitcher spinal cords, which was most evident in axons within the ventral white matter (compare Fig. 21A and 21B with 21E and 21F, respectively). Subsequent analysis of longitudinal sections of cords stained using the SMI32 antibody, which binds to dephosphorylated epitopes on NF-H, and using tissue isolated from the TWI-YFPax reporter model (Castelvetri et al., 2011), showed increased SMI32 immunostaining in Twitcher cords, especially in axons with clear signs of dystrophy (swellings, breaks; arrows in Fig. 21C, 21D and 21G). In contrast, WT axons were minimally stained with SMI32 (Fig. 21H). Finally, analysis of longitudinal sections of sciatic nerves from TWI-YFPax and age-matched WT-YFPax mice (P30) immunolabeled with the SMI31 antibody indicated a clear reduction in SMI31 binding in the mutant axons (compare Fig. 21I and 21J with 21L and 21M, respectively). Further assessment for changes in phosphorylation of NF in Twitcher mice, western blotting of protein extracts from sciatic nerves (obtained between P7 and P40) using antibody SMI31

revealed a clear reduction of phosphorylated NM-F levels at each developmental stage (Fig. 21K, pNFM). Analyses for the levels of both phosphorylated NF-M (Fig. 21N) and NF-H (Fig. 21O) showed significant ($p < 0.01$) reduction of these cytoskeletal proteins in mutant nerves at P15 and P30 but not at P7.

5.11 Increased activity of serine/threonine protein phosphatases in Twitcher sciatic nerves.

Phosphorylation of NFs is regulated by Erk1/2, CDK5, p35 and SAPK1b kinases and ser/thr protein phosphatases PP1 and PP2A (Perrot et al., 2008). To determine whether PP1 and/or PP2A were involved in abnormal dephosphorylation of mutant NFs, we first determined the activation levels for both phosphatases in protein extracts from WT and Twitcher sciatic nerves. Quantitative analysis indicated a significant increase in the activity for both PP1 and PP2A at P30, whereas at P7, only PP2A increased significantly in mutant sciatic nerves (Fig. 22A, 22B). Further analysis of longitudinal sections of sciatic nerves immunolabeled with antibodies against PP1 (Fig. 22C, 22E) and PP2A (Fig. 22D, 22F) revealed an increase in PP1 in mutant sciatic nerves (Fig. 22C) and an even greater increase in PP2A (Fig. 22D; black arrows indicate axons immunolabeled for PP2A; white arrow points to the surrounding area of myelin sheath).

5.12 Psychosine is sufficient to increase PP1 and PP2A activity in neuronal cells.

To test the possibility that psychosine might underlie the observed activation of PP1 and PP2A, we first carried out a correlation analysis of levels of all three molecules in mutant sciatic nerves. Indeed, we found a strong correlation between the elevated levels of psychosine (Fig. 23A) and PP2A activity in the mutant nerve at P7 and P30 ($r_{P7} = 0.994$ and $r_{P30} = 1$, respectively),

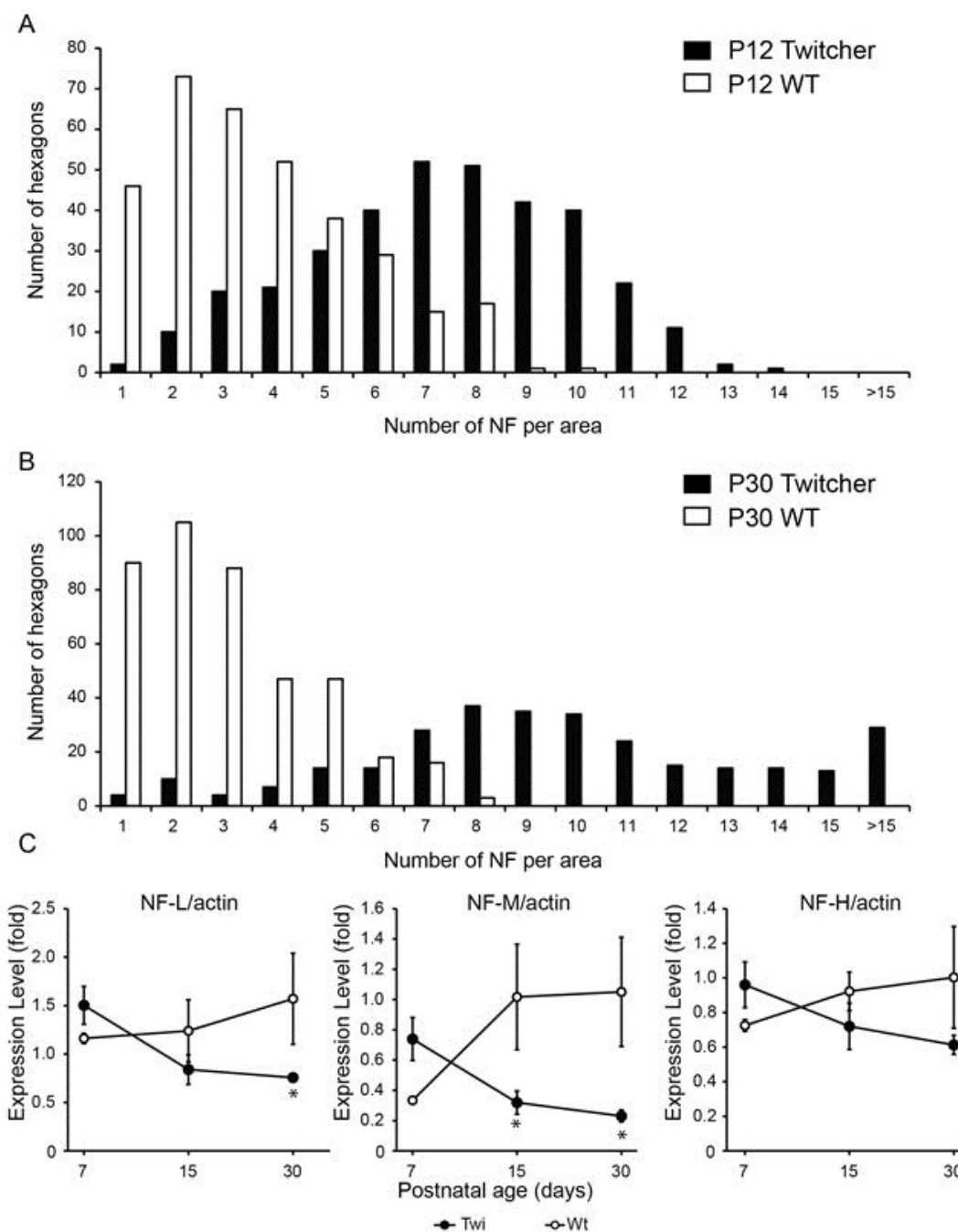


Figure 20 Lower levels of NFs in the Twitcher mouse

NF abnormalities in Twitcher sciatic nerves. A,B) NF density in P12 (A) and P30 (B) Wt and Twitcher sciatic nerves was quantitated by counting the NFs per hexagonal grid laid on high-magnification EM pictures of sciatic nerve coronal section. Twitcher axons had significantly more hexagons with higher number of NFs at both time points, indicating the increased NF density in Twitcher mice. C) Quantitation of Western blot analysis of NF-L, NF-M and NF-H in P7, P15 and P30 Wt and Twitcher sciatic nerves. Levels of all three proteins were decreased at P15 and P30, as assessed using ImageJ software and by normalizing to actin levels. Data are mean \pm SEM of four independent nerves per genotype per time point. Data were analyzed by ANOVA/post hoc paired test. Asterisk indicates $p < 0.05$.

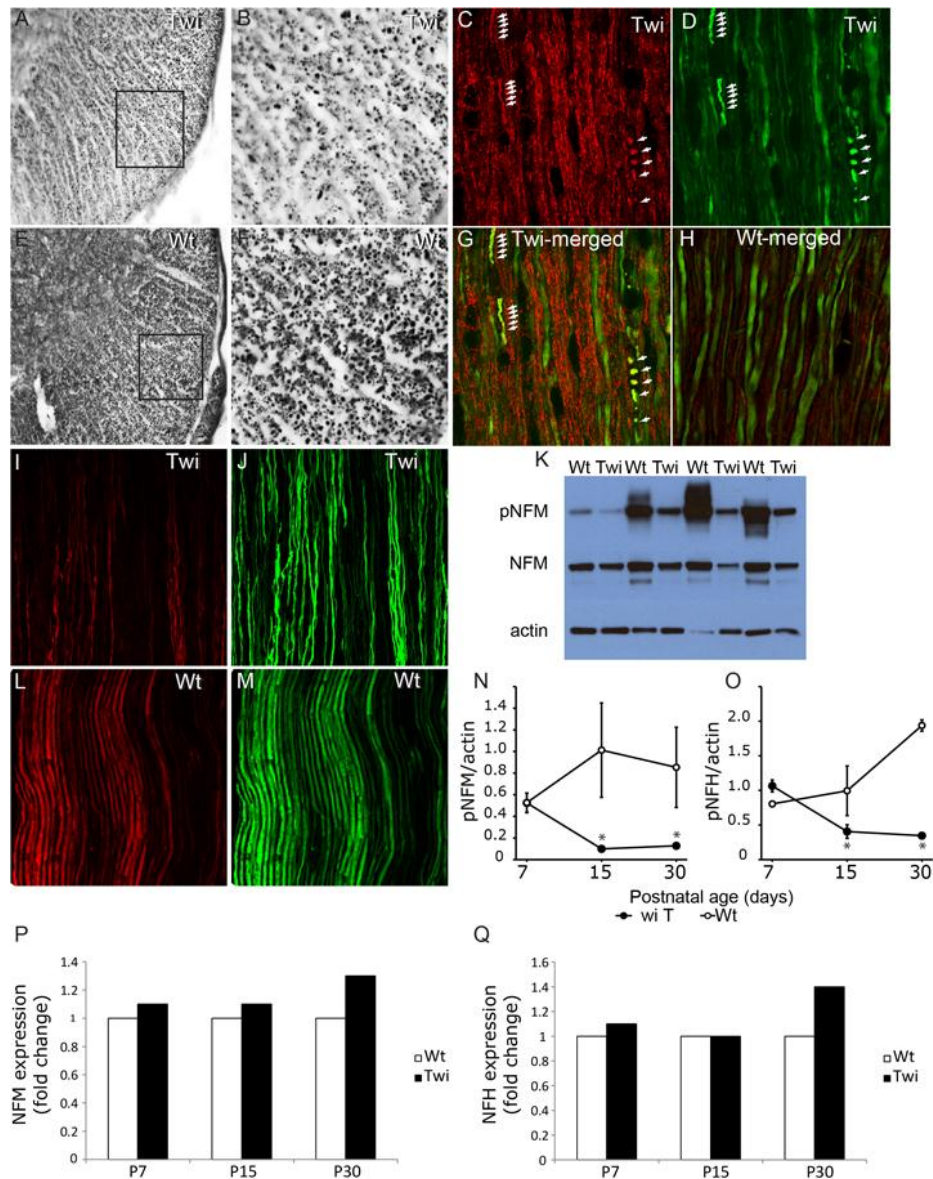


Figure 21 Reduced phosphorylation of mutant NFs

A, B, E, F) Immunohistochemical staining of P30 spinal cord coronal sections from twitcher (A, enlarged in B) and Wt (E, enlarged in F) with monoclonal antibody SMI31 shows a decrease in the density of SMI31+ fibers, especially in the ventral white matter, in Twitcher mice. C, D, G, H) Immunofluorescence staining of spinal cord longitudinal sections from WT-YFPax (H) and Twitcher-YFPax P30 mice (C, D and merged image in G) for SMI32 (red) and YFP (green) shows the stronger reactivity for SMI32 in the twitcher fibers and the accumulation of dephosphorylated NFs in sites of axonal swellings and breaks (white arrows). I, J, L, M) Immunofluorescence staining of sciatic nerve longitudinal sections from WT-YFPax (L and M) and Twitcher-YFPax (I and J) P30 mice for SMI31 (red) and YFP (green) shows stronger SMI31 reactivity in the WT tissue (L) as compared to Twitcher tissue (I), indicating the loss of NF phosphorylation in the Twitcher peripheral nervous system. K) Representative Western blot of phosphorylated NF (pNF-M, obtained with monoclonal antibody SMI31) and total NF-M (obtained with monoclonal antibody RMO189) of P10, P20, P30 and P40 Wt and twitcher sciatic nerves, with actin as a loading control. N, O) Quantitation of Western blot analyses of pNF-M and pNF-H, respectively, in sciatic nerves of P7, P15 and P30 WT and Twitcher mice and normalizing to actin. Data are mean \pm SEM of four replicates. Data were analyzed by ANOVA/post hoc paired test. Asterisk indicates $p < 0.01$. P, Q) qRT-PCR analysis of the mRNA for NFM and NFH in spinal cords of P7, P15 and P30 Wt and Twitcher animals.

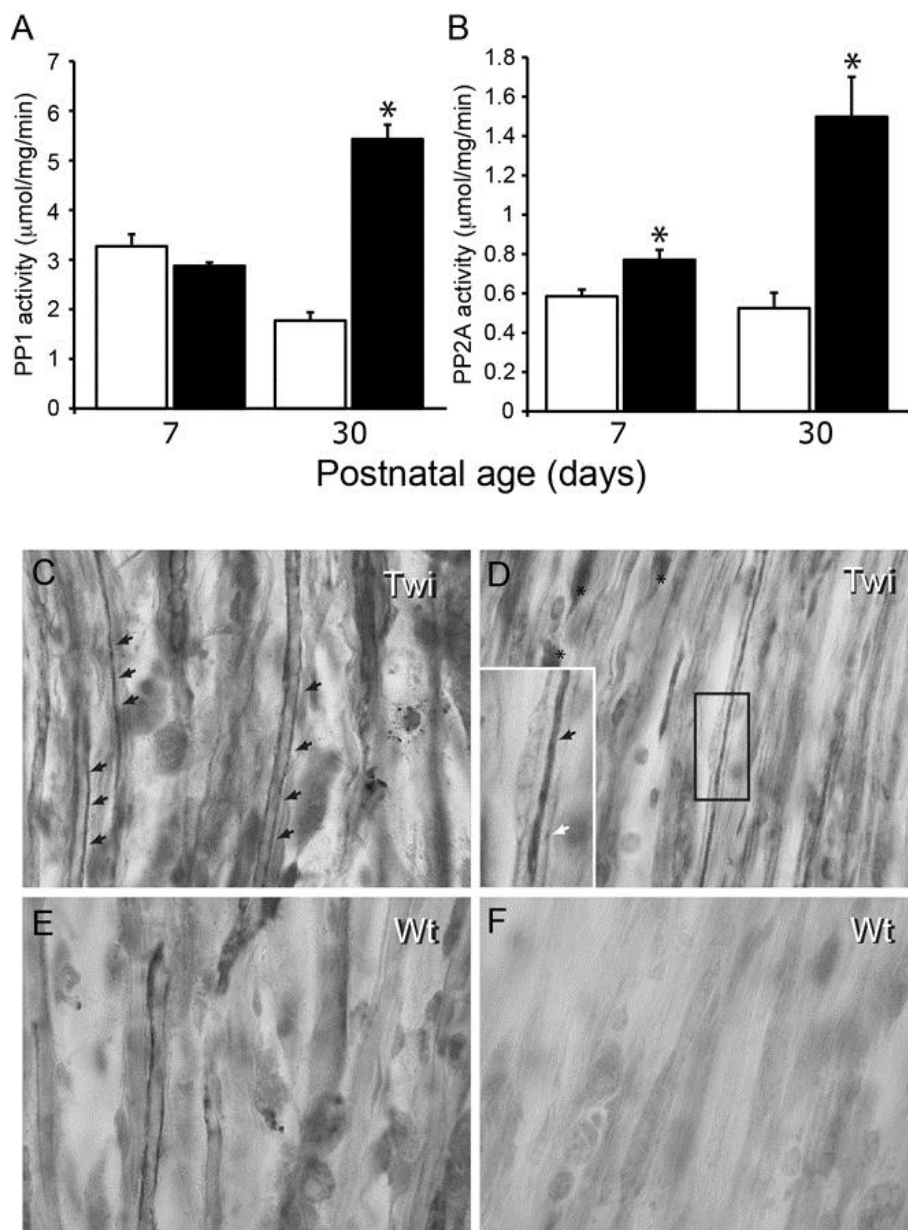


Figure 22 *Increased activity of serine/threonine protein phosphatases in Twitcher sciatic nerves*

Increased activation of PP1 and PP2A in the Twitcher sciatic nerve. A, B) Quantitation of PP1 (A) and PP2A (B) enzymatic activity in lysates from P7 and P30 sciatic nerves of Wt and twitcher mice showed that both enzymes in twitcher nerves were strongly over-activated at P30, while only PP2A was significantly more active in the P7 tissue. Activity is expressed as micromol substrate (DiFMUP)/mg protein/min. Data are mean \pm SEM of three replicates. Data were analyzed by ANOVA/post hoc paired test. Asterisk indicates $p < 0.01$. C–F) Representative immunohistochemical staining for PP2A in P30 Twitcher (C,D) and Wt (E,F) sciatic nerves shows the higher frequency of fibers intensely stained for PP2A in the twitcher nerve (black arrows in C and D). Rarely, PP2A+ myelinating Schwann cells were also detected in Twitcher tissue (asterisks in D). Enlarged in D, the presence of PP2A in a mutant axon is readily observed (black arrow in D), surrounded by the myelinating sheath (white arrow in D).

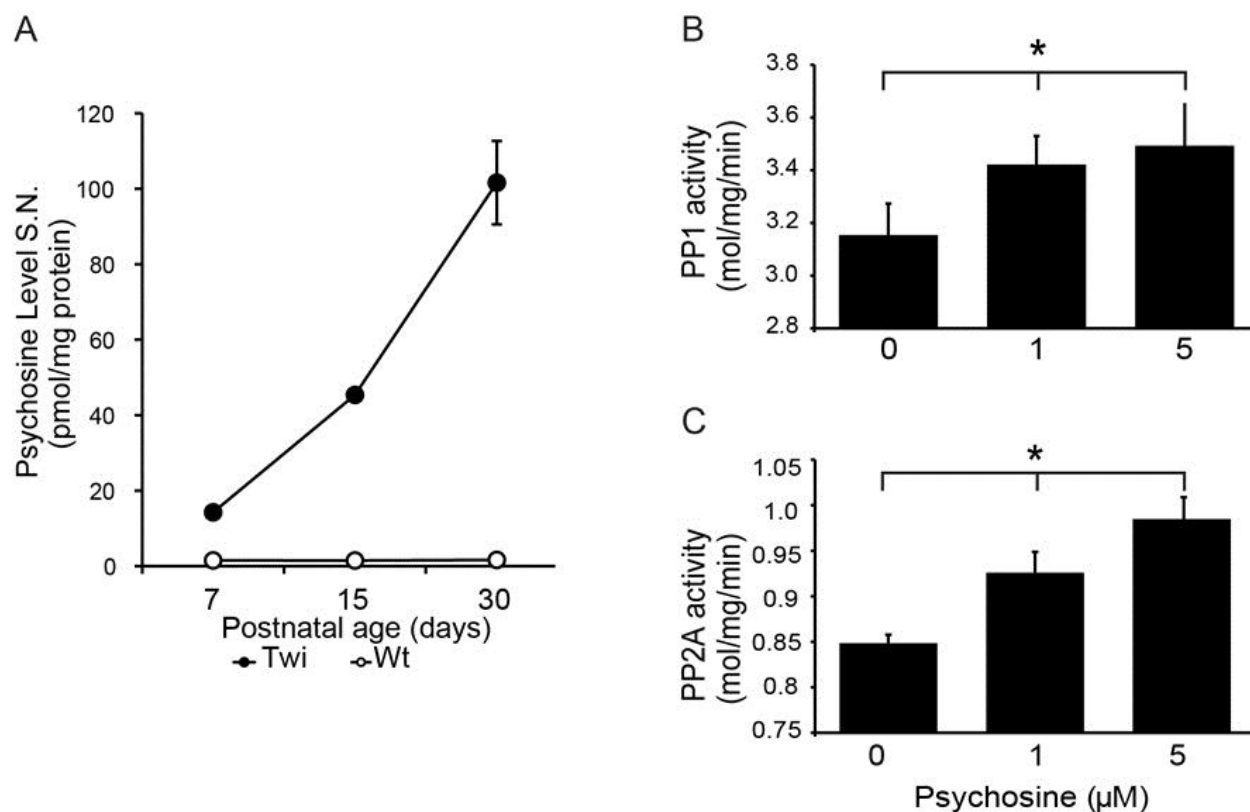


Figure 23 Psychosine is sufficient to increase PP1 and PP2A activity in neuronal cells NSC34

A) Quantitation of psychosine by mass spectrometry in P30 Wt and twitcher sciatic nerves indicated significantly higher levels of psychosine already at P7 in the Twitcher tissue, with accumulation progressively increasing over the course of the disease. Data are mean±SEM from 4 nerves per time point per genotype. Data were analyzed by ANOVA/post hoc paired test. Asterisk indicates $p < 0.01$. B,C) Quantitation of PP1 (B) and PP2A (C) enzymatic activities in NSC34 cells treated with 0, 1 or 5 μM psychosine for 3 h, showed that psychosine induces a dose-dependent increase in phosphatase activity. Activity is expressed as μmol substrate (DiFMUP)/mg protein/min. Data is mean±SEM of three replicates. Data were analyzed by t-test of Student. Asterisk indicates $p < 0.05$.

whereas the correlation with PP1 levels was significant only at P30 ($r_{P30}=0.932$). To test whether psychosine is sufficient to modify phosphatase activities, PP1 and PP2A activity was measured in immortalized NSC34 motor neuronal cells exposed to various concentrations of psychosine; activities of both PP1 and PP2A were significantly increased (Fig. 23B, 23C) in a psychosine concentration-dependent manner.

To determine whether psychosine leads to dephosphorylation of NFs through deregulated activities of PP1 and PP2A, we assessed these activities in NSC34 cells incubated with 5 μ M psychosine and with 10 nM okadaic acid, a broad phosphatase inhibitor that is non-toxic at this concentration (Atkinson et al., 2009). Induction of PP1 activity was efficiently blocked by 10 nM okadaic acid in these cultures, while blockage of PP2A activity was less efficient (Fig. 24A). Western analysis for changes in levels of phosphorylated NF using protein extracts from treated and control cells labeled with SMI31 monoclonal antibody showed that psychosine was sufficient to induce significant dephosphorylation of NF-M, while the presence of okadaic acid almost completely inhibited this psychosine-triggered dephosphorylation (Fig. 24B, 24C). In these experiments, psychosine was administered in the cell media, where appears to be rapidly taken up by the cells. To understand if GALC deficiency has a cell autonomous effect on neurons, we cultured Wt and Twitcher embryonic cortical neurons for 8 days. The cells were then collected and processed for immunoblot analysis for total and phosphorylated NFs. A significant reduction in NF phosphorylation was observed in the Twitcher cultures (Fig. 24 representative blot in D and quantification in E).

5.13 Fast axonal transport is reduced in Twitcher sciatic nerves.

To determine whether FAT was altered in the Twitcher mouse, we performed ligations of sciatic nerves. In this experimental model, accumulation of transported cargoes at the ligation site provides an indication of the transport efficiency. Wt and Twitcher mice at P30 were unilaterally ligated for 6 hours and imm of the proximal and distal stumps of the nerve (relative to the spinal cord) were collected and processed for immunoblot analysis. Reduced accumulations of KHC, the synaptic marker SNAP25, and the mitochondrial marker HSP60 were found in ligated Twitcher nerves (Fig. 25A, 25C). The decrease in the transport of mitochondria and synaptic vesicles, both with transport modalities substantially different, indicates in principle a general inhibition of the transport of axonal cargoes, rather than a defect in the transport of specific organelles.

Because axonal transport defects were observed in other myelin disorders (de Waegh and Brady, 1990; de Waegh and Brady, 1991; de Waegh et al., 1992), this raised the question whether demyelination was contributing to this defect. To investigate this possibility, ligation experiments were performed in P7 Wt and Twitcher animals. Again, significant reductions in the amount of accumulated markers were observed in mutant nerves (Fig. 25B). To confirm that these accumulations were consistent with membrane cargoes, TEM analyses were performed, which confirmed the immunoblotting results. Figure 26 shows visible reductions of accumulated membranous material in both myelinated and unmyelinated Twitcher axons (Fig. 26D, 26E, 26F). Vesicular structures and dense bodies were observed beneath the plasma membrane in the unligated Twitcher control (arrows in Fig. 26D). The presence of these vesicular accumulations might indicate a defect in the sorting of the transported cargoes, a process that is tightly regulated by specific enzymatic activities (Runnegar et al., 1999; Morfini et al., 2004; Morfini et al., 2007b; Hooper et al., 2008).

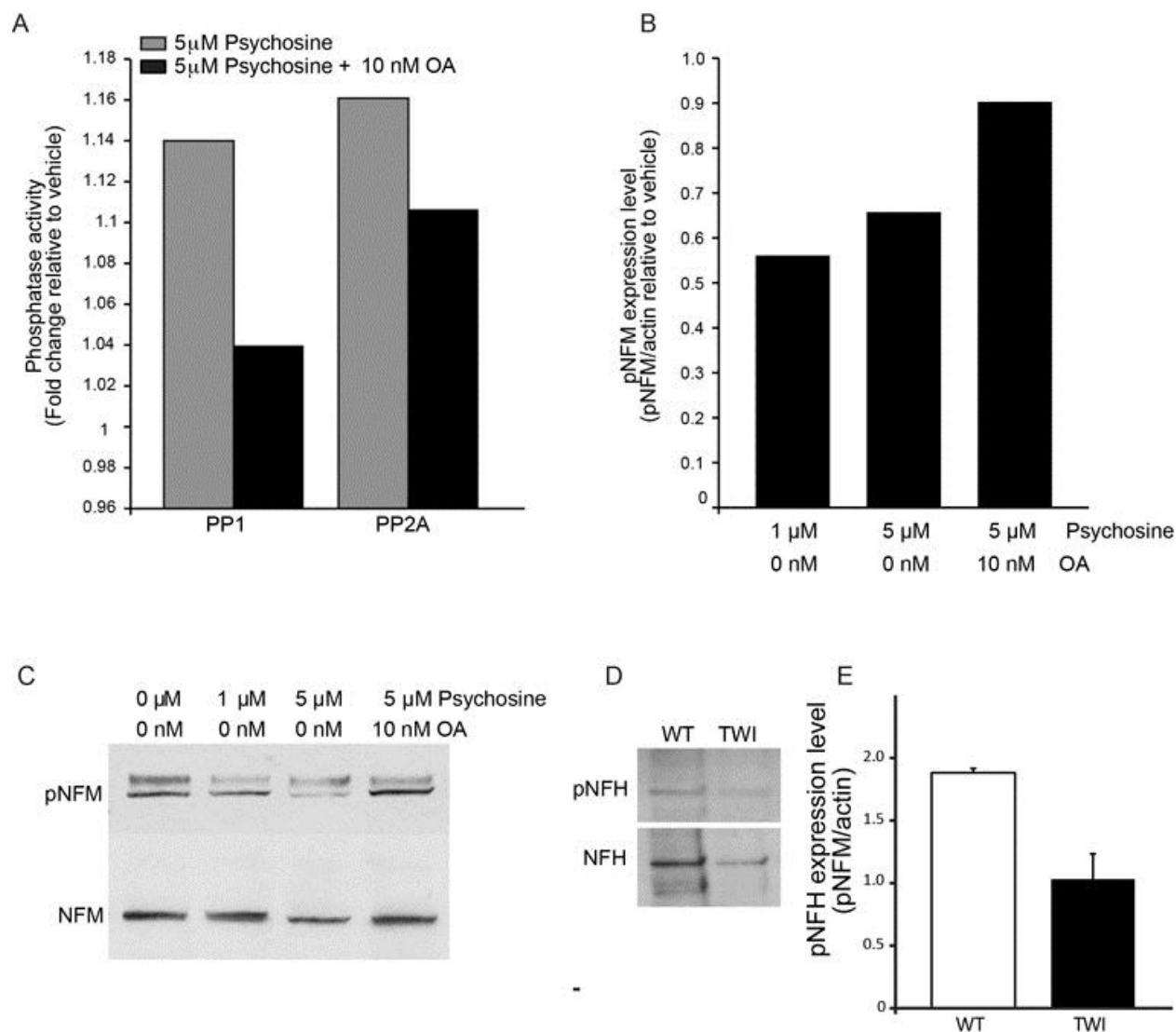


Figure 24 Psychosine induces the dephosphorylation of NFs through PP1 and PP2A

Okadaic acid protects NF from dephosphorylation triggered by psychosine. A) NSC34 cells incubated with 5 μ M psychosine and 10 nM okadaic acid (OA) for 3 h showed significant inhibition of both PP1 and PP2A activity. Data is expressed as fold-change of phosphatase enzymatic activity relative to the vehicle (n=3). B, C) Analysis of NSC34 cells treated with vehicle, 1 or 5 μ M psychosine for 3 h and processed for immunoblotting detection of pNF-M and total NF-M indicated that psychosine triggers NF-M dephosphorylation (quantitation in B using ImageJ and normalizing the amount of pNF-M with respect to actin; representative Western blot in C), and that OA prevents this dephosphorylation. Data is expressed as fold-change relative to the vehicle (n=3). D-E) Similar results were observed when primary cortical neurons were incubated with psychosine and a reduction in the pNF was observed (blot in D and quantification in E). F-G) Primary cortical neurons from Wt and Twitcher mice were cultured for 8 days and the amount of pNF was quantified by western blotting. A significant reduction in pNF was observed in the Twitcher neurons (blot in F and quantification in G). Data is mean \pm SEM of three replicates. Data were analyzed by t-test of Student. Asterisk indicates p<0.05.

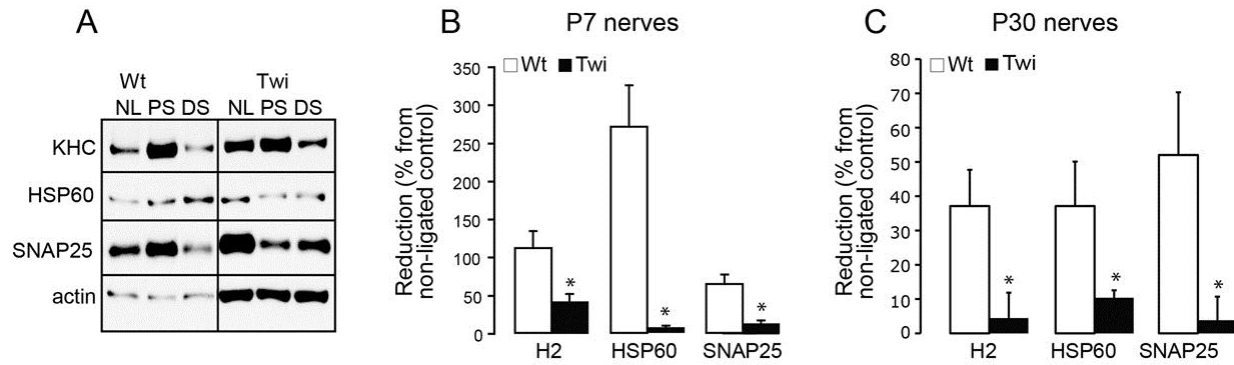


Figure 25 Evidence of defective axonal transport in the Twitcher mouse

A) Western blot analysis of the non-ligated control (NL) and of the proximal (PS) and distal (DS) stumps of the ligated Wt and twitcher (right panel) nerves. While the WT accumulates mitochondria (represented by the mitochondrial protein HSP60), synaptic vesicles (represented by the synaptic vesicle SNAP25) and KHC (antibody H2), ligated twitcher showed little or no accumulation of any of the transported molecules. The experiment was run in triplicates, and the bands of the immunoblot were quantified. Values were averaged and normalized to the loading control (actin). B-C) Quantification of the ligation experiment (proximal stumps) performed on the P7 (C) and P30 (D) Wt and twitcher animals. The decrease in the accumulation of transported cargoes was evident already at P7, when demyelination is not present. Data are mean \pm SEM of three replicates. Data were analyzed by t-test of Student. Asterisk indicates $p < 0.05$.

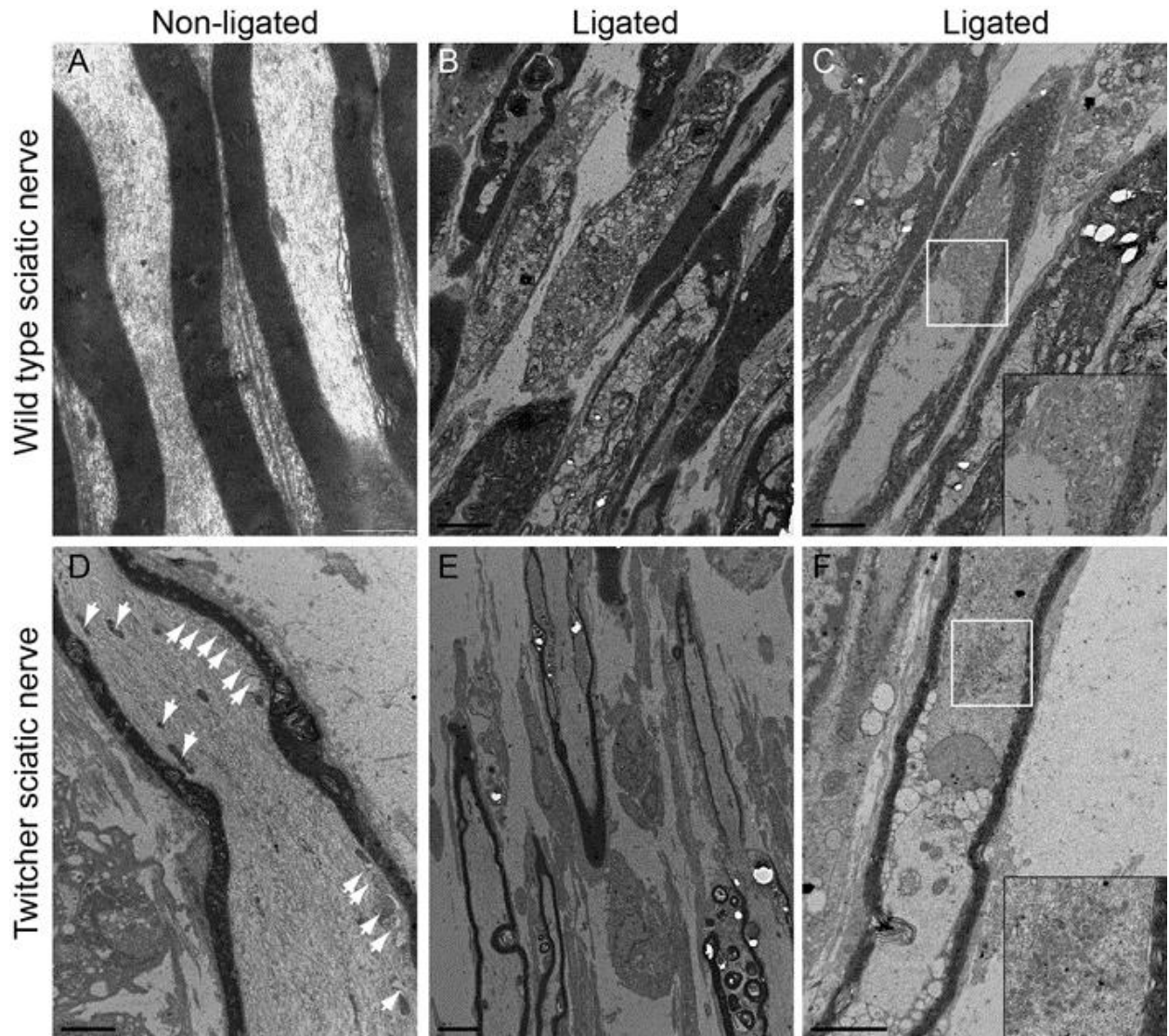


Figure 26 *FAT is deficient in myelinated Twitcher axons*

TEM pictures of non-ligated (A,D) and ligated (B,C,E,F) wild type (A-C) and twitcher (D-F) sciatic nerves. The Wt axons displayed abundant accumulation of vesicular material towards the site of ligation (B,C), while several twitcher axons was significantly less (E). Some mutant axons showed accumulation of vesicular material nearby the ligation zone (E, and boxed area), suggesting that FAT defects may not be affecting all of the axons. White arrows in D point to vesicular material already accumulating in unligated mutant axons. Bar=2 μ m

5.14 Defects in FAT involve GSK3 β

Defects in FAT could be affecting either or both anterograde and retrograde directions. Because of the complexity of this, we focused on the anterograde transport. We hypothesized that the observed FAT deficiency involved changes in phosphorylation of kinesins, and likely those involving the PP1/GSK3 β pathway, which has already been implicated in pathological alterations of FAT (Morfini et al., 2006; Morfini et al., 2009b; Kanaan et al., 2011). First, we measured for the activation of GSK3 β , by immunoblotting for total and phosphorylated GSK3 β . Phosphorylation of serine 9 of GSK3 β acts as an on/off-switch, inactivating the protein (Fig. 27). Therefore, the ratio of phosphorylated over total GSK3 β is an indirect measurement of the enzyme activation. Our analysis showed increased activation of GSK3 β in the Twitcher spinal cord and sciatic nerve, albeit at different time points. In the mutant spinal cord, more GSK3 β was activated at P7 than at P30, while the opposite was detected in the sciatic nerve (Fig. 28B-28E). The discrepancy in the time of activation of the kinase could be explained by the presence of GSK3 β in several cells of the nervous tissue, like myelinating glia and microglia (Ogata et al., 2004; Azim and Butt, 2011; Wang et al., 2011). GSK3 β has several functions, which often depend on the cell type and its kinase activity. Because the shown data were obtained from whole tissue lysates, it is likely that the change in ser9 phosphorylation in neurons is “diluted” by the overall enzyme levels in the tissue. It is also possible that GSK3 β activation might be differentially affected by the mutation, depending on the cell type. Further studies will be required to determine GSK3 β phosphorylation in other neural cell types.

GSK3 β regulates FAT mainly through the phosphorylation of KLC subunits of the motor complex, which induces the detachment of the cargo and the decrease in anterograde transport. Thus measurement of phosphorylated KLC is a good indicator of the status of this regulatory

pathway. To examine this aspect, we immunoblotted spinal cord and sciatic nerve lysates with the monoclonal antibody 63-90, which binds to a KLC epitope only if it is not phosphorylated by GSK3 β (Fig. 27). Not surprisingly, a decrease in the intensity of 63-90 binding to KLC was detected in both Twitcher spinal cord and sciatic nerve (Fig. 29A-29D). While these results significantly point to a defective regulation of phosphotransferase activities involved in FAT, we need to also examine for changes in expression of the various components of the motor families. In this respect, preliminary experiments indicate that RNA and protein levels of KIF5 are not significantly different in the twitcher mouse (data not shown).

5.15 Psychosine induces KLC phosphorylation through PP1 and GSK3 β

PP1 is a major regulator of GSK3 β , by dephosphorylating serine9. Because of the increased activation of PP1 observed in Twitcher sciatic nerves and in psychosine-treated cells, we speculated that psychosine could be facilitating the activation of GSK3 β through PP1. To test this hypothesis, NSC34 cells were treated with psychosine, and the protein lysates were analyzed by western blotting for total and phospho-GSK3 β . As expected, psychosine induced a dose-dependent increase in GSK3 β activity, which was completely prevented by 10 nM okadaic acid (Fig. 30A, 30B). Importantly, treatment with psychosine also increased KLC phosphorylation, as determined by the decrease in binding of the 63-90 antibody (Fig. 31A). To test whether psychosine increased KLC phosphorylation through the PP1/GSK3 β pathway, cells were treated with psychosine and either okadaic acid or TDZD8 (a specific non-competitive inhibitor of GSK3 β). Both treatments completely prevented KLC phosphorylation, strongly suggesting that psychosine effects on KLC phosphorylation are mediated by activities of PP1 and GSK3 β (Fig. 31A, 31B).

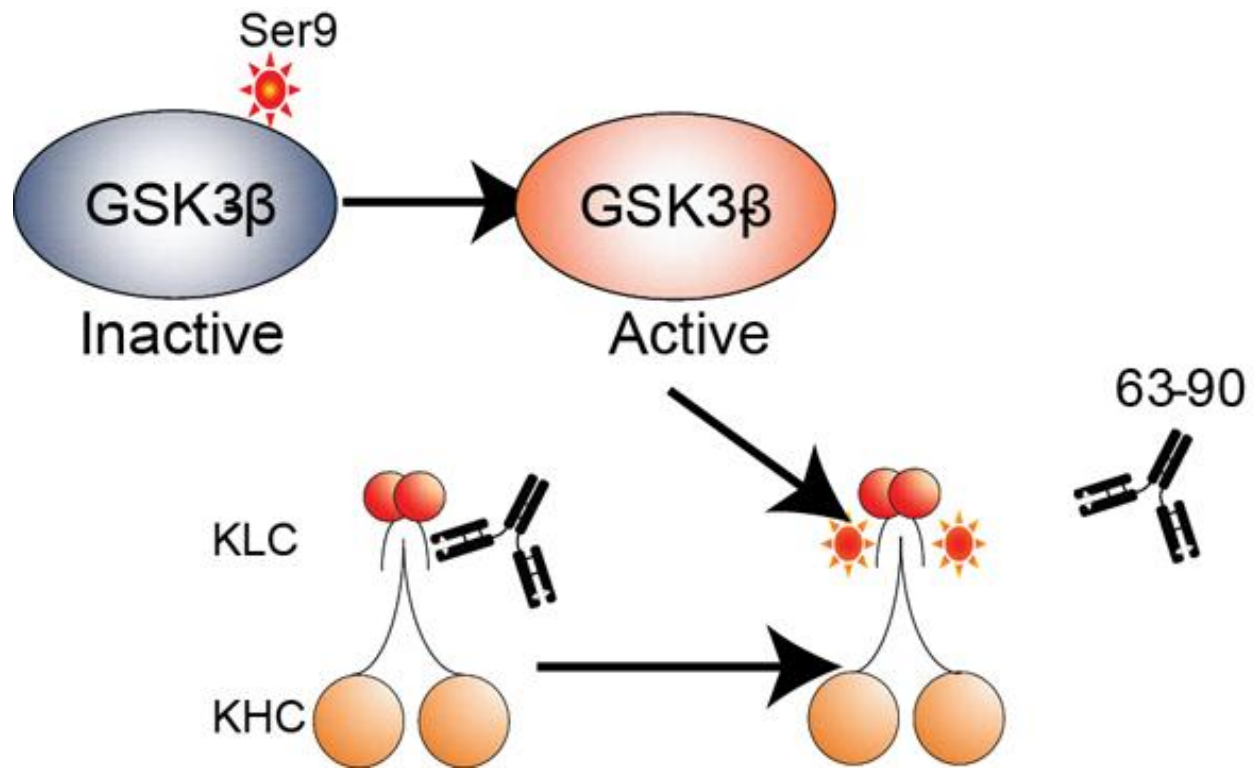


Figure 27 *GSK3 β regulates KLC phosphorylation.*

Removal of the phosphate group on serine 9 of GSK3 β causes its activation. GSK3 β directly phosphorylates KLC, triggering the release of its cargo. The antibody 63-90 binds to dephosphorylated KLC. An increase in KLC phosphorylation causes less immunoreactivity for this antibody.

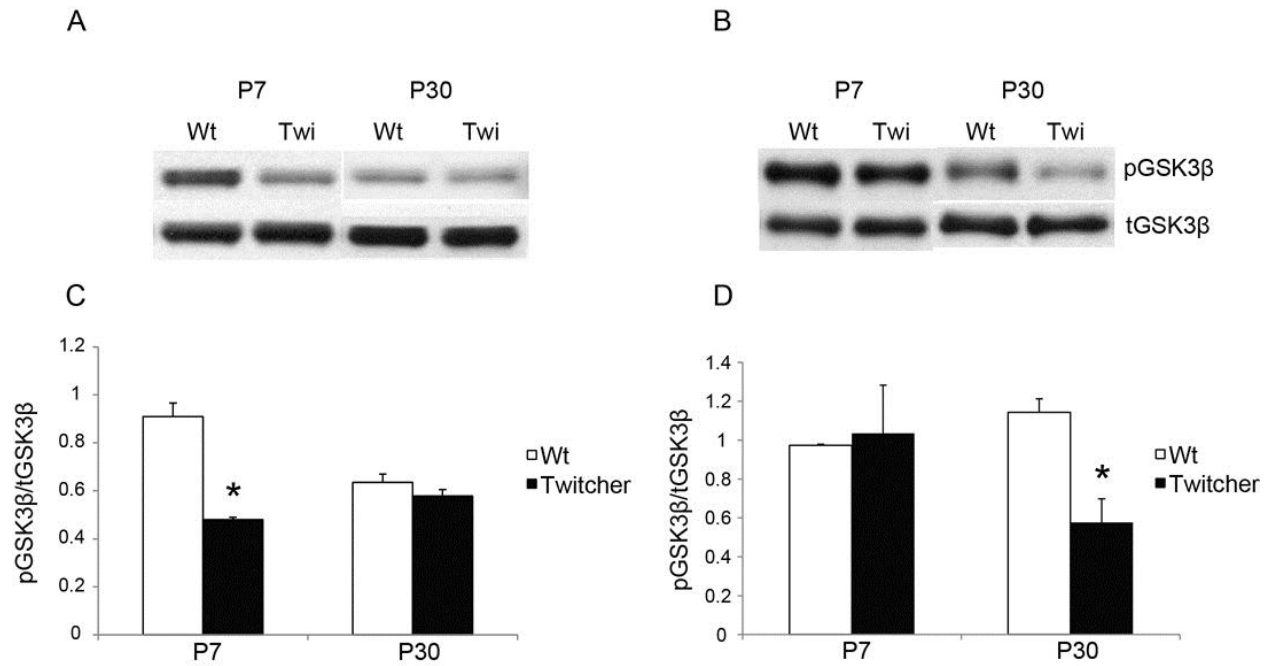


Figure 28 Activation of GSK3β in the Twitcher nervous system

A,B) western blot analysis for total and phospho-GSK3β (serine 9; inactive form) in spinal cord (A) and sciatic nerve (B) of Wt and Twitcher mice (quantification in C and D, respectively). Data are mean±SEM of three replicates. Data were analyzed by t-test of Student. Asterisk indicates $p < 0.05$.

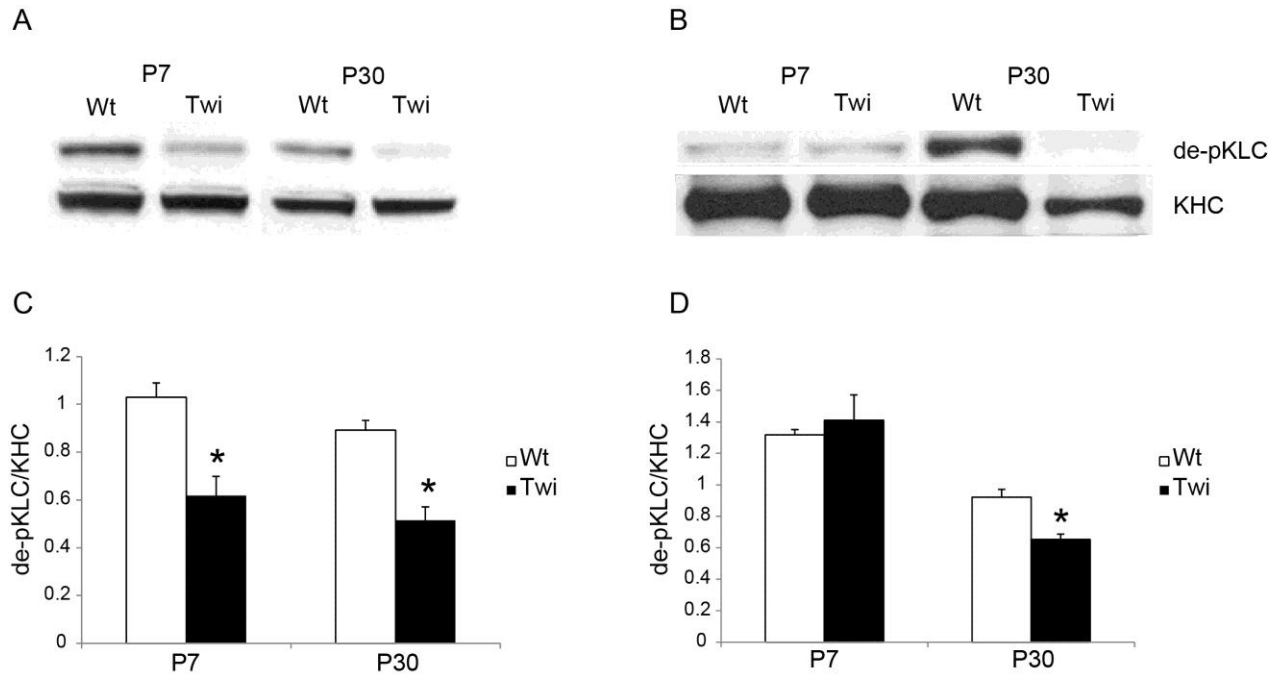


Figure 29 Increased KLC phosphorylation in the Twitcher nervous system

A-B) Western blot analysis for H2 (antibody against KHC) and 63-90 (pKLC) in spinal cord and sciatic nerve of Wt and twitcher mice shows the decrease in immunoreactivity of the antibody at P7 in the spinal cord and at P30 in the sciatic nerve (quantification in C and D, respectively). Data are mean \pm SEM of three replicates. Data were analyzed by t-test of Student. Asterisk indicates $p < 0.05$.

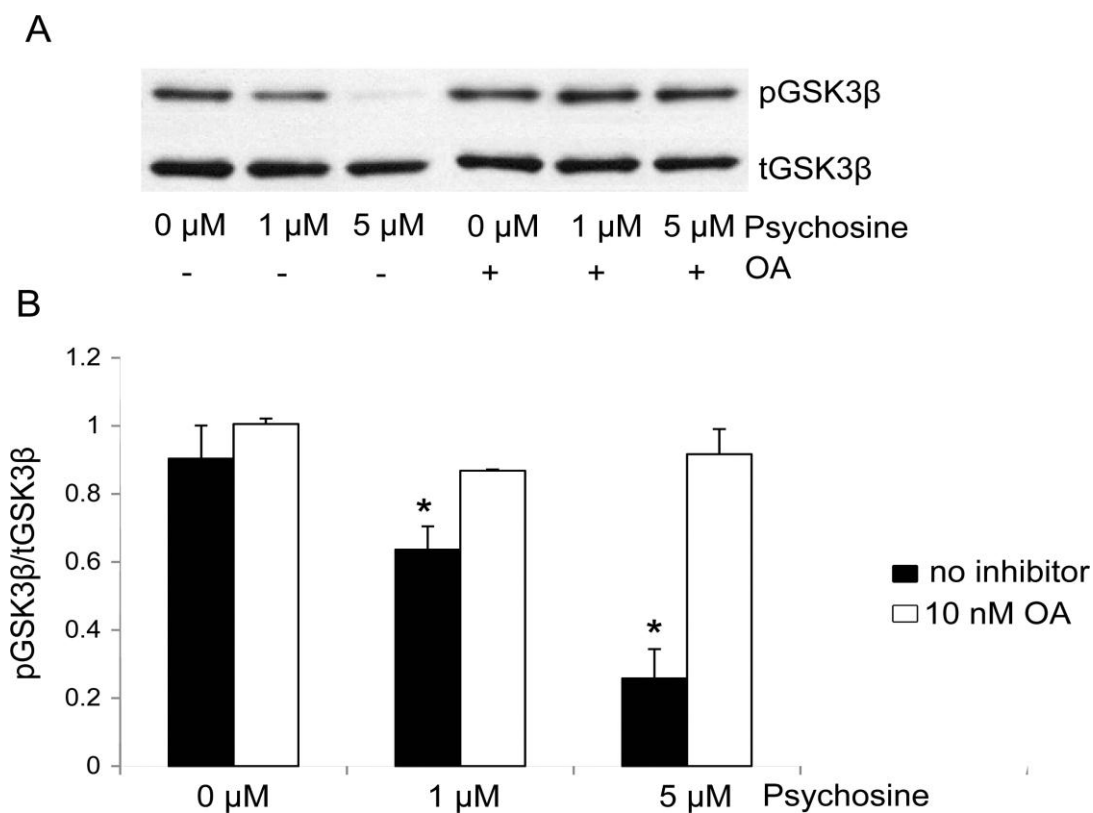


Figure 30 Psychosine induces GSK3β dephosphorylation

A-B) Western blot analysis of NSC34 cell after treatment with 1 and 5 μM psychosine shows the decrease in the amount of phospho-GSK3β (serine 9; inactive form). Co-administration of psychosine and 10 nM OA prevented GSK3β activation (representative bolt in A and quantification in B). Data are mean±SEM of three replicates. Data were analyzed by t-test of Student. Asterisk indicates p<0.05.

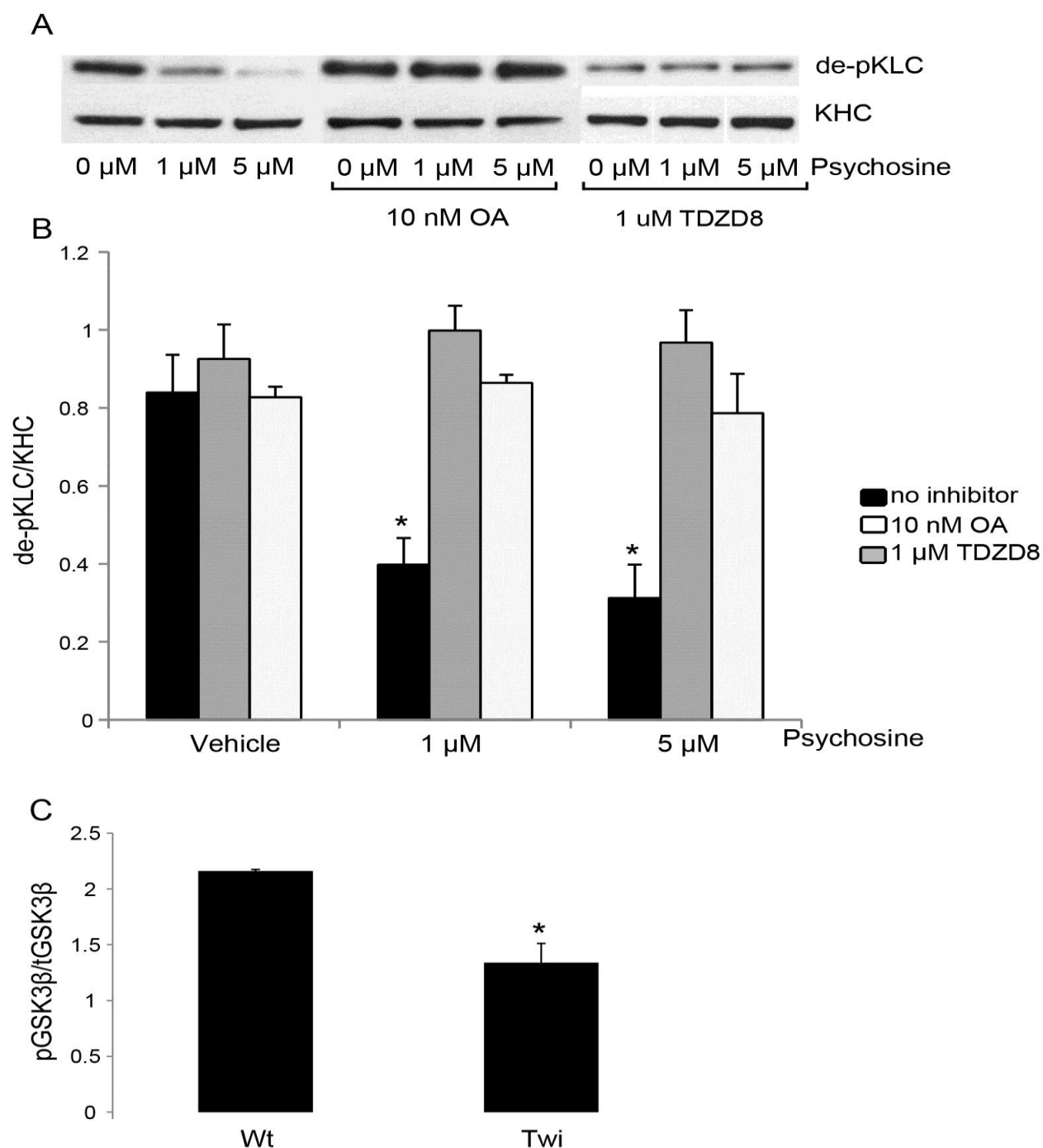


Figure 31 Psychosine induces KLC phosphorylation

A-B) Western blot analysis of psychosine treated cells for H2 (KHC) and 63-90 antibodies, showing that psychosine increases KLC phosphorylation. Both 10 nM OA and 1 μ M TDZD8, a specific non-competitive inhibitor of GSK3 β , prevented KLC phosphorylation, demonstrating the involvement of ser/thr PPs and GSK3 β in psychosine-mediated effect on KLC (representative blot in A and quantification in B). C) Cultures of embryonic Twitcher cortical neurons showed increased activation of GSK3 β , when compared to Wt control cultures (C). Data are mean \pm SEM of three replicates. Data were analyzed by t-test of Student. Asterisk indicates $p < 0.05$.

To understand if psychosine-induced GSK3 β activation was a cell autonomous effect, we measured for active GSK3 β in lysates of Wt and Twitcher primary cortical neurons. Figure 31C shows that indeed, Twitcher neurons contained increased levels of activated GSK3 β , supporting the idea of cell autonomous defect in Twitcher neurons.

5.16 Psychosine is present in Twitcher neurons.

The evidence presented so far suggests that psychosine may be a pathogenic molecule that triggers not only demyelination but also axonal and neurons defects. A relevant question is whether neurons are capable of producing psychosine. To address this possibility, we first determined expression levels of CGT, the enzyme responsible for the synthesis of psychosine (Cleland and Kennedy, 1960), in neurons. Immunohistochemical analysis revealed detectable levels of CGT expression in motoneurons (arrows Fig. 32A) and as expected, in oligodendroglial cells (not-shown). Immunoblotting and real time PCR analyses also showed CGT expression in protein extracts from NSC34 cells (Fig. 32C) and mRNA isolated from cortical neurons, (Fig. 32D). Neuronal expression of GALC was also confirmed by real time PCR, (Fig. 32D). Altogether, these results show that neurons contain the metabolic components for the potential production of psychosine. Next, we measured levels of neuronal psychosine in granule neurons – which are largely unmyelinated- isolated from Twitcher and wild type brains. High performance liquid chromatography tandem mass spectrometry (LC-MS-MS) showed three fold-increase of psychosine in mutant neurons respect levels in control neurons (Fig. 32E, 32F). These results provide evidence that a significant amount of psychosine may accumulate in some twitcher neurons. Further studies will need to address the accumulation of psychosine in other neuronal cells such as motoneurons.

5.17 Psychosine inhibits axonal transport.

Next, we tested whether psychosine was capable to impair vesicular traffic using two in vitro models of axonal transport. Vesicular transport measurements using axoplasm preparations from the squid *Loligo Pelai* have been extensively used to examine the effects and the mechanism of different pathogenic proteins on FAT (Morfini et al., 2002b; Morfini et al., 2004; Morfini et al., 2006; Morfini et al., 2007b; Pigino et al., 2009; Kanaan et al., 2011). Pure preparations of extruded axoplasm isolated from the squid were perfused with different concentrations of psychosine (or related controls) and the speed of vesicular cargoes was recorded over time. Figure 33 shows that perfusion of axoplasms with control D-Sphingosine, the sphingoid base of psychosine, or an enantiomer of psychosine (Kind gift of Dr Mark Sands, Washington University, St Louis) resulted in typical transport rates of 1,5-2 $\mu\text{m}/\text{sec}$ (anterograde FAT) and 1-1,4 $\mu\text{m}/\text{sec}$ (retrograde transport). In contrast, 1 μM and 5 μM psychosine resulted in a strong inhibition of both modes of axonal transport (Fig. 33A, 33B).

Using this model, we confirmed that the psychosine effect on FAT was mediated by the PP1/GSK3 β signaling pathway. Co-perfusion of psychosine and different inhibitors of PP1 (OA and inhibitor-2) or GSK3 β (ING35) showed to ameliorate FAT inhibition, (Fig. 34). Interestingly, the recovery of FAT was not complete, suggesting that other signaling pathways maybe involved in this defect.

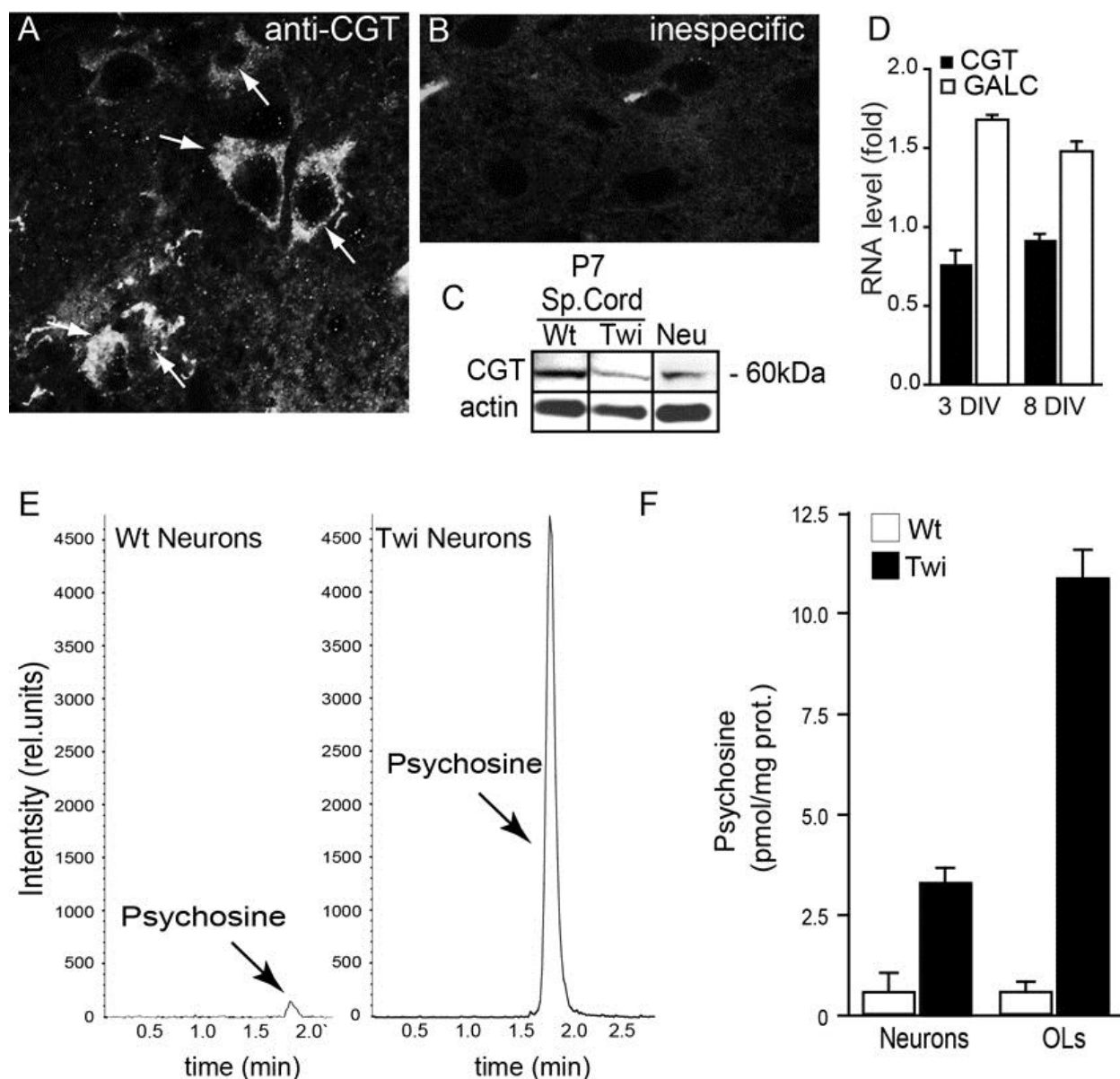


Figure 32 Psychosine in Twitcher neurons

A-B) Confocal imaging of the CGT enzyme in motor neurons from the ventral horns of the spinal cord of P7 wild-type mice. Non-specific binding of secondary antibodies is shown in B. C) Western blot analysis of CGT expression levels in lysates from P7 Wt and twitcher spinal (sp) cords and from NSC34 cells (Neu). Actin was used as a loading control. D) qRT-PCR analysis of GALC and CGT mRNA expression levels in wild-type primary cultures of cortical neurons cultured for 3 and 8 days in vitro (DIV). Results are shown as fold increase with respect to levels in one DIV cultures. E-F) Quantification of psychosine levels in Wt and twitcher primary neurons by LC-MS-MS. Chromatograms in E show the corresponding peak of psychosine in the Twitcher cells (arrow). Wt cells showed traces of the lipid. Quantification of psychosine levels in neurons and enriched cultures of Wt (white white bars) and twitcher (black bars) oligodendroglia is shown in F.

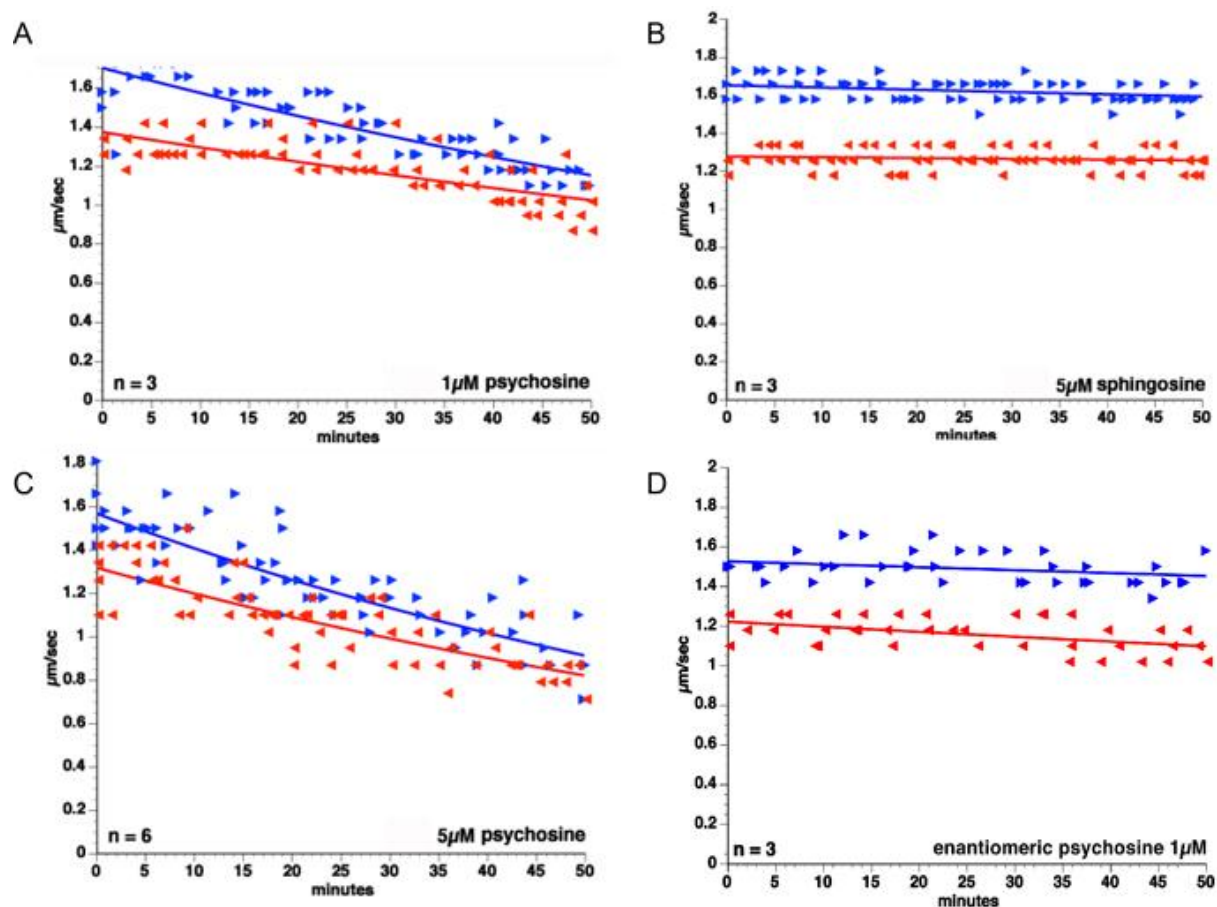


Figure 33 Psychosine inhibits FAT

Pure preparations of squid axoplasm were treated with 1 and 5 μM psychosine (A and C, respectively). The rates of fast anterograde (blue arrows) and retrograde (red arrows) transports were measured over time. Psychosine induced a strong decrease in FAT rates in both directions (A and C). D-Sphingosine had no effect on FAT (B). Psychosine enantiomer had no effect on FAT (D).

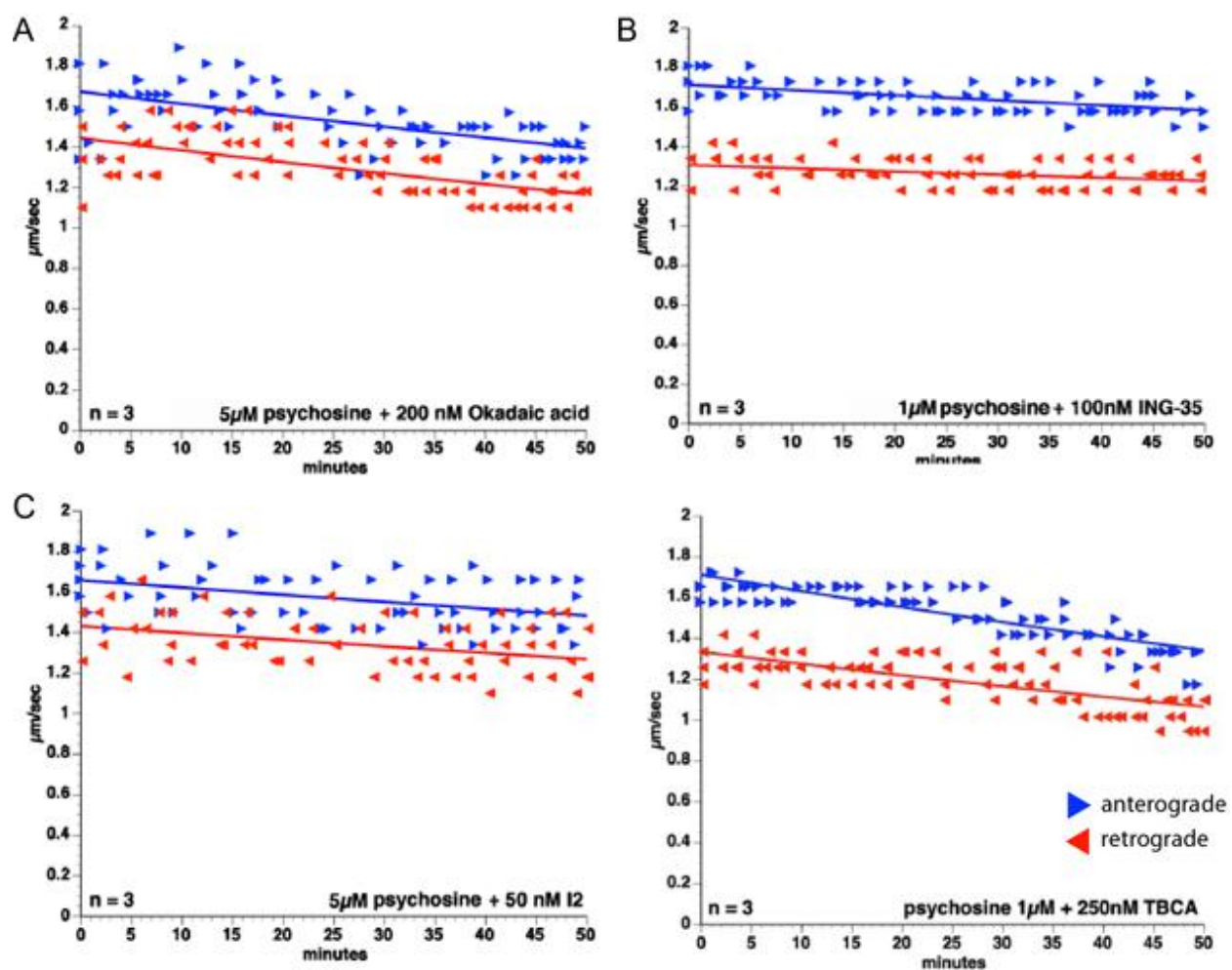


Figure 34 Psychosine inhibits FAT through PP1 and GSK3 β

Co-perfusion of squid axoplasm preparations with psychosine and OA (A) or inhibitor-2 (I2) (C), a PP1 specific inhibitor, resulted in almost complete protection of FAT rates. Similarly, ING-35, a GSK3 β specific inhibitor, prevented psychosine-mediated inhibition of FAT (B). TBCA, a CKII specific inhibitor, did not prevent the psychosine effect.

The inhibitory effect of psychosine on FAT was further confirmed by measuring the mitochondrial mobility in a motoneuronal cell line. NSC34 cells were cultured in the presence of psychosine and with Mitotracker green, a fluorescent live mitochondrial probe. Fluorescence pictures were taken every 10 seconds for 300 seconds. Quantification of the number of actively transported mitochondria per cell confirmed that psychosine is capable of significantly impair the transport of this organelle (Fig. 35). When NSC34 cells were co-treated with myristoylated-L803 (myr-L803), a competitive, cell-permeable inhibitor of GSK3 β , mitochondrial transport appeared protected, Fig. 35).

5.18 In vivo neuroprotection by inhibition of GSK3 β .

To determine if GSK3 β is a potential target for neuroprotection in KD, twitcher mice were injected intraperitoneally with 400 nmoles/day of myr-L803. Injections were started three days after birth and maintained on daily schedule for 20 days. Figure 36 shows that treatment with the inhibitor significantly normalized phosphorylation of KLC in sciatic nerves. This appears as a direct evidence of the abnormal phosphorylation of KLC by GSK3 β in the Twitcher mouse. Of functional relevance, treatment with myr-L803 also improved MCV in Twitcher animals (Fig. 37).

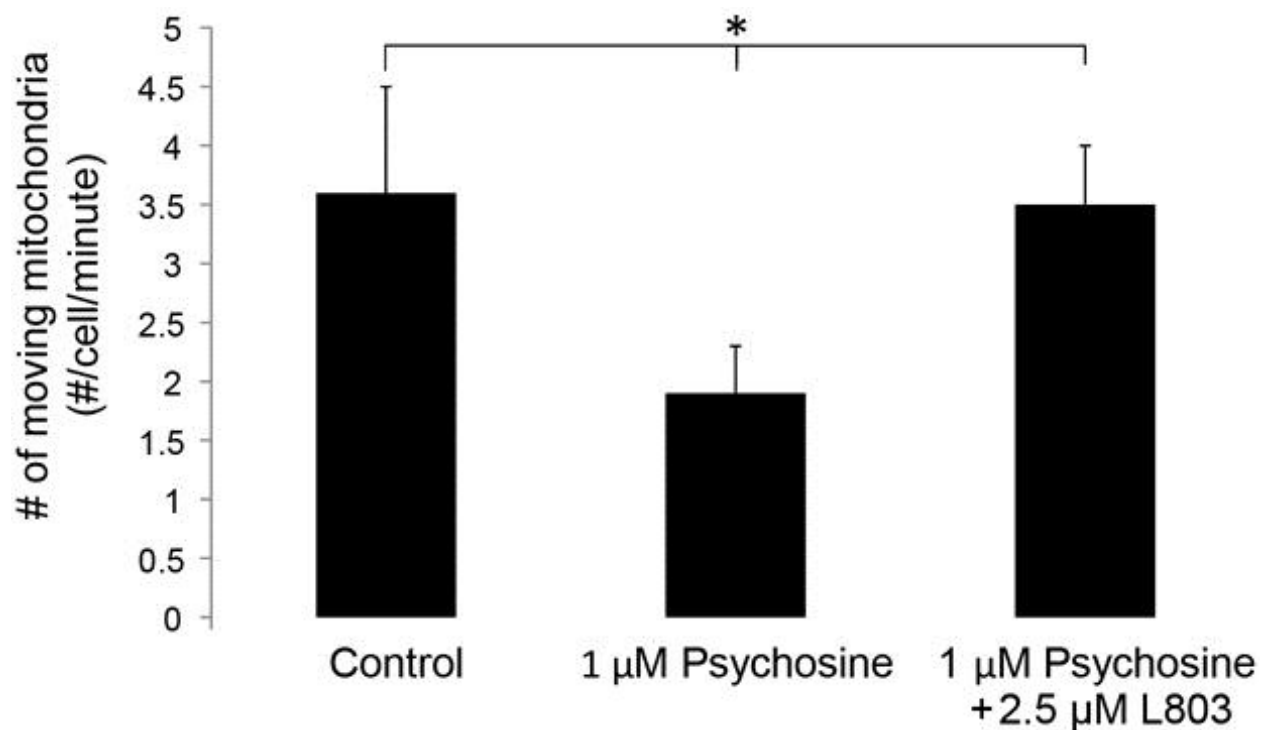


Figure 35 Psychosine inhibits mitochondrial transport

NSC34 were labeled for the mitochondrial probe MTG and visualized by time-lapse microscopy (pictures were taken every 10 seconds for 5 min.). The number of transported mitochondria per cell was counted. Psychosine treatment induced a decrease in the number of transported mitochondria. Myr L803, a cell-permeable, non-competitive inhibitor of GSK3 β , prevented the inhibition of mitochondrial transport. Data are mean \pm SEM of three replicates. Data were analyzed by t-test of Student. Asterisk indicates $p < 0.05$.

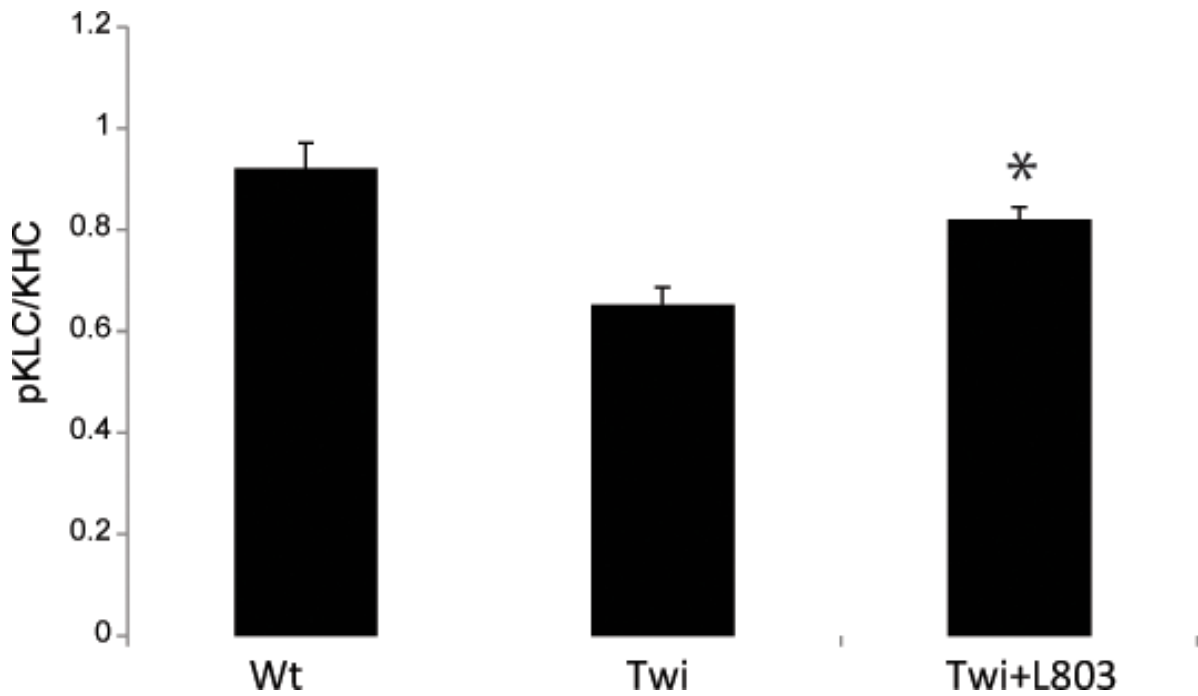


Figure 36 In vivo inhibition of GSK3 β prevents KLC phosphorylation

Quantification of the western blot analysis for the pKLC and KHC in the sciatic nerve of Wt and twitcher animals after treatment with myr-L803, a GSK3 β inhibitor. Daily intra-peritoneal injections of the twitcher animals with 400 nmoles of L803 prevented the phosphorylation of KLC in the P20 sciatic nerves of the Twitcher mouse. Data are mean \pm SEM of three replicates. Data were analyzed by t-test of Student. Asterisk indicates $p < 0.05$. $n = 3$

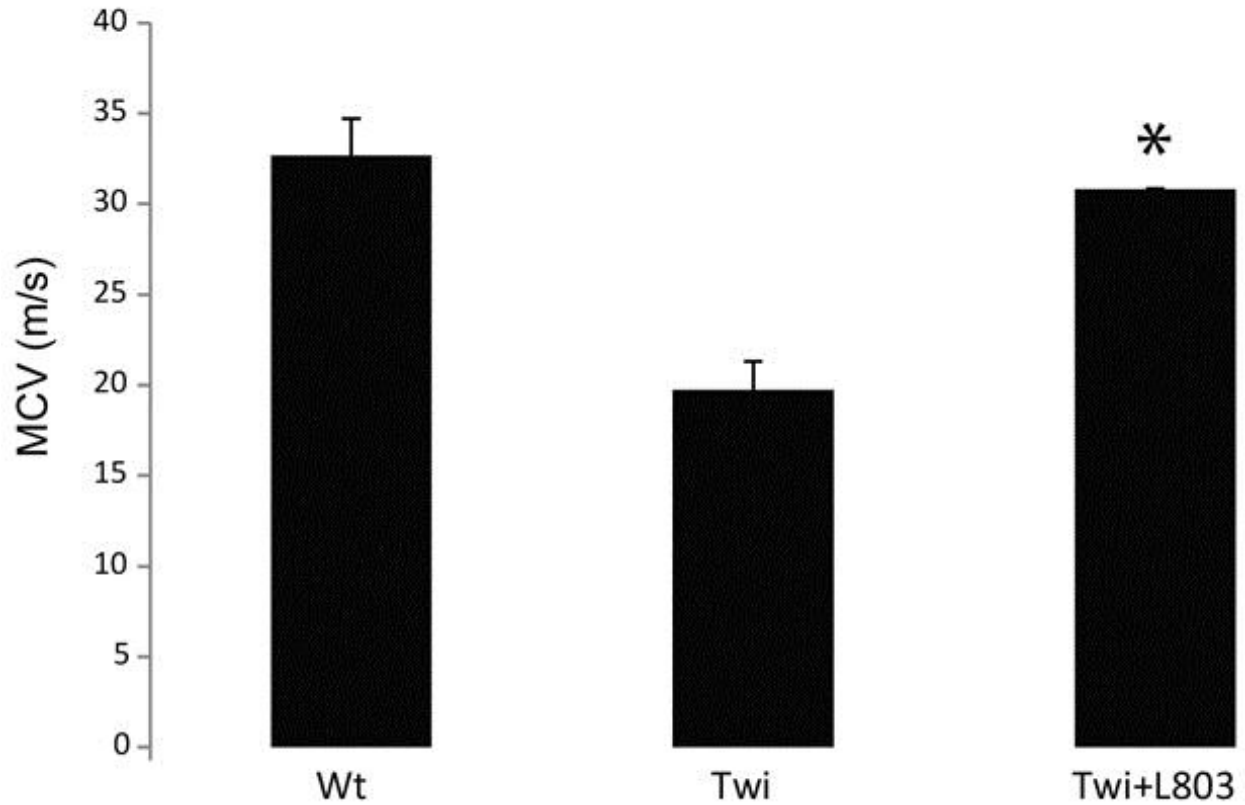


Figure 37 *In vivo* inhibition of KLC phosphorylation restores the MCV in the twitcher animal MCV recording on Wt and twitcher mice after treatment with myr-L803.

Daily intra-peritoneal injections of the twitcher animals with 400 nmoles of L803 prevented the decrease in MCV observed in the sciatic nerves of the Twitcher mouse at P20. Data are mean \pm SEM of three replicates. Data were analyzed by t-test of Student. Asterisk indicates $p < 0.05$. $n = 3$

CHAPTER 6 DISCUSSION

6.1 Summary

The aim of this study was to determine the extent and the molecular basis of neurodegeneration in KD. By examining the Twitcher mouse, an animal model of this disease, we demonstrated the existence of multiple levels of axonal pathology, including degeneration of nerve endings, muscle atrophy, axonal swelling, axonal caliber reduction, NF cytoskeleton defects and impairments in FAT. Our study shows that these pathological processes occur with minimal or no neuronal loss, which was only evidenced very late in the life of the Twitcher mouse. Our study also demonstrates that psychosine is capable per se of triggering some of these problems by deregulated changes in NFs and FAT, by recruitment of PP1, PP2A and GSK3- β activities. Our characterization of the Twitcher neurodegeneration proposes the existence of a dying-back axonopathy and develops a more complex neuropathological mechanism of this disease, where axonopathy appears as a compounding factor to demyelination (Figure 38).

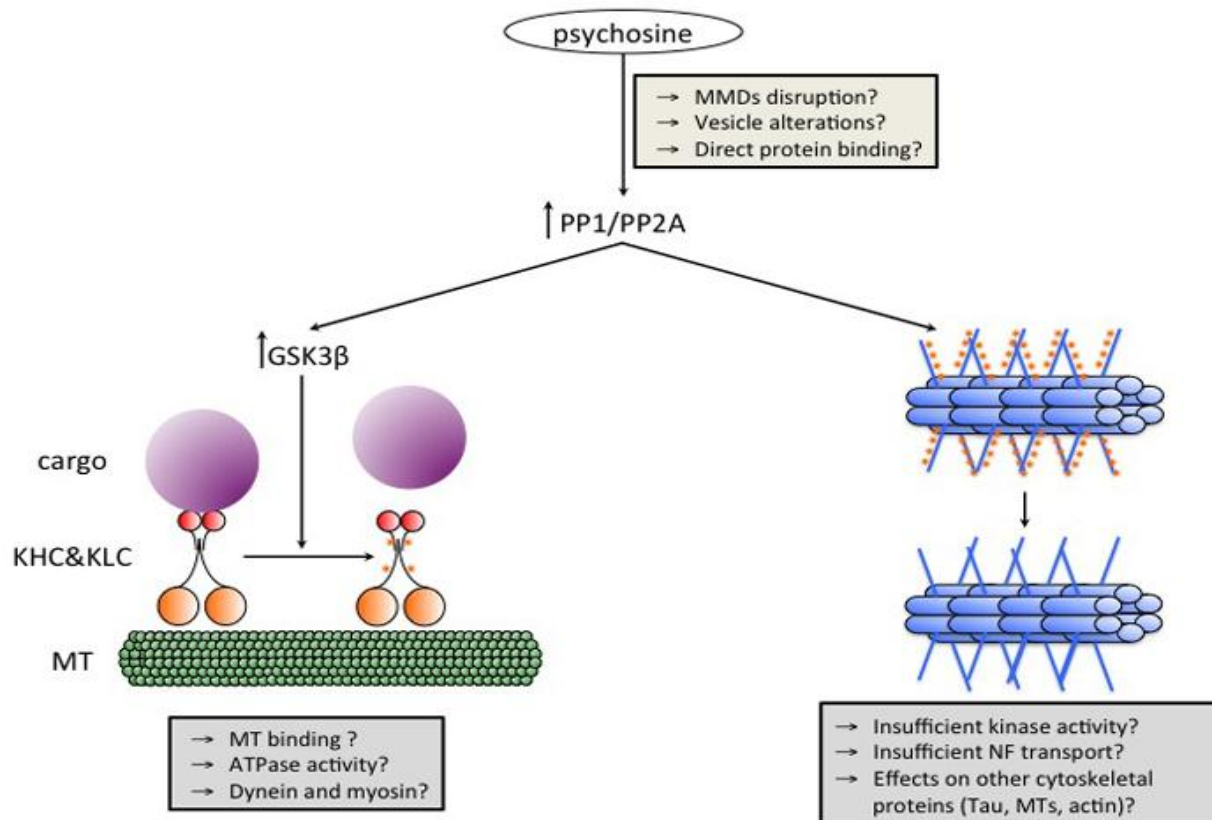


Figure 38 Model of psychosine-mediated axonopathy

Psychosine, by altering the membrane architecture of MMDs and vesicles, can cause defects in signaling, in particular through ser/thr phosphatases. The over-activation of phosphatases has two important consequences. First, it causes a decrease in the total NF phosphorylation. Possibly, other cytoskeletal proteins might be affected, like Tau or microtubules. Secondly, it triggers the activation of GSK3 β , which directly phosphorylates KLC, causing the release of cargoes. Psychosine might also affect other signaling pathways regulating kinesin, possibly interfering with microtubule binding and the ATPase domain of KHC. Furthermore, other molecular motors, like cytoplasmic dynein and the microfilament-binding myosin could be inhibited. Importantly, psychosine could affect both NFs and kinesin by direct binding and interference.

6.2 Axonal pathology in the Twitcher mouse.

Because of the severity of the white matter disorder in KD, most of the studies using Twitcher mice have focused on central and peripheral demyelination. Only few studies have examined axonal and neuronal abnormalities in this mutant. Impaired development of large diameter fibers was reported in Twitcher sciatic nerves but the cause for defect was never studied (Jacobs et al., 1982). Neuronal damage was observed in specific neuronal populations in the mutant brain and spinal cord (Dolcetta et al., 2005; Smith et al., 2011). Postural and motor

deficiencies the Twitcher mouse early in life (Olmstead, 1987). Altogether, these studies pointed to a neuropathogenic mechanism affecting the function of numerous neural paths. By studying the condition of Twitcher neurons and their connections during the progression of the disease, our study aimed at elucidating the nature of neurodegeneration of KD. This study focused on spinal cord motoneurons because of their accessibility and because of the extensive studies on Twitcher peripheral nerves (Duchen et al., 1980; Scaravilli and Jacobs, 1981; Jacobs et al., 1982; Powell et al., 1983; Kobayashi et al., 1988).

Our study on the Twitcher neurons demonstrates the existence of a clear axonal pathology in the Twitcher spinal cord and sciatic nerves. The Twitcher axonopathy is characterized by the early appearance of axonal swellings and breaks, many of which co-localized with local accumulations of dephosphorylated NFs (Castelvetri et al., 2011). The appearance and the progressive increase in the frequency of axonal abnormalities are paralleled by abnormalities of the NMJs and the progressive atrophy of the muscles of the lower limbs. These characteristics are consistent with a model of dying-back pathology, where axonal dysfunction, likely in the form of synaptic shut-down, precedes the death of the neuronal body (Sagot et al., 1995; Burne et al., 1996; Coleman and Perry, 2002; Whitmore et al., 2003; Coleman, 2005). In a dying-back pathology, an insult to the axons impairs the ability of the neurons to supply the synapses, leading first to their inability to properly transmit the electrical information and then to the retraction of the distal neurites. Importantly, the cell body of the affected neurons can be anatomically unaltered, while their synapses are shutting down and degenerating. Our experiments show indeed that the abundance of spinal cord motoneurons is similar in both Wt and Twitcher mice, and apoptotic motoneurons can be detected only after disease onset (P30), when the neuronal damage

might be caused by a combined effect of axonopathy, demyelination, inflammation and astrogliosis.

6.3 Muscular atrophy as a consequence of the Twitcher axonopathy

The abnormalities observed in the Twitcher NMJs help in understanding the muscular deficiencies observed in KD patients. Marjanović observed severe hypotonia and weakness in 12-months old KD patients. These authors suggested that the muscular phenotype may be caused by altered development of the muscle fibers (Marjanovic et al., 1996). The development of a functional muscle requires the precise coordination between muscle cells and nerve endings and the correct establishment of electrically-active NMJs (Witzemann, 2006). The contact and the exchange of signals between the growing neurite and the muscle cell direct the structural organization of the NMJ, as well as its molecular composition (Punga and Ruegg, 2012). A key event in the muscle development is the switch in the gene expression from the γ to the ϵ subunits of the AchR, which represents the transition from the fetal (γ subunit) into the mature (ϵ subunit) form of the AchR. The γ subunit is required for the nerve-induced clustering of the AchRs, but its expression is suppressed when the NMJ is electrically active and releasing Ach (Numberger et al., 1991; Duclert and Changeux, 1995). The expression of the γ subunit in postnatal life of the Twitcher mouse suggests the possibility of a compromise in the synaptic communication between the fiber ending and the muscle cells. The increased activation of caspase 3 in the terminal could effectively alter the NMJ functionality (Vohra et al., 2004; Vohra et al., 2006; Keller et al., 2011). Caspase 3, a well-known mediator of cell death, is also critical for long-term potentiation in the brain, and its inhibition results in strong impairment of synaptic plasticity. Although caspase 3 activity is essential for the proper development of synapses in the brain, its over-activation is

implicated in several late-onset neurological disorders, in which severe synaptic dysfunction is observed (Su et al., 2001; Martin et al., 2002). It is possible that caspase 3 over-activation in the Twitcher axons might lead to the NMJ inactivation, even in the absence of clear axonal retraction. Indeed, NMJ dysfunction has been observed, which lead to severe muscle atrophy even in the absence of NMJ loss (Pinter et al., 1995; Balice-Gordon et al., 2000). In line with this idea, our group has shown activation of caspase 3 in fibers of the twitcher sciatic nerve as well as in the ventral funiculus of the twitcher cord (Smith et al., 2011), which contain the anterior corticospinal tract and the lateral vestibulospinal tract. Demise or dysfunction of these tracts, which carry the information to lower limb muscles, may affect their muscle connections, furthering the loss of muscle connections and, eventually, muscle wasting (Ludolph et al., 1987; Ugawa et al., 1991). It is feasible that the mutant muscle attempts to preserve NMJs by upregulating the AchR γ subunit. However, the decrease in the electrical activity of the sciatic nerve, together with the activation of caspases in the presynaptic terminals, and demyelination may cause the shut-down of the synapse.

These alterations of the NMJ in Twitcher muscles appear to also be compounded by the deregulation of the AKT-muscle growth-signaling pathway. The activity of AKT has been shown to act as molecular switch between protein synthesis and degradation, therefore determining the overall growth or reduction of the muscle mass (Dobrowolny et al.; Alessi et al., 1996; Bodine et al., 2001; Millino et al., 2009). We found that phosphorylation of AKT, which is directly proportional to its activity, was strongly decreased in Twitcher soleus muscle. One of the functional consequences of a decrease in phospho-AKT in muscle cells is an increase in protein ligases, like atrogen-1, and the corresponding increase in ubiquitination of the muscle proteins and their degradation (Glass, 2003b, a). This leads to reduction in muscle mass. All together our results provide a first understanding of the muscle atrophy in this mutant. While it is still possible

that GALC deficiency has a direct effect on muscle cells, this possibility is beyond the scope of this work and is going to be explored at a later time.

6.4 Alterations in NFs

The changes of the Twitcher NMJs suggest that all or some of the nerve terminals are dysfunctional. One interpretation is that Twitcher axons are unable to properly maintain electrical stimulation of muscles, leading to alteration in the NMJs. Consistent with this idea, we observed an increase in the frequency of small diameter fibers in the Twitcher sciatic nerves. The prevalence of small diameter fibers suggests a problem in the development of large myelinated fibers in the Twitcher mouse. During development, axons may grow up to 15 times their original diameter after establishing their synapses (Goldberg and Frank, 1979; Graf von Keyserlingk and Schramm, 1984). This has profound implications on the function of the axons, as a larger diameter increases the propagation speed of the axon potential. Thus, the prevalence of small diameter fibers can contribute significantly to the decreased propagation speed observed in the Twitcher peripheral nerves (Takei et al., 2000; Eng et al., 2001; Wang et al., 2006; Lin et al., 2011b).

NFs are critical mediators of the increase of the axonal caliber. Variations in NF gene expression, transport and phosphorylation have been implicated in unrelated neurodegenerative disorders, such as ALS (Hirano et al., 1984; Hirano et al., 1984), Parkinson disease (Brownlee et al., 2002) Pappolla, 1986) and Charcot–Marie–Tooth disease (Brownlee et al., 2002). Of fundamental importance, small changes in NF composition or function can lead to changes in the diameter of the axons and to severe muscle pathology (Shen et al., 2011; Wakeling et al., 2011). Our analysis shows a decrease in the amount (in the case of NFM) and organization of NFs in

most of axons of the Twitcher sciatic nerve. These changes are not caused by variations in gene expression as we could not detect significant changes in mRNA and protein levels for the different NFs in the spinal cord of the Twitcher mice. On the other hand, dephosphorylation of NFs could significantly affect both the assembly and the transport of NFs along the nerve. NF phosphorylation is the result of the overall activity of ser/thr phosphatases, like PP1 and PP2A, and specific kinases, like Erk1/2, CDK5, p35 and SAPK1b (Perrot et al., 2008); Perrot et al., 2008). Importantly, phosphorylation of NF side chains regulates not only the assembly and transport of NFs, but also the radial growth of the axons, by virtue of the repulsive forces generated between the numerous phosphate groups of the NFs. If the balance between phosphorylation and dephosphorylation is shifted, alterations in NF dynamics will consequently occur. Consistent with this idea, the activity of PP2A is significantly increased in the Twitcher nervous system already after one week of life. The increase in phosphatase activity could explain the decrease in the axon diameter and, consequently, contribute to a low MCV.

It is important to remember that, during development, the thickness of the myelin and the fiber size are adjusted to optimize the speed of electrical conduction. Signals between the axon and myelin allows for their coordinated growth. Importantly, the crosstalk between the two allows for the local regulation of axonal diameter, so that the axon is smaller at the nodes of Ranvier. Local regulation of phosphotransferase activity and NF phosphorylation seem fundamental for the determination of the fiber size. Accordingly, thinner myelin was observed around P18 in the twitcher sciatic nerve (Jacobs et al., 1982) Thus, our observations on the axonal phosphatases and the fiber size might represent a more complex problem of interaction between myelin and the axon. Alterations in the activity of phosphatases could affect axonal growth and this, in turn,

influence the process of myelination. Further studies will be required to understand how GALC deficiency affects the crosstalk between myelin and the axon.

6.5 Fast axonal transport as a pathological mechanism in KD.

A general defect in transport can create localized bottlenecks, causing the accumulation of unsorted cargoes. If this condition persists, the neuron might not be able to supply its neurites, leading to further damage along the axons. Axonal dystrophy is considered a histological symptom of axonopathy, even if the axonal insult is not limited to the area of the swelling. Importantly, axonal dystrophy can be caused by a deficiency in FAT. Our experiments on the Twitcher mouse concur with this idea. FAT deficiency was first determined at P7, when the first axonal swellings were also detected in Twitcher mice (Castelvetri et al., 2011). Interestingly, our TEM analysis of ligated nerves showed that not all axons were similarly affected by FAT deficiencies. FAT defects could be affecting mutant neurons to different extents, so that axonal degeneration develops differently in neurons located in the same area of the nervous system. Collectively, our observations support this notion. For instance, axonal swellings are observed in several, but not all the fibers of sciatic nerve and spinal cord. It is therefore possible that GALC deficiency leads to a selective neuronal vulnerability, similarly to other neurological disorders. For instance, ALS strikes cholinergic motoneurons, while hippocampal and cortical pyramidal neurons are affected in AD. The reason for this selectivity is still unclear. In the case of the twitcher mouse, we found that the increase in PP1 and PP2A catalytic subunits is localized to specific fibers of the sciatic nerve. The defect in sphingolipid metabolism might alter axonal phosphotransferases differently, depending on the neuronal type. Furthermore, different neuronal

populations might require different levels of GALC activity, and this would also affect the specific levels of psychosine.

Our results raise an important question: what is the initial insult that triggers the defect in FAT in the Twitcher mutant? Our work advances one hypothesis: small but significant amounts of psychosine are responsible for the FAT defect. Psychosine concentration is significantly higher already in the P7 Twitcher sciatic nerve, when compared to the Wt control, suggesting that the synthesis and accumulation of this sphingolipid starts before, possibly during the embryonic life. Unpublished data from the dissertation work of Hongling Zhu in our laboratory confirmed that indeed, psychosine is already accumulated in twitcher embryos (Zhu and Bongarzone, unpublished results). Therefore, small but considerable amounts of psychosine may be sufficient to affect FAT, even in the absence of demyelination or inflammation. Indeed, psychosine alone was sufficient to inhibit FAT, both in the model of extruded squid axoplasm and in cultured cells. This inhibitory effect is specific for psychosine, as D-sphingosine does not exert any effects on the transport rates in either model. Our results showed an abnormal activation of the PP1/GSK3 β pathway likely leading to the release of transported MBOs from kinesin-based motors. A similar situation was previously shown to affect anterograde transport in AD (Morfini et al., 2004; LaPointe et al., 2009; Kanaan et al., 2011). In particular, the aggregation of tau, a microtubule associated protein involved in the pathogenesis of AD, exposes a phosphatase-activating domain which, in turns, activates the PP1-GSK3 β pathway. Upregulation of this path by aggregated tau is therefore a toxic gain-of-function that alters FAT and, consequently, that alters neuronal survivability. The PP1/GSK3 β pathway seems to regulate only anterograde transport (Morfini et al., 2002a; Morfini et al., 2004). In our study, we show that psychosine affects both antero- and retrograde directions. Likely, psychosine activates multiple pathways, possibly regulating both

directions of FAT. In line with this idea, we observed that the protection of FAT rates with inhibitors of PP1 and GSK3 β is not complete. We are currently investigating if other signaling enzymes are activated by psychosine. These enzymes might alter other properties of the molecular motors, like the microtubule binding or the ATPase activity of KHC and dynein regulation.

Our experiments on primary cultures of Wt and Twitcher cortical neurons suggest that GSK3 β activation occurs autonomously, independent of myelin defects. It is however possible that the initial accumulation of psychosine subtly affects the myelin-axon interaction and, as a result, the myelin-related regulation of FAT might be altered in the mutant axons. For example, defects in myelin proteins result in significant changes in axonal transport, causing axonal swellings despite the presence of normal-appearing myelin (Lappe-Siefke et al., 2003). These swellings occur at the nodes of Ranvier, which are considered an important delivery destination of nodal proteins, like ion channels. Because GALC deficiency affects the differentiation of oligodendrocytes as well, it will be important to understand whether psychosine affects intracellular transport in myelinating glia as well. Kinesin-based transport is important for myelination, because several myelin proteins or their mRNAs are transported along the myelinating processes (Ainger et al., 1993; Carson et al., 1997; Song et al., 2003). Defects in kinesin-based transport in oligodendrocytes are indeed sufficient to alter myelination and to induce axonal abnormalities (Lyons et al., 2009; Kreutzer et al., 2011).

6.6 Is psychosine as a natural regulator of axonal phosphotransferases?

The current work describes how the NF cytoskeleton and FAT are both affected in the Twitcher mouse. How is it possible that these two critical axonal components are affected by GALC deficiency? We answered this question, at least partially, by demonstrating that psychosine alone can decrease both NF phosphorylation and the rate of FAT, in the absence of

any glia-derived effect. Further these effects were mediated by specific enzymes: the ser/thr phosphatases PP1 and PP2A and the kinase GSK3 β .

These enzymes are among a larger number of regulators of NFs and axonal transport. PP1 and PP2A account for 15% and 60% of the total dephosphorylation activity of the NFs, representing the most important NF-associated phosphatases (Strack et al., 1997b). Differential localization of these phosphatases along the axon allows the neurons to regulate the local phosphorylation of NFs, tightly controlling axonal diameter. The activity of PP1 is also important to activate GSK3 β which, in turn, phosphorylates KLC and induces the release of its cargo (Morfini et al., 2002b; Morfini et al., 2002a; Morfini et al., 2004). On the other hand, GSK3 β also phosphorylates NFs on specific epitopes, likely regulating their assembly along the axon (Sasaki et al., 2002; DeFuria and Shea, 2007; Sasaki et al., 2009). The crosstalk between these enzymes is therefore quite complex, and involves several levels of regulations. PP1 and GSK3 β , for example, colocalize on transported vesicles, suggesting that the signals required for FAT regulation travel directly with kinesin (Morfini et al., 2002a). By activating PP1 and GSK3 β at specific locations, the neuron regulates where and when kinesin cargoes are released. NF phosphorylation is also spatially regulated along myelinated axons (Mata et al., 1992). The NFs underlying the nodes of Ranvier are markedly less phosphorylated than the adjacent NFs spanning the internode (de Waegh et al., 1992). Studies on the *trembler* mouse, a mutant of the myelin protein PMP-22, confirmed that myelin differentially regulates the phosphorylation state of NFs, depending whether they are underlying the node or the internode. If psychosine alone is able to increase the activities of ser/thr phosphatases and kinases, which are critical for the regulation of NF and FAT, even small concentrations of the lipid could severely undermine mutant axons.

Now, one relevant question is how psychosine activates PP1, PP2A and GSK3 β . An obvious possibility is that psychosine directly binds to specific signaling proteins, altering their regulation or activities. Despite several efforts, the existence of a “psychosine receptor” has never been demonstrated. It is however possible to speculate that proteins involved in the regulation of PP1 and PP2A might be able to bind psychosine. For example, ceramide can bind inhibitor 2, a specific phosphatase inhibitory subunit, triggering the release and the activation of the phosphatase (Mukhopadhyay et al., 2009). Certain phospholipids also bind NFs (Kim et al., 2011). Our laboratory is working to identify potential psychosine binding motifs in proteins that regulate PP1 and PP2A. While binding motifs have not been described for psychosine, the fact that this lipid is degraded by GALC and no other hydrolase implies a specific recognition, and hence, potential binding motifs. The consequence of this binding may vary, depending on the binding partners. If this is true, then such differential binding may help to explain why psychosine has different effects on NFs and KLC.

An alternative –yet maybe additive mechanism- is that that psychosine alters membrane dynamics. Our laboratory has previously shown that psychosine specifically accumulates in lipid rafts and interferes with the associated signaling complexes (Keller and Simons, 1998; Manes et al., 1999; White et al., 2009). Several critical signaling enzymes, like AKT and PKC, require re-localization to the rafts to be properly activated, and the disruption of these domains significantly compromises their signaling pathways (Zundel et al., 2000; Elhyany et al., 2004; White et al., 2009). PP2A is present in rafts, where cholesterol levels modulate its activity (Berrou and Bryckaert, 2009). Importantly, all three enzymes were present in rafts isolated from cultured neuronal cells, but their association to the membrane decreases after psychosine treatment (data not shown).

Finally, it is also possible that psychosine accumulates in the membranes of the transported vesicles, which can carry specific lipids. The presence of psychosine in transported cargoes would provide a mean to transport psychosine along the axons. Importantly, because PP1 and GSK3 β are associated with the transported vesicles, psychosine could directly affect the FAT—regulatory enzymes (Morfini et al., 2004). Our laboratory is currently investigating this possibility.

6.7 GALC deficiency may generate a cell autonomous pathogenic defect in neurons

What is the source of psychosine in Twitcher neurons? Significant levels of psychosine can be detected in brain lipid rafts at P3, a much earlier developmental time than previously suggested (Suzuki, 1998; White et al., 2009). The presence of psychosine before major myelination raised the possibility that psychosine may be synthesized by other neural cells such as neurons in addition to myelinating glia. Our studies on cultured neurons showed that CGT, the enzyme responsible for psychosine synthesis, and GALC are present in primary cultures of neurons and in spinal cord motoneurons (Castelvetri et al., 2011). Cultures of acutely isolated neurons from wild type and Twitcher mice showed that not only does psychosine accumulate significantly in these cells but also that mutant neurons degenerate faster than wild type controls. This indicates that Twitcher neurons maybe affected by an intrinsic mechanism of degeneration.

In culture, Twitcher neurons accumulated psychosine to lower levels than mutant oligodendrocytes. Despite this difference, the accumulation of low amounts of psychosine may still be significantly toxic to neurons. In fact, we found that even a low concentration of psychosine (1 μ M) was sufficient to activate PP1, PP2A, and GSK3 β , and, eventually, to alter NF and KLC phosphorylation levels. This may mimic conditions seen during the first week of life of

the animal. While accumulation of psychosine in neurons may be primarily the result of endogenous neuronal synthesis, it is still possible that the neuronal concentrations of psychosine might be even higher, if non-neuronal psychosine reaches the neuronal compartment. For example, the transfer of certain phosphoinositides from myelin to axons has been already proven (Ledeen and Haley, 1983; Toews et al., 1988; Ledeen et al., 1992). If this is true, psychosine could be synthesized by glial cells and then transferred to the neuron. The modality of this transfer could be based on cell-to-cell contact and/or mediated by mobilized vesicles. Recent studies indeed show that the lysosomal activity regulates the release of exosomes which carry proteins and lipids from one cell to another (Subra et al., 2007; Alvarez-Erviti et al., 2011; Fitzner et al., 2011; Strauss et al., 2011; Yuyama et al., 2012). For example, neurons carrying the mutation of Niemann-Pick disease type C, which accumulate cholesterol release cholesterol-enriched exosomes, to reduce the burden (Strauss et al., 2011). It is therefore possible that the constant accumulation of psychosine and the lack of lysosomal degradation in the Twitcher might cause release of this sphingolipid from myelinating glia into the extracellular environment and its redistribution to other cell types.

6.8 Neurodegeneration as a new target for KD therapy.

The data presented in this work have important therapeutic implications. The main goal of the traditional therapies such as BMT for KD has been to reconstitute GALC activity in the nervous system and to assume that the enzyme would help in the clearance of the sphingolipid accumulation. Numerous studies have demonstrated that GALC reconstitution in the nervous

system provides several benefits, although the extent of therapeutic success depends on the protocol used. However, the inability to completely arrest the development of the disease is a shared pitfall in all of these studies (Ichioka et al., 1987; Kondo et al., 1988; Krivit et al., 1998; Escolar et al., 2005; Siddiqi et al., 2006; Galbiati et al. 2009). Various limitations may intervene to reduce the benefits of BMT. Maybe the biggest obstacle is the timing for cross-correction in the nervous system. Donor-derived macrophages take about 30-45 days to infiltrate the nervous system and cross-correct host cells (Wu et al., 2000; Galbiati et al., 2008). Thus, during this lag of time the protective value of BMT correction of the nervous system might be significantly reduced in comparison to the periphery. In other words, before sufficient GALC enzyme is produced in the brain, cord and nerves, mutant neurons and axons may have already been damaged. Our findings on the changes in FAT and NF phosphorylation support this idea and indicate the importance of protecting peripheral fibers during the early life of the mutant animal.

PP1, PP2A and GSK3 β , as mediators of psychosine effects on FAT and NFs, represent new potential targets for KD therapy. Pharmacological inhibition of PP1, PP2A and GSK3 β may be helpful to slow or halt the effect of psychosine on these enzymes, preventing or reducing axonal burden. Inhibition of these enzymatic activities may prove to be relevant since the first days of life, when psychosine is known to be already accumulating in the membranes of the GALC deficient cells (White et al., 2009). As such, a pharmacological treatment is likely to be insufficient with increasing concentrations of psychosine. However, a combination of this pharmacological intervention and BMT may prove to add synergy to the treatment. Our laboratory is currently working on these ideas and a number of combined protocols are in the process of experimentation.

6.9 Relevance of this study in other lysosomal storage diseases

This work focused on the Twitcher mouse, a model of KD with accumulation of psychosine. Our studies determined how psychosine triggers neuropathogenic mechanisms compromising the function of the nervous system, in addition to demyelination. Of relevance, psychosine may have natural targets such as PKC, PP1, PP2A and GSK3 β , which may regulate under normal metabolic conditions. Our laboratory is currently investigating whether normal concentrations of psychosine may elicit specific effects on these pathways.

Our findings may be relevant to other LSDs. Various sphingolipidosis cause severe neurological symptoms, suggesting that other accumulated substrates may be toxic to neural cells. We speculate that if psychosine regulates specific kinases and phosphatases, it is possible that other LSD substrates have similar effects. To challenge this hypothesis, we administered gangliosides GM1 and GM2, which accumulate in GM1 gangliosidosis, Tay-sachs disease and Sandhoff disease (O'Brien et al., 1965; Balint and Kyriakides, 1968; Sandhoff et al., 1971; Srivastava and Beutler, 1973) to squid axoplasm preparations. We observed that these sphingolipids are potent inhibitors of anterograde FAT (data not shown). Sphingomyelin, which accumulates in Niemann-Pick disease type A (Brady et al., 1966), has a similar inhibitory effect on anterograde FAT (data not shown). Interestingly, co-administration of these sphingolipids with inhibitors of the p38 MAP kinase completely prevented their inhibitory effects (data not shown). In light of these observations, we speculate that different sphingolipids may regulate different phosphotransferase activities, and this regulation is altered with supra-physiological levels of these lipids. Furthermore, we hypothesize that many of the neurological symptoms in these diseases may arise from axonal defects through FAT deregulation. It is fascinating to think that defects in sphingolipid-regulated signaling might be a common pathogenic mechanism in several

unrelated LSDs. Identification of the kinases and phosphatases affected in different LSDs might provide novel targets to develop new and more potent pharmacological treatments for these diseases.

CHAPTER 7 CONCLUSIONS AND FUTURE DIRECTIONS

We provide evidence of an early axonopathy affecting the nervous system of the twitcher mouse. This is the first description of how a sphingolipidosis affects axonal stability by dysregulating FAT and the NF cytoskeleton, leading to a subtle defect in the fibers of the mutant. Our experiments show that the twitcher axonopathy starts during the first week of postnatal life and that it is the likely cause of synaptic dysfunction and muscle atrophy. Because no evident loss of fiber is observed, the twitcher axonopathy has remained undetected, and most of the scientific community has focused on the pathogenesis of demyelination and inflammation in the twitcher. However, the described axonopathy represents a major obstacle to the therapy of the disease, because most of the available therapies require several days to restore GALC activity in the nervous system. During this time, the axons of the twitcher are exposed to a progressive insult, which might irretrievably compromise their function. This effect is particularly prominent in spinal cord motoneurons. However, other neuronal cell types might be affected. Further studies are required to understand how this sphingolipidosis affects other neurons.

We conclude that the twitcher axonopathy is caused by the accumulation of psychosine in the nervous system of the newborn mutant. Psychosine alters some phosphotransferase activities of the axons. Consequent changes in the phosphorylation state of NFs and kinesin dramatically impair the ability of the neuron to sustain its functions. We identified PP1, PP2A and GSK3 β as mediators of psychosine neurotoxicity on the axons. Although psychosine might affect other molecules, we show that the inhibition of these enzymes provides protection against psychosine effects. In particular, GSK3 β inhibition restores the conduction velocity of the peripheral nerve. Because the current therapies are mostly limited to the CNS, our experiments set the basis for new

pharmacological treatments. Possibly, inhibition of GSK3 β will protect the mutant fibers during the first weeks of life, until the GALC replacement therapies provide sufficient enzyme to rescue the genetic defect in the entire nervous system. We are currently investigating the extent of the axonal protection provided by different GSK3 β inhibitors. To the best of our knowledge, this is the first report on the regulatory effect of a sphingolipid on motor based transport. The question then rises: is the defect in transport limited to neurons? Because kinesin and dynein are widely expressed, a defect in transport might affect other cell types. For example, specific isoforms of kinesin transport the mRNA of myelin proteins, and are required for the proper development of myelin (Lyons et al., 2009). It is possible that psychosine could affect myelinating glia by interfering with the kinesin-based transport of important myelin components. Our laboratory is investigating if defects in motor-based transport are present in myelinating glia in the Twitcher mouse and at the core of the demyelinating mechanism.

Finally, is FAT dysregulation a common pathological mechanism in different LSDs? Possibly, different sphingolipids could affect motor-based transport, by regulating specific signaling pathways. Our preliminary data on the effects of sphingomyelin and the gangliosides GM1 and GM2 on FAT suggest that defects in FAT might be part of the pathogenesis of GM1 gangliosidosis, Tay-sachs disease and Sandhoff disease. Studying the extent and relevance of FAT defects in sphingolipidosis will deepen our knowledge on the functions of sphingolipids, while also providing potential new target for pharmacological treatments for these devastating pediatric neurological diseases.

REFERENCES

- Aicardi J. 1993 The inherited leukodystrophies: a clinical overview. *J Inherit Metab Dis* 16:733-743.
- Ainger K., Avossa D., Morgan F., Hill S. J., Barry C., Barbarese E., Carson J. H. 1993 Transport and localization of exogenous myelin basic protein mRNA microinjected into oligodendrocytes. *J Cell Biol* 123:431-441.
- Alessi D. R., Andjelkovic M., Caudwell B., Cron P., Morrice N., Cohen P., Hemmings B. A. 1996 Mechanism of activation of protein kinase B by insulin and IGF-1. *EMBO J* 15:6541-6551.
- Alvarez-Erviti L., Seow Y., Schapira A. H., Gardiner C., Sargent I. L., Wood M. J., Cooper J. M. 2011 Lysosomal dysfunction increases exosome-mediated alpha-synuclein release and transmission. *Neurobiol Dis* 42:360-367.
- Angelides K. J., Smith K. E., Takeda M. 1989 Assembly and exchange of intermediate filament proteins of neurons: neurofilaments are dynamic structures. *J Cell Biol* 108:1495-1506.
- Atkinson T., Whitfield J., Chakravarthy B. 2009 The phosphatase inhibitor, okadaic acid, strongly protects primary rat cortical neurons from lethal oxygen-glucose deprivation. *Biochem Biophys Res Commun* 378:394-398.
- Azim K., Butt A. M. 2011 GSK3beta negatively regulates oligodendrocyte differentiation and myelination in vivo. *Glia* 59:540-553.
- Baker R. H., Trautmann J. C., Younge B. R., Nelson K. D., Zimmerman D. 1990 Late juvenile-onset Krabbe's disease. *Ophthalmology* 97:1176-1180.
- Balice-Gordon R. J., Smith D. B., Goldman J., Cork L. C., Shirley A., Cope T. C., Pinter M. J. 2000 Functional motor unit failure precedes neuromuscular degeneration in canine motor neuron disease. *Ann Neurol* 47:596-605.
- Balint J. A., Kyriakides E. C. 1968 Studies of red cell stromal proteins in Tay-Sachs disease. *J Clin Invest* 47:1858-1864.
- Bashir A., Haq E. 2011 Effect of psychosine on inducible nitric-oxide synthase expression under different culture conditions: implications for Krabbe disease. *Eur Rev Med Pharmacol Sci* 15:1282-1287.
- Berrou E., Bryckaert M. 2009 Recruitment of protein phosphatase 2A to dorsal ruffles by platelet-derived growth factor in smooth muscle cells: dephosphorylation of Hsp27. *Exp Cell Res* 315:836-848.

- Betz W. J., Caldwell J. H., Ribchester R. R. 1979 The size of motor units during post-natal development of rat lumbrical muscle. *J Physiol* 297:463-478.
- Bodine S. C., Stitt T. N., Gonzalez M., Kline W. O., Stover G. L., Bauerlein R., Zlotchenko E., Scrimgeour A., Lawrence J. C., Glass D. J., Yancopoulos G. D. 2001 Akt/mTOR pathway is a crucial regulator of skeletal muscle hypertrophy and can prevent muscle atrophy in vivo. *Nat Cell Biol* 3:1014-1019.
- Brady R. O., Kanfer J. N., Mock M. B., Fredrickson D. S. 1966 The metabolism of sphingomyelin. II. Evidence of an enzymatic deficiency in Niemann-Pick disease. *Proc Natl Acad Sci U S A* 55:366-369.
- Brady S. T. 1995 A kinesin medley: biochemical and functional heterogeneity. *Trends Cell Biol* 5:159-164.
- Brown A. 2003 Axonal transport of membranous and nonmembranous cargoes: a unified perspective. *J Cell Biol* 160:817-821.
- Brown H. G., Hoh J. H. 1997 Entropic exclusion by neurofilament sidearms: a mechanism for maintaining interfilament spacing. *Biochemistry* 36:15035-15040.
- Brown M. C., Jansen J. K., Van Essen D. 1976 Polyneuronal innervation of skeletal muscle in new-born rats and its elimination during maturation. *J Physiol* 261:387-422.
- Brownlee J., Yates A., Bajaj N. P., Davis D., Anderton B. H., Leigh P. N., Shaw C. E., Miller C. C. 2000 Phosphorylation of neurofilament heavy chain side-arms by stress activated protein kinase-1b/Jun N-terminal kinase-3. *J Cell Sci* 113 (Pt 3):401-407.
- Brownlee J., Ackerley S., Grierson A. J., Jacobsen N. J., Shea K., Anderton B. H., Leigh P. N., Shaw C. E., Miller C. C. 2002 Charcot-Marie-Tooth disease neurofilament mutations disrupt neurofilament assembly and axonal transport. *Hum Mol Genet* 11:2837-2844.
- Buonanno A., Apone L., Morasso M. I., Beers R., Brenner H. R., Eftimie R. 1992 The MyoD family of myogenic factors is regulated by electrical activity: isolation and characterization of a mouse Myf-5 cDNA. *Nucleic Acids Res* 20:539-544.
- Burne J. F., Staple J. K., Raff M. C. 1996 Glial cells are increased proportionally in transgenic optic nerves with increased numbers of axons. *J Neurosci* 16:2064-2073.
- Cannizzaro L. A., Chen Y. Q., Rafi M. A., Wenger D. A. 1994 Regional mapping of the human galactocerebrosidase gene (GALC) to 14q31 by in situ hybridization. *Cytogenet Cell Genet* 66:244-245.
- Carden M. J., Trojanowski J. Q., Schlaepfer W. W., Lee V. M. 1987 Two-stage expression of neurofilament polypeptides during rat neurogenesis with early establishment of adult phosphorylation patterns. *J Neurosci* 7:3489-3504.

- Carson J. H., Worboys K., Ainger K., Barbarese E. 1997 Translocation of myelin basic protein mRNA in oligodendrocytes requires microtubules and kinesin. *Cell Motil Cytoskeleton* 38:318-328.
- Castelvetri L. C., Givogri M. I., Zhu H., Smith B., Lopez-Rosas A., Qiu X., van Breemen R., Bongarzone E. R. 2011 Axonopathy is a compounding factor in the pathogenesis of Krabbe disease. *Acta Neuropathol.*
- Chen Y. Q., Rafi M. A., de Gala G., Wenger D. A. 1993 Cloning and expression of cDNA encoding human galactocerebrosidase, the enzyme deficient in globoid cell leukodystrophy. *Hum Mol Genet* 2:1841-1845.
- Cho H., Mu J., Kim J. K., Thorvaldsen J. L., Chu Q., Crenshaw E. B., 3rd, Kaestner K. H., Bartolomei M. S., Shulman G. I., Birnbaum M. J. 2001 Insulin resistance and a diabetes mellitus-like syndrome in mice lacking the protein kinase Akt2 (PKB beta). *Science* 292:1728-1731.
- Cleland W. W., Kennedy E. P. 1960 The enzymatic synthesis of psychosine. *J Biol Chem* 235:45-51.
- Cole J. S., Messing A., Trojanowski J. Q., Lee V. M. 1994 Modulation of axon diameter and neurofilaments by hypomyelinating Schwann cells in transgenic mice. *J Neurosci* 14:6956-6966.
- Coleman M. 2005 Axon degeneration mechanisms: commonality amid diversity. *Nat Rev Neurosci* 6:889-898.
- Coleman M. P., Perry V. H. 2002 Axon pathology in neurological disease: a neglected therapeutic target. *Trends Neurosci* 25:532-537.
- Coleman M. P., Adalbert R., Beirowski B. 2005 Neuroprotective strategies in MS: lessons from C57BL/Wld(S) mice. *J Neurol Sci* 233:133-138.
- Costantino-Ceccarini E., Luddi A., Volterrani M., Strazza M., Rafi M. A., Wenger D. A. 1999 Transduction of cultured oligodendrocytes from normal and twitcher mice by a retroviral vector containing human galactocerebrosidase (GALC) cDNA. *Neurochem Res* 24:287-293.
- Cragg B. G. 1970 What is the signal for chromatolysis? *Brain Res* 23:1-21.
- De Gasperi R., Gama Sosa M. A., Sartorato E. L., Battistini S., MacFarlane H., Gusella J. F., Krivit W., Kolodny E. H. 1996 Molecular heterogeneity of late-onset forms of globoid-cell leukodystrophy. *Am J Hum Genet* 59:1233-1242.

- de Waegh S., Brady S. T. 1990 Altered slow axonal transport and regeneration in a myelin-deficient mutant mouse: the trembler as an in vivo model for Schwann cell-axon interactions. *J Neurosci* 10:1855-1865.
- de Waegh S. M., Brady S. T. 1991 Local control of axonal properties by Schwann cells: neurofilaments and axonal transport in homologous and heterologous nerve grafts. *J Neurosci Res* 30:201-212.
- de Waegh S. M., Lee V. M., Brady S. T. 1992 Local modulation of neurofilament phosphorylation, axonal caliber, and slow axonal transport by myelinating Schwann cells. *Cell* 68:451-463.
- DeFuria J., Shea T. B. 2007 Arsenic inhibits neurofilament transport and induces perikaryal accumulation of phosphorylated neurofilaments: roles of JNK and GSK-3beta. *Brain Res* 1181:74-82.
- Dobrowolny G., Aucello M., Musaro A. Muscle atrophy induced by SOD1G93A expression does not involve the activation of caspase in the absence of denervation. *Skelet Muscle* 1:3.
- Dobrowolny G., Aucello M., Musaro A. 2011 Muscle atrophy induced by SOD1G93A expression does not involve the activation of caspase in the absence of denervation. *Skelet Muscle* 1:3.
- Dolcetta D., Amadio S., Guerrini U., Givogri M. I., Perani L., Galbiati F., Sironi L., Del Carro U., Roncarolo M. G., Bongarzone E. 2005 Myelin deterioration in Twitcher mice: motor evoked potentials and magnetic resonance imaging as in vivo monitoring tools. *J Neurosci Res* 81:597-604.
- Dolcetta D., Perani L., Givogri M. I., Galbiati F., Amadio S., Del Carro U., Finocchiaro G., Fanzani A., Marchesini S., Naldini L., Roncarolo M. G., Bongarzone E. 2006 Design and optimization of lentiviral vectors for transfer of GALC expression in Twitcher brain. *J Gene Med* 8:962-971.
- Duchen L. W., Eicher E. M., Jacobs J. M., Scaravilli F., Teixeira F. 1980 Hereditary leucodystrophy in the mouse: the new mutant twitcher. *Brain* 103:695-710.
- Duclert A., Changeux J. P. 1995 Acetylcholine receptor gene expression at the developing neuromuscular junction. *Physiol Rev* 75:339-368.
- Dunn H. G., Lake B. D., Dolman C. L., Wilson J. 1969 THE NEUROPATHY OF KRABBE'S INFANTILE CEREBRAL SCLEROSIS: GLOBOID CELL LEUCODYSTROPHY. *Brain* 92:329-344.
- Elhyany S., Assa-Kunik E., Tsory S., Muller T., Fedida S., Segal S., Fishman D. 2004 The integrity of cholesterol-enriched microdomains is essential for the constitutive high activity of protein kinase B in tumour cells. *Biochem Soc Trans* 32:837-839.

- Eng S. R., Gratwick K., Rhee J. M., Fedtsova N., Gan L., Turner E. E. 2001 Defects in sensory axon growth precede neuronal death in Brn3a-deficient mice. *J Neurosci* 21:541-549.
- English A. W., Schwartz G. 1995 Both basic fibroblast growth factor and ciliary neurotrophic factor promote the retention of polyneuronal innervation of developing skeletal muscle fibers. *Dev Biol* 169:57-64.
- Escolar M. L., Poe M. D., Provenzale J. M., Richards K. C., Allison J., Wood S., Wenger D. A., Pietryga D., Wall D., Champagne M., Morse R., Krivit W., Kurtzberg J. 2005 Transplantation of umbilical-cord blood in babies with infantile Krabbe's disease. *N Engl J Med* 352:2069-2081.
- Feng G., Mellor R. H., Bernstein M., Keller-Peck C., Nguyen Q. T., Wallace M., Nerbonne J. M., Lichtman J. W., Sanes J. R. 2000 Imaging neuronal subsets in transgenic mice expressing multiple spectral variants of GFP. *Neuron* 28:41-51.
- Fitzner D., Schnaars M., van Rossum D., Krishnamoorthy G., Dibaj P., Bakhti M., Regen T., Hanisch U. K., Simons M. 2011 Selective transfer of exosomes from oligodendrocytes to microglia by macropinocytosis. *J Cell Sci* 124:447-458.
- Floyd C. C., Grant P., Gallant P. E., Pant H. C. 1991 Principal neurofilament-associated protein kinase in squid axoplasm is related to casein kinase I. *J Biol Chem* 266:4987-4994.
- Formichi P., Radi E., Battisti C., Pasqui A., Pompella G., Lazzerini P. E., Laghi-Pasini F., Leonini A., Di Stefano A., Federico A. 2007 Psychosine-induced apoptosis and cytokine activation in immune peripheral cells of Krabbe patients. *J Cell Physiol* 212:737-743.
- Fratantoni J. C., Hall C. W., Neufeld E. F. 1968 The defect in Hurler's and Hunter's syndromes: faulty degradation of mucopolysaccharide. *Proc Natl Acad Sci U S A* 60:699-706.
- Friede R. L., Samorajski T. 1970 Axon caliber related to neurofilaments and microtubules in sciatic nerve fibers of rats and mice. *Anat Rec* 167:379-387.
- Funai K., Parkington J. D., Carambula S., Fielding R. A. 2006 Age-associated decrease in contraction-induced activation of downstream targets of Akt/mTOR signaling in skeletal muscle. *Am J Physiol Regul Integr Comp Physiol* 290:R1080-1086.
- Futerman A. H., van Meer G. 2004 The cell biology of lysosomal storage disorders. *Nat Rev Mol Cell Biol* 5:554-565.
- Galbiati F., Givogri M. I., Cantuti L., Lopez Rosas A., Cao H., van Breemen R., Bongarzone E. R. 2009a Combined hematopoietic and lentiviral gene-transfer therapies in newborn Twitcher mice reveal contemporaneous neurodegeneration and demyelination in Krabbe disease. *J Neurosci Res*.

- Galbiati F., Givogri M. I., Cantuti L., Rosas A. L., Cao H., van Breemen R., Bongarzone E. R. 2009b Combined hematopoietic and lentiviral gene-transfer therapies in newborn Twitcher mice reveal contemporaneous neurodegeneration and demyelination in Krabbe disease. *J Neurosci Res* 87:1748-1759.
- Galbiati F., Givogri M., Cantuti L., Lopez Rosas A., Marchesini S., Amadio S., Cao H., van Breemen R., Bongarzone E. 2008 Combined hematopoietic and lentiviral gene-transfer therapies in newborn twitcher mice reveal undergoing neurodegenerative processes in Krabbe disease. *In review J Neurosci*.
- Galbiati F., Basso V., Cantuti L., Givogri M. I., Lopez-Rosas A., Perez N., Vasu C., Cao H., van Breemen R., Mondino A., Bongarzone E. R. 2007 Autonomic denervation of lymphoid organs leads to epigenetic immune atrophy in a mouse model of Krabbe disease. *J Neurosci* 27:13730-13738.
- Garcia M. L., Lobsiger C. S., Shah S. B., Deerinck T. J., Crum J., Young D., Ward C. M., Crawford T. O., Gotow T., Uchiyama Y., Ellisman M. H., Calcutt N. A., Cleveland D. W. 2003 NF-M is an essential target for the myelin-directed "outside-in" signaling cascade that mediates radial axonal growth. *J Cell Biol* 163:1011-1020.
- Gavrieli Y., Sherman Y., Ben-Sasson S. A. 1992 Identification of programmed cell death in situ via specific labeling of nuclear DNA fragmentation. *J Cell Biol* 119:493-501.
- Giri S., Khan M., Rattan R., Singh I., Singh A. K. 2006 Krabbe disease: psychosine-mediated activation of phospholipase A2 in oligodendrocyte cell death. *J Lipid Res* 47:1478-1492.
- Giri S., Jatana M., Rattan R., Won J. S., Singh I., Singh A. K. 2002 Galactosylsphingosine (psychosine)-induced expression of cytokine-mediated inducible nitric oxide synthases via AP-1 and C/EBP: implications for Krabbe disease. *Faseb J* 16:661-672.
- Glass D. J. 2003a Molecular mechanisms modulating muscle mass. *Trends Mol Med* 9:344-350.
- Glass D. J. 2003b Signalling pathways that mediate skeletal muscle hypertrophy and atrophy. *Nat Cell Biol* 5:87-90.
- Glicksman M. A., Soppet D., Willard M. B. 1987 Posttranslational modification of neurofilament polypeptides in rabbit retina. *J Neurobiol* 18:167-196.
- Goldberg S., Frank B. 1979 The guidance of optic axons in the developing and adult mouse retina. *Anat Rec* 193:763-774.
- Goldstein L. S., Yang Z. 2000 Microtubule-based transport systems in neurons: the roles of kinesins and dyneins. *Annu Rev Neurosci* 23:39-71.

- Goldstein M. E., Weiss S. R., Lazzarini R. A., Shneidman P. S., Lees J. F., Schlaepfer W. W. 1988 mRNA levels of all three neurofilament proteins decline following nerve transection. *Brain Res* 427:287-291.
- Gosmanov A. R., Umpierrez G. E., Karabell A. H., Cuervo R., Thomason D. B. 2004 Impaired expression and insulin-stimulated phosphorylation of Akt-2 in muscle of obese patients with atypical diabetes. *Am J Physiol Endocrinol Metab* 287:E8-E15.
- Graf von Keyserlingk D., Schramm U. 1984 Diameter of axons and thickness of myelin sheaths of the pyramidal tract fibres in the adult human medullary pyramid. *Anat Anz* 157:97-111.
- Grafstein B., Forman D. S. 1980 Intracellular transport in neurons. *Physiol Rev* 60:1167-1283.
- Haddad F., Adams G. R. 2006 Aging-sensitive cellular and molecular mechanisms associated with skeletal muscle hypertrophy. *J Appl Physiol* 100:1188-1203.
- Hannun Y. A., Bell R. M. 1987 Lysosphingolipids inhibit protein kinase C: implications for the sphingolipidoses. *Science* 235:670-674.
- Heeroma J. H., Plomp J. J., Roubos E. W., Verhage M. 2003 Development of the mouse neuromuscular junction in the absence of regulated secretion. *Neuroscience* 120:733-744.
- Heins S., Wong P. C., Muller S., Goldie K., Cleveland D. W., Aebi U. 1993 The rod domain of NF-L determines neurofilament architecture, whereas the end domains specify filament assembly and network formation. *J Cell Biol* 123:1517-1533.
- Henneman E. 1985 The size-principle: a deterministic output emerges from a set of probabilistic connections. *J Exp Biol* 115:105-112.
- Hirano A., Donnenfeld H., Sasaki S., Nakano I. 1984 Fine structural observations of neurofilamentous changes in amyotrophic lateral sclerosis. *J Neuropathol Exp Neurol* 43:461-470.
- Hoffman P. N. 1988 Distinct roles of neurofilament and tubulin gene expression in axonal growth. *Ciba Found Symp* 138:192-204.
- Hoffman P. N., Griffin J. W., Price D. L. 1984 Control of axonal caliber by neurofilament transport. *J Cell Biol* 99:705-714.
- Hoffman P. N., Thompson G. W., Griffin J. W., Price D. L. 1985 Changes in neurofilament transport coincide temporally with alterations in the caliber of axons in regenerating motor fibers. *J Cell Biol* 101:1332-1340.
- Hoogerbrugge P. M., Poorthuis B. J., Romme A. E., van de Kamp J. J., Wagemaker G., van Bekkum D. W. 1988a Effect of bone marrow transplantation on enzyme levels and clinical course in the neurologically affected twitcher mouse. *J Clin Invest* 81:1790-1794.

- Hoogerbrugge P. M., Suzuki K., Suzuki K., Poorthuis B. J., Kobayashi T., Wagemaker G., van Bekkum D. W. 1988b Donor-derived cells in the central nervous system of twitcher mice after bone marrow transplantation. *Science* 239:1035-1038.
- Hooper C., Killick R., Lovestone S. 2008 The GSK3 hypothesis of Alzheimer's disease. *J Neurochem* 104:1433-1439.
- Ichioka T., Kishimoto Y., Brennan S., Santos G. W., Yeager A. M. 1987 Hematopoietic cell transplantation in murine globoid cell leukodystrophy (the twitcher mouse): effects on levels of galactosylceramidase, psychosine, and galactocerebrosides. *Proc Natl Acad Sci U S A* 84:4259-4263.
- Igisu H., Suzuki K. 1984a Progressive accumulation of toxic metabolite in a genetic leukodystrophy. *Science* 224:753-755.
- Igisu H., Suzuki K. 1984b Analysis of galactosylsphingosine (psychosine) in the brain. *J Lipid Res* 25:1000-1006.
- Jacobs J. M., Scaravilli F., De Aranda F. T. 1982 The pathogenesis of globoid cell leucodystrophy in peripheral nerve of the mouse mutant twitcher. *J Neurol Sci* 55:285-304.
- Jatana M., Giri S., Singh A. K. 2002 Apoptotic positive cells in Krabbe brain and induction of apoptosis in rat C6 glial cells by psychosine. *Neurosci Lett* 330:183-187.
- Julien J. P., Mushynski W. E. 1982 Multiple phosphorylation sites in mammalian neurofilament polypeptides. *J Biol Chem* 257:10467-10470.
- Julien J. P., Mushynski W. E. 1983 The distribution of phosphorylation sites among identified proteolytic fragments of mammalian neurofilaments. *J Biol Chem* 258:4019-4025.
- Julien J. P., Mushynski W. E. 1998 Neurofilaments in health and disease. *Prog Nucleic Acid Res Mol Biol* 61:1-23.
- Kablar B., Rudnicki M. A. 1999 Development in the absence of skeletal muscle results in the sequential ablation of motor neurons from the spinal cord to the brain. *Dev Biol* 208:93-109.
- Kablar B., Krastel K., Ying C., Tapscott S. J., Goldhamer D. J., Rudnicki M. A. 1999 Myogenic determination occurs independently in somites and limb buds. *Dev Biol* 206:219-231.
- Kaech S., Banker G. 2006 Culturing hippocampal neurons. *Nat Protoc* 1:2406-2415.
- Kagitani-Shimono K., Mohri I., Fujitani Y., Suzuki K., Ozono K., Urade Y., Taniike M. 2005 Anti-inflammatory therapy by ibudilast, a phosphodiesterase inhibitor, in demyelination of twitcher, a genetic demyelination model. *J Neuroinflammation* 2:10.

- Kanaan N. M., Morfini G. A., LaPointe N. E., Pigino G. F., Patterson K. R., Song Y., Andreadis A., Fu Y., Brady S. T., Binder L. I. 2011 Pathogenic forms of tau inhibit kinesin-dependent axonal transport through a mechanism involving activation of axonal phosphotransferases. *J Neurosci* 31:9858-9868.
- Kanazawa T., Nakamura S., Momoi M., Yamaji T., Takematsu H., Yano H., Sabe H., Yamamoto A., Kawasaki T., Kozutsumi Y. 2000 Inhibition of cytokinesis by a lipid metabolite, psychosine. *J Cell Biol* 149:943-950.
- Karcher R. L., Deacon S. W., Gelfand V. I. 2002 Motor-cargo interactions: the key to transport specificity. *Trends Cell Biol* 12:21-27.
- Karnes H. E., Kaiser C. L., Durham D. 2009 Deafferentation-induced caspase-3 activation and DNA fragmentation in chick cochlear nucleus neurons. *Neuroscience* 159:804-818.
- Keller L. C., Cheng L., Locke C. J., Muller M., Fetter R. D., Davis G. W. 2011 Glial-derived prodegenerative signaling in the Drosophila neuromuscular system. *Neuron* 72:760-775.
- Keller P., Simons K. 1998 Cholesterol is required for surface transport of influenza virus hemagglutinin. *J Cell Biol* 140:1357-1367.
- Kim S. K., Kim H., Yang Y. R., Suh P. G., Chang J. S. 2011 Phosphatidylinositol phosphates directly bind to neurofilament light chain (NF-L) for the regulation of NF-L self assembly. *Exp Mol Med* 43:153-160.
- Kobayashi S., Katayama M., Satoh J., Suzuki K., Suzuki K. 1988 The twitcher mouse. An alteration of the unmyelinated fibers in the PNS. *Am J Pathol* 131:308-319.
- Kobayashi T., Yamanaka T., Jacobs J. M., Teixeira F., Suzuki K. 1980 The Twitcher mouse: an enzymatically authentic model of human globoid cell leukodystrophy (Krabbe disease). *Brain Res* 202:479-483.
- Kong L., Wang X., Choe D. W., Polley M., Burnett B. G., Bosch-Marce M., Griffin J. W., Rich M. M., Sumner C. J. 2009 Impaired synaptic vesicle release and immaturity of neuromuscular junctions in spinal muscular atrophy mice. *J Neurosci* 29:842-851.
- Kornek B., Storch M. K., Bauer J., Djamshidian A., Weissert R., Wallstroem E., Stefferl A., Zimprich F., Olsson T., Linington C., Schmidbauer M., Lassmann H. 2001 Distribution of a calcium channel subunit in dystrophic axons in multiple sclerosis and experimental autoimmune encephalomyelitis. *Brain* 124:1114-1124.
- Kozutsumi Y., Kanazawa T., Sun Y., Yamaji T., Yamamoto H., Takematsu H. 2002 Sphingolipids involved in the induction of multinuclear cell formation. *Biochim Biophys Acta* 1582:138-143.

- Krabbe K. 1916 A new familial, infantile form of diffuse brain. sclerosis. *Brain* 39:74-114.
- Kreutzer M., Seehusen F., Kreutzer R., Pringproa K., Kummerfeld M., Claus P., Deschl U., Kalkul A., Beineke A., Baumgartner W., Ulrich R. 2011 Axonopathy Is Associated with Complex Axonal Transport Defects in a Model of Multiple Sclerosis. *Brain Pathol.*
- Kumar S., Hoh J. H. 2004 Modulation of repulsive forces between neurofilaments by sidearm phosphorylation. *Biochem Biophys Res Commun* 324:489-496.
- Kurtz H. J., Fletcher T. F. 1970 The peripheral neuropathy of canine globoid-cell leukodystrophy (krabbe-type). *Acta Neuropathol* 16:226-232.
- Kwon Y. W., Gurney M. E. 1996 Brain-derived neurotrophic factor transiently stabilizes silent synapses on developing neuromuscular junctions. *J Neurobiol* 29:503-516.
- LaPointe N. E., Morfini G., Pigino G., Gaisina I. N., Kozikowski A. P., Binder L. I., Brady S. T. 2009 The amino terminus of tau inhibits kinesin-dependent axonal transport: implications for filament toxicity. *J Neurosci Res* 87:440-451.
- Lappe-Siefke C., Goebbels S., Gravel M., Nicksch E., Lee J., Braun P. E., Griffiths I. R., Nave K. A. 2003 Disruption of Cnp1 uncouples oligodendroglial functions in axonal support and myelination. *Nat Genet* 33:366-374.
- Ledeen R. W., Haley J. E. 1983 Axon-myelin transfer of glycerol-labeled lipids and inorganic phosphate during axonal transport. *Brain Res* 269:267-275.
- Ledeen R. W., Golly F., Haley J. E. 1992 Axon-myelin transfer of phospholipids and phospholipid precursors. Labeling of myelin phosphoinositides through axonal transport. *Mol Neurobiol* 6:179-190.
- Leger B., Vergani L., Soraru G., Hespel P., Derave W., Gobelet C., D'Ascenzio C., Angelini C., Russell A. P. 2006a Human skeletal muscle atrophy in amyotrophic lateral sclerosis reveals a reduction in Akt and an increase in atrogin-1. *FASEB J* 20:583-585.
- Leger B., Cartoni R., Praz M., Lamon S., Deriaz O., Crettenand A., Gobelet C., Rohmer P., Konzelmann M., Luthi F., Russell A. P. 2006b Akt signalling through GSK-3beta, mTOR and Foxo1 is involved in human skeletal muscle hypertrophy and atrophy. *J Physiol* 576:923-933.
- Li A. M., Ma H., Villarreal A. 2008 Acetylcholine receptor gamma-subunits mRNA isoforms expressed in denervated rat muscle. *Mol Neurobiol* 37:164-170.
- Ligon L. A., Steward O. 2000 Movement of mitochondria in the axons and dendrites of cultured hippocampal neurons. *J Comp Neurol* 427:340-350.

- Lin D. S., Hsiao C. D., Liao I., Lin S. P., Chiang M. F., Chuang C. K., Wang T. J., Wu T. Y., Jian Y. R., Huang S. F., Liu H. L. 2011a CNS-targeted AAV5 gene transfer results in global dispersal of vector and prevention of morphological and function deterioration in CNS of globoid cell leukodystrophy mouse model. *Mol Genet Metab* 103:367-377.
- Lin L., Lee V. M., Wang Y., Lin J. S., Sock E., Wegner M., Lei L. 2011b Sox11 regulates survival and axonal growth of embryonic sensory neurons. *Dev Dyn* 240:52-64.
- Livak K. J., Schmittgen T. D. 2001 Analysis of relative gene expression data using real-time quantitative PCR and the 2(-Delta Delta C(T)) Method. *Methods* 25:402-408.
- Lorenz T., Willard M. 1978 Subcellular fractionation of intra-axonally transport polypeptides in the rabbit visual system. *Proc Natl Acad Sci U S A* 75:505-509.
- Luddi A., Volterrani M., Strazza M., Smorlesi A., Rafi M. A., Datto J., Wenger D. A., Costantino-Ceccarini E. 2001 Retrovirus-mediated gene transfer and galactocerebrosidase uptake into twitcher glial cells results in appropriate localization and phenotype correction. *Neurobiol Dis* 8:600-610.
- Ludolph A. C., Elger C. E., Gossling J. H., Brune G. G. 1987 [Study of long spinal pathways in amyotrophic lateral sclerosis. Electrophysiologic and clinical findings]. *Nervenarzt* 58:543-548.
- Luzi P., Rafi M. A., Wenger D. A. 1995 Structure and organization of the human galactocerebrosidase (GALC) gene. *Genomics* 26:407-409.
- Luzio J. P., Pryor P. R., Bright N. A. 2007 Lysosomes: fusion and function. *Nat Rev Mol Cell Biol* 8:622-632.
- Lycke J. N., Karlsson J. E., Andersen O., Rosengren L. E. 1998 Neurofilament protein in cerebrospinal fluid: a potential marker of activity in multiple sclerosis. *J Neurol Neurosurg Psychiatry* 64:402-404.
- Lyons D. A., Naylor S. G., Scholze A., Talbot W. S. 2009 Kif1b is essential for mRNA localization in oligodendrocytes and development of myelinated axons. *Nat Genet* 41:854-858.
- Malmstrom C., Haghghi S., Rosengren L., Andersen O., Lycke J. 2003 Neurofilament light protein and glial fibrillary acidic protein as biological markers in MS. *Neurology* 61:1720-1725.
- Manes S., Mira E., Gomez-Mouton C., Lacalle R. A., Keller P., Labrador J. P., Martinez A. C. 1999 Membrane raft microdomains mediate front-rear polarity in migrating cells. *EMBO J* 18:6211-6220.

- Marjanovic B.,Cvetkovic D.,Dozic S.,Todorovic S., Djuric M. 1996 Association of Krabbe leukodystrophy and congenital fiber type disproportion. *Pediatr Neurol* 15:79-82.
- Martin D. S.,Lonergan P. E.,Boland B.,Fogarty M. P.,Brady M.,Horrobin D. F.,Campbell V. A., Lynch M. A. 2002 Apoptotic changes in the aged brain are triggered by interleukin-1beta-induced activation of p38 and reversed by treatment with eicosapentaenoic acid. *J Biol Chem* 277:34239-34246.
- Mata M.,Kupina N., Fink D. J. 1992 Phosphorylation-dependent neurofilament epitopes are reduced at the node of Ranvier. *J Neurocytol* 21:199-210.
- Matsushima G. K.,Taniike M.,Glimcher L. H.,Grusby M. J.,Frelinger J. A.,Suzuki K., Ting J. P. 1994 Absence of MHC class II molecules reduces CNS demyelination, microglial/macrophage infiltration, and twitching in murine globoid cell leukodystrophy. *Cell* 78:645-656.
- McCurdy C. E., Cartee G. D. 2005 Akt2 is essential for the full effect of calorie restriction on insulin-stimulated glucose uptake in skeletal muscle. *Diabetes* 54:1349-1356.
- McCurdy C. E.,Davidson R. T., Cartee G. D. 2005 Calorie restriction increases the ratio of phosphatidylinositol 3-kinase catalytic to regulatory subunits in rat skeletal muscle. *Am J Physiol Endocrinol Metab* 288:E996-E1001.
- McGraw P.,Liang L.,Escolar M.,Mukundan S.,Kurtzberg J., Provenzale J. M. 2005 Krabbe disease treated with hematopoietic stem cell transplantation: serial assessment of anisotropy measurements--initial experience. *Radiology* 236:221-230.
- Mikoshiha K.,Fujishiro M.,Kohsaka S.,Okano H.,Takamatsu K., Tsukada Y. 1985 Disorders in myelination in the twitcher mutant: immunohistochemical and biochemical studies. *Neurochem Res* 10:1129-1141.
- Millino C.,Fanin M.,Vettori A.,Laveder P.,Mostacciuolo M. L.,Angelini C., Lanfranchi G. 2009 Different atrophy-hypertrophy transcription pathways in muscles affected by severe and mild spinal muscular atrophy. *BMC Med* 7:14.
- Mishina M.,Takai T.,Imoto K.,Noda M.,Takahashi T.,Numa S.,Methfessel C., Sakmann B. 1986 Molecular distinction between fetal and adult forms of muscle acetylcholine receptor. *Nature* 321:406-411.
- Morfini G.,Szebenyi G.,Elluru R.,Ratner N., Brady S. T. 2002a Glycogen synthase kinase 3 phosphorylates kinesin light chains and negatively regulates kinesin-based motility. *Embo J* 21:281-293.
- Morfini G.,Pigino G.,Beffert U.,Busciglio J., Brady S. T. 2002b Fast axonal transport misregulation and Alzheimer's disease. *Neuromolecular Med* 2:89-99.

- Morfini G.,Pigino G.,Mizuno N.,Kikkawa M., Brady S. T. 2007a Tau binding to microtubules does not directly affect microtubule-based vesicle motility. *J Neurosci Res* 85:2620-2630.
- Morfini G.,Pigino G.,Szebenyi G.,You Y.,Pollema S., Brady S. T. 2006 JNK mediates pathogenic effects of polyglutamine-expanded androgen receptor on fast axonal transport. *Nat Neurosci* 9:907-916.
- Morfini G.,Szebenyi G.,Brown H.,Pant H. C.,Pigino G.,DeBoer S.,Beffert U., Brady S. T. 2004 A novel CDK5-dependent pathway for regulating GSK3 activity and kinesin-driven motility in neurons. *Embo J* 23:2235-2245.
- Morfini G.,Pigino G.,Opalach K.,Serulle Y.,Moreira J. E.,Sugimori M.,Llinas R. R., Brady S. T. 2007b 1-Methyl-4-phenylpyridinium affects fast axonal transport by activation of caspase and protein kinase C. *Proc Natl Acad Sci U S A* 104:2442-2447.
- Morfini G. A.,You Y. M.,Pollema S. L.,Kaminska A.,Liu K.,Yoshioka K.,Bjorkblom B.,Coffey E. T.,Bagnato C.,Han D.,Huang C. F.,Banker G.,Pigino G., Brady S. T. 2009a Pathogenic huntingtin inhibits fast axonal transport by activating JNK3 and phosphorylating kinesin. *Nat Neurosci* 12:864-871.
- Morfini G. A.,Burns M.,Binder L. I.,Kanaan N. M.,LaPointe N.,Bosco D. A.,Brown R. H., Jr.,Brown H.,Tiwari A.,Hayward L.,Edgar J.,Nave K. A.,Garberrn J.,Atagi Y.,Song Y.,Pigino G., Brady S. T. 2009b Axonal transport defects in neurodegenerative diseases. *J Neurosci* 29:12776-12786.
- Morris R. L., Hollenbeck P. J. 1993 The regulation of bidirectional mitochondrial transport is coordinated with axonal outgrowth. *J Cell Sci* 104 (Pt 3):917-927.
- Mukhopadhyay A.,Saddoughi S. A.,Song P.,Sultan I.,Ponnusamy S.,Senkal C. E.,Snook C. F.,Arnold H. K.,Sears R. C.,Hannun Y. A., Oqretmen B. 2009 Direct interaction between the inhibitor 2 and ceramide via sphingolipid-protein binding is involved in the regulation of protein phosphatase 2A activity and signaling. *FASEB J* 23:751-763.
- Muma N. A.,Hoffman P. N.,Slunt H. H.,Applegate M. D.,Lieberburg I., Price D. L. 1990 Alterations in levels of mRNAs coding for neurofilament protein subunits during regeneration. *Exp Neurol* 107:230-235.
- Nagara H.,Kobayashi T.,Suzuki K., Suzuki K. 1982 The twitcher mouse: normal pattern of early myelination in the spinal cord. *Brain Res* 244:289-294.
- Nagara H.,Ogawa H.,Sato Y.,Kobayashi T., Suzuki K. 1986 The twitcher mouse: degeneration of oligodendrocytes in vitro. *Brain Res* 391:79-84.
- Nakamura Y.,Hashimoto R.,Kashiwagi Y.,Wada Y.,Sakoda S.,Miyamae Y.,Kudo T., Takeda M. 1999 Casein kinase II is responsible for phosphorylation of NF-L at Ser-473. *FEBS Lett* 455:83-86.

- Nixon R. A., Shea T. B. 1992 Dynamics of neuronal intermediate filaments: a developmental perspective. *Cell Motil Cytoskeleton* 22:81-91.
- Numberger M.,Durr I.,Kues W.,Koenen M., Witzemann V. 1991 Different mechanisms regulate muscle-specific AChR gamma- and epsilon-subunit gene expression. *EMBO J* 10:2957-2964.
- O'Brien J. S.,Stern M. B.,Landing B. H.,O'Brien J. K., Donnell G. N. 1965 Generalized Gangliosidosis: Another Inborn Error of Ganglioside Metabolism? *Am J Dis Child* 109:338-346.
- O'Brien R. A., Vrbova G. 1978 Acetylcholine synthesis in nerve endings to slow and fast muscles of developing chicks: effect of muscle activity. *Neuroscience* 3:1227-1230.
- O'Brien R. A.,Ostberg A. J., Vrbova G. 1978 Observations on the elimination of polyneuronal innervation in developing mammalian skeletal muscle. *J Physiol* 282:571-582.
- Oblinger M. M.,Wong J., Parysek L. M. 1989a Axotomy-induced changes in the expression of a type III neuronal intermediate filament gene. *J Neurosci* 9:3766-3775.
- Oblinger M. M.,Brady S. T.,McQuarrie I. G., Lasek R. J. 1987 Cytotypic differences in the protein composition of the axonally transported cytoskeleton in mammalian neurons. *J Neurosci* 7:453-462.
- Oblinger M. M.,Szumlas R. A.,Wong J., Liuzzi F. J. 1989b Changes in cytoskeletal gene expression affect the composition of regenerating axonal sprouts elaborated by dorsal root ganglion neurons in vivo. *J Neurosci* 9:2645-2653.
- Ogata T.,Iijima S.,Hoshikawa S.,Miura T.,Yamamoto S.,Oda H.,Nakamura K., Tanaka S. 2004 Opposing extracellular signal-regulated kinase and Akt pathways control Schwann cell myelination. *J Neurosci* 24:6724-6732.
- Ohno M.,Komiyama A.,Martin P. M., Suzuki K. 1993 Proliferation of microglia/macrophages in the demyelinating CNS and PNS of twitcher mouse. *Brain Res* 602:268-274.
- Olmstead C. E. 1987 Neurological and neurobehavioral development of the mutant 'twitcher' mouse. *Behav Brain Res* 25:143-153.
- Olsen I.,Dean M. F.,Harris G., Muir H. 1981 Direct transfer of a lysosomal enzyme from lymphoid cells to deficient fibroblasts. *Nature* 291:244-247.
- Ontell M., Kozeka K. 1984 The organogenesis of murine striated muscle: a cytoarchitectural study. *Am J Anat* 171:133-148.

- Oppenheim R. W. 1984 Cell death of motoneurons in the chick embryo spinal cord. VIII. Motoneurons prevented from dying in the embryo persist after hatching. *Dev Biol* 101:35-39.
- Pasqui A. L., Di Renzo M., Auteri A., Federico G., Puccetti L. 2007 Increased TNF-alpha production by peripheral blood mononuclear cells in patients with Krabbe's disease: effect of psychosine. *Eur J Clin Invest* 37:742-745.
- Paturi S., Gutta A. K., Katta A., Kakarla S. K., Arvapalli R. K., Gadde M. K., Nalabotu S. K., Rice K. M., Wu M., Blough E. Effects of aging and gender on muscle mass and regulation of Akt-mTOR-p70s6k related signaling in the F344BN rat model. *Mech Ageing Dev* 131:202-209.
- Perrot R., Berges R., Bocquet A., Eyer J. 2008 Review of the multiple aspects of neurofilament functions, and their possible contribution to neurodegeneration. *Mol Neurobiol* 38:27-65.
- Pigino G., Morfini G., Atagi Y., Deshpande A., Yu C., Jungbauer L., LaDu M., Busciglio J., Brady S. 2009 Disruption of fast axonal transport is a pathogenic mechanism for intraneuronal amyloid beta. *Proc Natl Acad Sci U S A* 106:5907-5912.
- Pinter M. J., Waldeck R. F., Wallace N., Cork L. C. 1995 Motor unit behavior in canine motor neuron disease. *J Neurosci* 15:3447-3457.
- Powell H. C., Knobler R. L., Myers R. R. 1983 Peripheral neuropathy in the Twitcher mutant. A new experimental model of endoneurial edema. *Lab Invest* 49:19-25.
- Punga A. R., Ruegg M. A. 2012 Signaling and aging at the neuromuscular synapse: lessons learnt from neuromuscular diseases. *Curr Opin Pharmacol*.
- Rafi M. A., Luzi P., Chen Y. Q., Wenger D. A. 1995 A large deletion together with a point mutation in the GALC gene is a common mutant allele in patients with infantile Krabbe disease. *Hum Mol Genet* 4:1285-1289.
- Rafi M. A., Fugaro J., Amini S., Luzi P., de Gala G., Victoria T., Dubell C., Shahinfar M., Wenger D. A. 1996 Retroviral vector-mediated transfer of the galactocerebrosidase (GALC) cDNA leads to overexpression and transfer of GALC activity to neighboring cells. *Biochem Mol Med* 58:142-150.
- Rao M., Mayor S. 2005 Use of Forster's resonance energy transfer microscopy to study lipid rafts. *Biochim Biophys Acta* 1746:221-233.
- Reid E., Kloos M., Ashley-Koch A., Hughes L., Bevan S., Svenson I. K., Graham F. L., Gaskell P. C., Dearlove A., Pericak-Vance M. A., Rubinsztein D. C., Marchuk D. A. 2002 A kinesin heavy chain (KIF5A) mutation in hereditary spastic paraplegia (SPG10). *Am J Hum Genet* 71:1189-1194.

- Runnegar M. T., Wei X., Hamm-Alvarez S. F. 1999 Increased protein phosphorylation of cytoplasmic dynein results in impaired motor function. *Biochem J* 342 (Pt 1):1-6.
- Sagot Y., Dubois-Dauphin M., Tan S. A., de Bilbao F., Aebischer P., Martinou J. C., Kato A. C. 1995 Bcl-2 overexpression prevents motoneuron cell body loss but not axonal degeneration in a mouse model of a neurodegenerative disease. *J Neurosci* 15:7727-7733.
- Saito T., Shima H., Osawa Y., Nagao M., Hemmings B. A., Kishimoto T., Hisanaga S. 1995 Neurofilament-associated protein phosphatase 2A: its possible role in preserving neurofilaments in filamentous states. *Biochemistry* 34:7376-7384.
- Sakmann B. 1978 Acetylcholine-induced ionic channels in rat skeletal muscle. *Fed Proc* 37:2654-2659.
- Sandhoff K., Harzer K., Wassele W., Jatzkewitz H. 1971 Enzyme alterations and lipid storage in three variants of Tay-Sachs disease. *J Neurochem* 18:2469-2489.
- Sando G. N., Neufeld E. F. 1977 Recognition and receptor-mediated uptake of a lysosomal enzyme, alpha-l-iduronidase, by cultured human fibroblasts. *Cell* 12:619-627.
- Sandri M., Sandri C., Gilbert A., Skurk C., Calabria E., Picard A., Walsh K., Schiaffino S., Lecker S. H., Goldberg A. L. 2004 Foxo transcription factors induce the atrophy-related ubiquitin ligase atrogin-1 and cause skeletal muscle atrophy. *Cell* 117:399-412.
- Sasaki T., Ishiguro K., Hisanaga S. 2009 Novel axonal distribution of neurofilament-H phosphorylated at the glycogen synthase kinase 3beta-phosphorylation site in its E-segment. *J Neurosci Res* 87:3088-3097.
- Sasaki T., Taoka M., Ishiguro K., Uchida A., Saito T., Isobe T., Hisanaga S. 2002 In vivo and in vitro phosphorylation at Ser-493 in the glutamate (E)-segment of neurofilament-H subunit by glycogen synthase kinase 3beta. *J Biol Chem* 277:36032-36039.
- Scaravilli F., Jacobs J. M. 1981 Peripheral nerve grafts in hereditary leukodystrophic mutant mice (twitcher). *Nature* 290:56-58.
- Scaravilli F., Suzuki K. 1983 Enzyme replacement in grafted nerve of twitcher mouse. *Nature* 305:713-715.
- Schlaepfer W. W., Prensky A. L. 1972 Quantitative and qualitative study of sural nerve biopsies in Krabbe's disease. *Acta Neuropathol* 20:55-66.
- Shen H., Barry D. M., Dale J. M., Garcia V. B., Calcutt N. A., Garcia M. L. 2011 Muscle pathology without severe nerve pathology in a new mouse model of Charcot-Marie-Tooth disease type 2E. *Hum Mol Genet* 20:2535-2548.

- Shen J. S., Watabe K., Ohashi T., Eto Y. 2001 Intraventricular administration of recombinant adenovirus to neonatal twitcher mouse leads to clinicopathological improvements. *Gene Ther* 8:1081-1087.
- Shen J. S., Meng X. L., Yokoo T., Sakurai K., Watabe K., Ohashi T., Eto Y. 2005 Widespread and highly persistent gene transfer to the CNS by retrovirus vector in utero: implication for gene therapy to Krabbe disease. *J Gene Med* 7:540-551.
- Shinoda H., Kobayashi T., Katayama M., Goto I., Nagara H. 1987 Accumulation of galactosylsphingosine (psychosine) in the twitcher mouse: determination by HPLC. *J Neurochem* 49:92-99.
- Smith B., Galbiati F., Castelvetti L. C., Givogri M. I., Lopez-Rosas A., Bongarzone E. R. 2011 Peripheral neuropathy in the Twitcher mouse involves the activation of axonal caspase 3. *ASN Neuro* 3.
- Snider W. D., Silos-Santiago I. 1996 Dorsal root ganglion neurons require functional neurotrophin receptors for survival during development. *Philos Trans R Soc Lond B Biol Sci* 351:395-403.
- Song J., Carson J. H., Barbarese E., Li F. Y., Duncan I. D. 2003 RNA transport in oligodendrocytes from the taiep mutant rat. *Mol Cell Neurosci* 24:926-938.
- Sourander P., Olsson Y. 1968 Peripheral neuropathy in globoid cell leucodystrophy (morbus Krabbe). *Acta Neuropathol* 11:69-81.
- Srivastava S. K., Beutler E. 1973 Hexosaminidase-A and hexosaminidase-B: studies in Tay-Sachs' and Sandhoff's disease. *Nature* 241:463.
- Sternberger L. A., Sternberger N. H. 1983 Monoclonal antibodies distinguish phosphorylated and nonphosphorylated forms of neurofilaments in situ. *Proc Natl Acad Sci U S A* 80:6126-6130.
- Stitt T. N., Drujan D., Clarke B. A., Panaro F., Timofeyeva Y., Kline W. O., Gonzalez M., Yancopoulos G. D., Glass D. J. 2004 The IGF-1/PI3K/Akt pathway prevents expression of muscle atrophy-induced ubiquitin ligases by inhibiting FOXO transcription factors. *Mol Cell* 14:395-403.
- Strack S., Barban M. A., Wadzinski B. E., Colbran R. J. 1997a Differential inactivation of postsynaptic density-associated and soluble Ca²⁺/calmodulin-dependent protein kinase II by protein phosphatases 1 and 2A. *J Neurochem* 68:2119-2128.
- Strack S., Westphal R. S., Colbran R. J., Ebner F. F., Wadzinski B. E. 1997b Protein serine/threonine phosphatase 1 and 2A associate with and dephosphorylate neurofilaments. *Brain Res Mol Brain Res* 49:15-28.

- Strauss K.,Goebel C.,Runz H.,Mobius W.,Weiss S.,Feussner I.,Simons M., Schneider A. 2011 Exosome secretion ameliorates lysosomal storage of cholesterol in Niemann-Pick type C disease. *J Biol Chem* 285:26279-26288.
- Su J. H.,Zhao M.,Anderson A. J.,Srinivasan A., Cotman C. W. 2001 Activated caspase-3 expression in Alzheimer's and aged control brain: correlation with Alzheimer pathology. *Brain Res* 898:350-357.
- Subra C.,Laulagnier K.,Perret B., Record M. 2007 Exosome lipidomics unravels lipid sorting at the level of multivesicular bodies. *Biochimie* 89:205-212.
- Suzuki K. 1998 Twenty five years of the "psychosine hypothesis": a personal perspective of its history and present status. *Neurochem Res* 23:251-259.
- Suzuki K., Suzuki K. 1990 Myelin pathology in the twitcher mouse. *Ann N Y Acad Sci* 605:313-324.
- Svennerholm L.,Vanier M. T., Mansson J. E. 1980 Krabbe disease: a galactosylsphingosine (psychosine) lipidosis. *J Lipid Res* 21:53-64.
- Takahashi H., Suzuki K. 1982 Globoid cell leukodystrophy: specialized contact of globoid cell with astrocyte in the brain of twitcher mouse. *Acta Neuropathol* 58:237-242.
- Takahashi H.,Igisu H.,Suzuki K., Suzuki K. 1983 The twitcher mouse: an ultrastructural study on the oligodendroglia. *Acta Neuropathol* 59:159-166.
- Takei Y.,Teng J.,Harada A., Hirokawa N. 2000 Defects in axonal elongation and neuronal migration in mice with disrupted tau and map1b genes. *J Cell Biol* 150:989-1000.
- Taniike M.,Mohri I.,Eguchi N.,Irikura D.,Urade Y.,Okada S., Suzuki K. 1999 An apoptotic depletion of oligodendrocytes in the twitcher, a murine model of globoid cell leukodystrophy. *J Neuropathol Exp Neurol* 58:644-653.
- Thompson W. 1983 Synapse elimination in neonatal rat muscle is sensitive to pattern of muscle use. *Nature* 302:614-616.
- Thompson W.,Kuffler D. P., Jansen J. K. 1979 The effect of prolonged, reversible block of nerve impulses on the elimination of polyneuronal innervation of new-born rat skeletal muscle fibers. *Neuroscience* 4:271-281.
- Toews A. D.,Armstrong R.,Ray R.,Gould R. M., Morell P. 1988 Deposition and transfer of axonally transported phospholipids in rat sciatic nerve. *J Neurosci* 8:593-601.
- Tsai J.,Grutzendler J.,Duff K., Gan W. B. 2004 Fibrillar amyloid deposition leads to local synaptic abnormalities and breakage of neuronal branches. *Nat Neurosci* 7:1181-1183.

- Ugawa Y., Rothwell J. C., Day B. L., Thompson P. D., Marsden C. D. 1991 Percutaneous electrical stimulation of corticospinal pathways at the level of the pyramidal decussation in humans. *Ann Neurol* 29:418-427.
- Vale R. D., Reese T. S., Sheetz M. P. 1985 Identification of a novel force-generating protein, kinesin, involved in microtubule-based motility. *Cell* 42:39-50.
- Veeranna, Shetty K. T., Link W. T., Jaffe H., Wang J., Pant H. C. 1995 Neuronal cyclin-dependent kinase-5 phosphorylation sites in neurofilament protein (NF-H) are dephosphorylated by protein phosphatase 2A. *J Neurochem* 64:2681-2690.
- Verhey K. J., Lizotte D. L., Abramson T., Barenboim L., Schnapp B. J., Rapoport T. A. 1998 Light chain-dependent regulation of Kinesin's interaction with microtubules. *J Cell Biol* 143:1053-1066.
- Vohra B. P., Groshong J. S., Zayas R., Wollmann R. L., Gomez C. M. 2006 Activation of apoptotic pathways at muscle fiber synapses is circumscribed and reversible in a slow-channel syndrome model. *Neurobiol Dis* 23:462-470.
- Vohra B. P., Groshong J. S., Maselli R. A., Verity M. A., Wollmann R. L., Gomez C. M. 2004 Focal caspase activation underlies the endplate myopathy in slow-channel syndrome. *Ann Neurol* 55:347-352.
- von Figura K., Hasilik A. 1986 Lysosomal enzymes and their receptors. *Annu Rev Biochem* 55:167-193.
- Wakeling E. N., Joussemet B., Costiou P., Fanuel D., Moullier P., Barkats M., Fyfe J. C. 2011 Failure of lower motor neuron radial outgrowth precedes retrograde degeneration in a feline model of SMA. *J Comp Neurol*.
- Wang M. J., Huang H. Y., Chen W. F., Chang H. F., Kuo J. S. 2011 Glycogen synthase kinase-3beta inactivation inhibits tumor necrosis factor-alpha production in microglia by modulating nuclear factor kappaB and MLK3/JNK signaling cascades. *J Neuroinflammation* 7:99.
- Wang Y., Zhang J., Mori S., Nathans J. 2006 Axonal growth and guidance defects in Frizzled3 knock-out mice: a comparison of diffusion tensor magnetic resonance imaging, neurofilament staining, and genetically directed cell labeling. *J Neurosci* 26:355-364.
- Wenger D. A., Rafi M. A., Luzi P. 1997 Molecular genetics of Krabbe disease (globoid cell leukodystrophy): diagnostic and clinical implications. *Hum Mutat* 10:268-279.
- Wenger D. A., Rafi M. A., Luzi P., Datto J., Costantino-Ceccarini E. 2000 Krabbe disease: genetic aspects and progress toward therapy. *Mol Genet Metab* 70:1-9.

- White A. B., Givogri M. I., Lopez-Rosas A., Cao H., van Breemen R., Thinakaran G., Bongarzone E. R. 2009 Psychosine accumulates in membrane microdomains in the brain of Krabbe patients, disrupting the raft architecture. *J Neurosci* 29:6068-6077.
- White A. B., Galbiati F., Givogri M. I., Lopez Rosas A., Qiu X., van Breemen R., Bongarzone E. R. 2011 Persistence of psychosine in brain lipid rafts is a limiting factor in the therapeutic recovery of a mouse model for Krabbe disease. *J Neurosci Res* 89:352-364.
- Whitmore A. V., Lindsten T., Raff M. C., Thompson C. B. 2003 The proapoptotic proteins Bax and Bak are not involved in Wallerian degeneration. *Cell Death Differ* 10:260-261.
- Wijsman J. H., Jonker R. R., Keijzer R., van de Velde C. J., Cornelisse C. J., van Dierendonck J. H. 1993 A new method to detect apoptosis in paraffin sections: in situ end-labeling of fragmented DNA. *J Histochem Cytochem* 41:7-12.
- Willard M., Simon C. 1983 Modulations of neurofilament axonal transport during the development of rabbit retinal ganglion cells. *Cell* 35:551-559.
- Witzemann V. 1989 Control of acetylcholine receptors in skeletal muscle. *J Protein Chem* 8:333-335.
- Witzemann V. 2006 Development of the neuromuscular junction. *Cell Tissue Res* 326:263-271.
- Witzemann V., Barg B., Criado M., Stein E., Sakmann B. 1989 Developmental regulation of five subunit specific mRNAs encoding acetylcholine receptor subtypes in rat muscle. *FEBS Lett* 242:419-424.
- Witzemann V., Schwarz H., Koenen M., Berberich C., Villarroel A., Wernig A., Brenner H. R., Sakmann B. 1996 Acetylcholine receptor epsilon-subunit deletion causes muscle weakness and atrophy in juvenile and adult mice. *Proc Natl Acad Sci U S A* 93:13286-13291.
- Wu Y. P., Matsuda J., Kubota A., Suzuki K., Suzuki K. 2000 Infiltration of hematogenous lineage cells into the demyelinating central nervous system of twitcher mice. *J Neuropathol Exp Neurol* 59:628-639.
- Xu C., Sakai N., Taniike M., Inui K., Ozono K. 2006 Six novel mutations detected in the GALC gene in 17 Japanese patients with Krabbe disease, and new genotype-phenotype correlation. *J Hum Genet* 51:548-554.
- Yamada H., Martin P., Suzuki K. 1996 Impairment of protein kinase C activity in twitcher Schwann cells in vitro. *Brain Res* 718:138-144.
- Yeager A. M., Brennan S., Tiffany C., Moser H. W., Santos G. W. 1984 Prolonged survival and remyelination after hematopoietic cell transplantation in the twitcher mouse. *Science* 225:1052-1054.

- Yildiz A.,Tomishige M.,Vale R. D., Selvin P. R. 2004 Kinesin walks hand-over-hand. *Science* 303:676-678.
- Yuyama K.,Sun H.,Mitsutake S., Igarashi Y. 2012 Sphingolipid-modulated exosome secretion promotes the clearance of amyloid-beta by microglia. *J Biol Chem*.
- Zaka M., Wenger D. A. 2004 Psychosine-induced apoptosis in a mouse oligodendrocyte progenitor cell line is mediated by caspase activation. *Neurosci Lett* 358:205-209.
- Zhao C.,Takita J.,Tanaka Y.,Setou M.,Nakagawa T.,Takeda S.,Yang H. W.,Terada S.,Nakata T.,Takei Y.,Saito M.,Tsuji S.,Hayashi Y., Hirokawa N. 2001 Charcot-Marie-Tooth disease type 2A caused by mutation in a microtubule motor KIF1Bbeta. *Cell* 105:587-597.
- Zhao J. X.,Ohnishi A.,Itakura C.,Mizutani M.,Yamamoto T.,Hojo T., Murai Y. 1995 Smaller axon and unaltered numbers of microtubules per axon in relation to number of myelin lamellae of myelinated fibers in the mutant quail deficient in neurofilaments. *Acta Neuropathol* 89:305-312.
- Zundel W.,Swiersz L. M., Giaccia A. 2000 Caveolin 1-mediated regulation of receptor tyrosine kinase-associated phosphatidylinositol 3-kinase activity by ceramide. *Mol Cell Biol* 20:1507-1514.

CURRICULUM VITAE LUDOVICO CANTUTI CASTELVETRI

University of Illinois at Chicago (UIC), Department of Anatomy and Cell Biology,
808 S Wood Street, Chicago, 60612, Illinois, USA
312-355-3952 (work); 312-927-5933 (mobile); Email: cantuti@uic.edu

EDUCATION:

- 2007-Present Ph.D. in Anatomy and Cell Biology. University of Illinois at Chicago** Advisor: Prof. Ernesto Bongarzone. GPA: 3.82/4 Dissertation Title: Mechanism of Axonopathy in Krabbe Disease.
- 2005-2007 Master degree in Medical, Molecular and Cellular Biotechnology (Laurea Magistrale in Biotecnologie Mediche, Molecolari e Cellulari). Istituto Vita-Salute San Raffaele (Milan).** Advisor: Prof. Ernesto Bongarzone Supervisors: Prof. Fabio Grohovaz and Prof. Ottavio Cremona. Dissertation Title: Effect of galactosyl-sphingosine on the neuronal cytoskeleton. Final Grade: 110/110 cum laude.
- 2002-2005 Bachelor degree in Medical and Pharmaceutical Biotechnology (Laurea in Biotecnologie Mediche e Farmaceutiche). Istituto Vita-Salute San Raffaele (Milan).** Advisor: Prof. Ernesto Bongarzone. Supervisor: Prof. Fabio Grohovaz. Final grade: 110/110

EXPERIENCE:

- 2007-Present Graduate Research Assistant. Supervisor: Prof. Ernesto Bongarzone. Department of Anatomy and Cell Biology, University of Illinois at Chicago, Chicago.**
Analysis of the mechanisms leading to axonopathy in Krabbe disease under the supervision of Prof. Ernesto Bongarzone at the University of Illinois at Chicago. This work focused on characterizing the extent and the molecular mechanisms of axonopathy in the Twitcher mouse, the spontaneous model of Krabbe disease. Alterations in axonal transport and neurofilament phosphorylation were identified as pathological mechanisms leading to axonal damage. Finally, the enzymes responsible for these alterations were identified. The project provided me with multiple levels of experiences, ranging from different experimental techniques to grant and paper writing.
- 2005-2006 Undergraduate Research Assistant. Supervisor: Prof. Ernesto Bongarzone. University of Illinois at Chicago, Chicago.** Immunofluorescence, flow cytometry, western blotting and cell cultures of PC12 neuroblastoma cells. Analysis of psychosine effect on neuronal cytoskeleton.
- 2003-2004 Undergraduate Research Assistant. Supervisor: Prof. Ernesto Bongarzone. Telethon Institute for the Gene Therapy (TIGET), Milan.** Immunohistochemistry, immunofluorescence, confocal microscopy on stained cells and stained tissue. Analysis of SDF1⁺ and RANTES⁺ cells in the nervous system of Krabbe disease.

HONORS AND AWARDS:

- 3/6/12 Travel award assigned from the UIC Graduate Council and the Graduate Student Council to attend the SfN meeting in Washington DC.
- 4/20/10 Dean's Scholar award - UIC Graduate College
- 3/30/09 Travel award assigned from the UIC Graduate Council and the Graduate Student Council to attend the ASN meeting in Charleston.

MEMBERSHIPS:

Member of the Society for Neuroscience (SfN) since 2008.

Member of the American Society for Neurochemistry (ASN) since 2009.

PUBLICATIONS:

Cantuti Castelvetri L, Givogri M.I. , Hongling Z., Lopez-Rosas A, Morfini G., Pigino G., Cao, H.; van Breemen R.; Brady S. and Bongarzone E. Inhibition of fast axonal transport is a pathogenic mechanism contributing to neuropathology in Krabbe disease. (manuscript in submission)

Cantuti Castelvetri L, Hongling Z., Givogri M.I., Chidavaenzi R., Lopez-Rosas A and Bongarzone E. Psychosine induces the dephosphorylation of neurofilaments by deregulation of PP1 and PP2A. *Neurobiol Dis.* 2012 Feb 4.

Smith B, Galbiati F, **Cantuti-Castelvetri L**, Givogri MI, Lopez-Rosas A, Bongarzone ER. Peripheral neuropathy in the Twitcher mouse involves the activation of axonal caspase 3. *ASN Neuro.* 2011 Sep 19.

Castelvetri LC, Givogri MI, Zhu H, Smith B, Lopez-Rosas A, Qiu X, van Breemen R, Bongarzone ER. Axonopathy is a compounding factor in the pathogenesis of Krabbe disease. *Acta Neuropathologica* 2011 Jul;122(1):35-48. 2011 Mar 4.

Galbiati F., Givogri M.I., **Cantuti L.**, Rosas A.L., Cao H., van Breemen R., Bongarzone E.R.. Combined hematopoietic and lentiviral gene-transfer therapies in newborn Twitcher mice reveal contemporaneous neurodegeneration and demyelination in Krabbe disease. *Journal of Neuroscience Research* 2009 Jun;87(8):1748-59.

Galbiati F., Basso V., **Cantuti L.**, Givogri M.I., Lopez-Rosas A., Perez N., Vasu C., Cao H., van Breemen R., Mondino A., Bongarzone E.R.. "Autonomic denervation of lymphoid organs leads to epigenetic immune atrophy in a mouse model of Krabbe disease." *Journal of Neuroscience.* 2007 Dic 12;27(50):13730-8.

PRESENTATIONS AND CONFERENCES:

- 05/21/12 Invited talk to the 32nd Blankenese meeting in Hamburg (Germany)
- 11/13/11 Presentation at the Annual Meeting of the Society for Neuroscience in Washington DC
- 4/19/11 Presentation at the Annual Meeting of the American Society for Neurochemistry in Saint Louis
- 3/6-10/10 Presentation at the Annual Meeting of the American Society for Neuroscience in Chicago

- 1/11/2009 Invited talk at the Department of Chemistry of the Università di Modena.
Title: Neurodegenerazione nella malattia di Krabbe: un problema di percorso
(Neurodegeneration in Krabbe disease: a problem of transit)
- 17-21/10/2009 Presentation at the Annual Meeting of the Society for Neuroscience in Chicago
- 3-5/11/2009 Presentation at the Great Lake Glia Meeting, in Traverse City (Michigan)
- 7-11/3/2009 Presentation at the annual meeting of the American Society for Neurochemistry in Charleston (South Carolina)
- 12/18/2008 Invited talk at the Circolo del Casino in Reggio Emilia (Italy). Title:
Neurodegenerazione: un nemico invisibile (Neurodegeneration: an invisible
enemy)

LABORATORY SKILLS

- Handling and genotyping of mice. Surgical procedures: sciatic nerve ligation, percutaneous intravenous injections in neonatal mice and retro-orbital injection in adult mice.
- Handling of cell lines (PC12, N2A, Hela and NSC34 cells) and preparation of primary cultures of neurons (embryonic cortical neurons and postnatal cerebellar granule neurons).
- Techniques for immunohistochemistry (intra-cardiac perfusion of mice, tissue collection, tissue embedding and sectioning, staining) and immunocytochemistry.
- Techniques for RNA quantification: RNA purification (TRIZOL), retro-transcription, design and optimization of primers for real time polymerase chain reaction (RTPCR) and quantification by RTPCR.
- Western blotting.
- Techniques for real time imaging of fluorescently labeled organelles, epi- and confocal fluorescence microscopy.
- Preparation of microsomal fraction by ultracentrifugation.
- Preparation of lipid rafts fractions from tissue or cell cultures.

OTHER SKILLS

- Fluent in Italian, Proficient in English and German.
- Experience in imaging software (Adobe Photoshop, Adobe Illustrator, Powerpoint and imageJ).

Teaching experiences with rotation students and as a teaching assistant in the class of Human Neur